



Lineage tracing of metastasis in a mouse model for Non-small cell lung cancer (NSCLC)

Untersuchung metastatischer Prozesse durch genetische Zellmarkierung in einem Mausmodell des nichtkleinzelligen Lungenkarzinoms (NSCLC)

Doctoral thesis for a doctoral degree
at the Graduate School of Life Sciences,
Julius-Maximilians-Universität Würzburg,

Section Infection and Immunity

Submitted by

Chitra Thakur

from

Bhopal, India

Würzburg 2012

Submitted on:

Office stamp

Members of the Promotion Committee

Chairperson: Prof. Dr. rer. nat. Thomas Hünig

Primary Supervisor: Prof. Dr. Ulf R. Rapp

Supervisor (Second): PD Dr. Rudolf Götz

Supervisor (Third): Prof. Dr. Thomas Rudel

Supervisor (Fourth): PD Dr. Jörg Wischhusen

Date of Public Defense:

Date of receipt of Certificates:

“That in all things He may have the preeminence! Colossians 1:18”

Dedicated to My Parents

Table of Contents

Table of Contents	1
Zusammenfassung	6
Summary	8
1 Introduction	10
1.1 Non small cell lung cancer (NSCLC)	10
1.1.1 The mitogenic cascade and Ras/Raf signaling	11
1.1.1.1 Ras/Raf signaling	12
1.2 Molecular abnormalities found in human lung cancer	14
1.2.1 Raf protein.....	15
1.2.2 The RAS genes	16
1.2.3 The MYC proto-oncogenes.....	16
1.2.4 Tumor suppressor genes.....	17
1.3 Metastasis	17
1.3.1 Collective migration	18
1.4 Cellular architecture of the lung	19
1.4.1 Cell populations involved in the homeostasis and injury repair of the distal lung	21
1.5 Genetic lineage tracing	24
1.5.1 What is lineage tracing?.....	24
1.5.2 Need of lineage tracing strategy in pulmonary/oncology research	25
1.5.3 Reporter molecules employed for lineage labeling experiments	26
1.5.3.1 Fluorescent reporter proteins.....	26
1.5.3.2 Advantage of fluorescent reporters over conventional marking systems	26
1.5.3.3 Red Fluorescent protein (DsRed).....	27
1.6 In vivo imaging	28
1.7 Mouse models for studying tumor progression and metastasis	29
1.7.1 Tetracycline-controlled transcriptional activation.....	30
1.7.1.1 Tet Off.....	30
1.7.1.2 Tet On.....	31

1.7.2 The Cre-loxP technology	32
2 Experimental design and goals of the project.....	35
2.1 Goals of the project	36
2.2 Transgenic mice used for the study	36
3 Materials.....	40
3.1 Instruments	40
3.2 Chemical Reagents.....	42
3.3 Antibodies	45
3.3.1 Primary antibodies.....	45
3.3.2 Secondary antibodies.....	46
3.3.3 Antibodies for immunoblotting	47
3.4 Enzymes.....	47
3.5 Kits.....	48
3.6 Oligonucleotides	49
3.7 Oligos for expression analysis	50
3.8 Solutions and buffers.....	52
4 Methods	54
4.1 Molecular Biology Methods.....	54
4.1.1 Measurement of DNA concentration.....	54
4.1.2 Polymerase Chain Reaction (PCR).....	54
4.1.3 Agarose-gel electrophoresis of DNA molecules.....	54
4.1.4 Isolation of RNA.....	55
4.1.5 cDNA synthesis	55
4.1.6 Real-time PCR.....	56
4.2 Biochemistry methods.....	56
4.2.1 Preparation of whole protein lysates from cells and tissues.....	56
4.2.2 Measurement of protein concentration	56
4.2.3 SDS PAGE.....	57
4.2.4 Immunoblotting.....	58
4.2.5 Membrane stripping	58

4.2.6 Eukaryotic cell culture technique.....	59
4.2.7 Freezing cell lines	59
4.2.8 Analysis of cultured cells via immunocytochemistry	60
4.3 Histological methods	60
4.3.1 Paraffin-embedding and sectioning of tissue	60
4.3.2 Optimal cutting temperature (O.C.T.) - embedding and cryosectioning of tissue	61
4.3.3 Haematoxylin and Eosin Staining	61
4.3.4 Immunohistochemical stainings (Enzymatic based detection).....	62
4.3.5 Alcian Blue Staining.....	65
4.3.6 Immunofluorescence stainings	66
4.3.7 X Gal staining on frozen sections	66
4.3.8 X Gal staining of FACS sorted DsRed cells.....	67
4.3.9 X-Gal : Whole mount tissue preparation.....	67
4.3.10 FACS sorting of DsRed cells from triple transgenic reporter mice	68
4.4 Animal Experiments	69
4.4.1 Generation of reporter transgenic mouse lines for lineage tracing experiments.....	69
4.4.2 Breeding of mice.....	69
4.4.3 Genotyping of transgenic mice.....	70
4.4.4 Sacrificiation of mice.....	71
4.4.5 Transplantation – experiments.....	71
4.5 Statistical Analysis	72
5 Results.....	73
5.1 Transgenic reporter mice for lineage labeling studies in a murine NSCLC model.....	73
5.1.1 The Red Fluorescent protein (RFP) mice	73
5.1.2 Generation of compound transgenic reporter mice for lineage tracing experiments	73
5.1.3 Testing of the compound reporter transgenic mice generated for the expression of the reporter gene.....	77
5.1.3.1 Lung targeted expression of the reporter gene in the DsRed mice.	77
5.1.3.2 FACS sorted DsRed cells cultured on matrigel	82
5.1.4 Labeling tumor cells induced by oncogenic C RAF	84
5.1.4.1 Lung tumor formation in C RAF BXB-DsRed induced mice exhibiting cuboidal tumor cell phenotype	85
5.1.4.2 Evaluation of the tumor for the expression of the lineage marker and the transgene	86

5.1.4.3 Labeling small cryptic lesions at earlier time points.....	87
5.1.4.4 C RAF BXB-DsRed transgenic mice exhibit proliferating bronchiolar hyperplasia.....	88
5.1.5 Labeling tumor cells generated in a reporter metastatic NSCLC model	90
5.1.6 Introduction of Myc induces a new phenotype: premalignant lesions.....	93
5.1.7 Evaluation and characterization of the primary tumor.....	95
5.1.8 Tumor progression concomitant with angiogenesis in the absence of EMT.....	96
5.1.9 Labeling efficiency in the transgenic compound reporter mice	98
5.1.10 Proliferation and apoptosis in the primary tumor.....	99
5.1.11 Status of p53 in the compound transgenic reporter animals.....	101
5.1.12 Screening for DsRed positive cells via Flow Cytometry.....	102
5.1.13 Loss of SpC and TTF-1 in the primary tumors: Hallmarks for metastatic progression	103
5.1.14 Evidence of circulating Bronchioalveolar stem cells (BASCs) in the tumors.....	105
5.1.15 Detection of the tumor specific transcripts in compound transgenic reporter mice via gene expression analysis.....	107
5.1.16 Gene expression profiling of the primary lung tumor.....	109
5.1.17 Survival curve and tumor burden of the reporter transgenic animals.....	111
5.2 Analysis of liver metastases	114
5.2.1 Anatomical and morphological characterization of the metastatic lesions	114
5.2.2 SpC expression is detected in cystic metastases	117
5.2.3 DsRed is detected in the single cluster of cell including the cystic and the papillary lesions of metastatic colonization	118
5.2.4 Evaluation of metastases for the expression of progenitor markers/lineage selectors.....	120
5.2.5 Clara cell emerges at the mixed cystic papillary stage of liver metastases	123
5.2.6 Presence of Bronchioalveolar stem cells (BASCs) in the metastases.....	125
6 Discussion	127
6.1 Novel transgenic murine model for lineage tracing of alveolar type II cells in NSCLC metastasis	127
6.2 Alveolar type II cells in NSCLC tumor initiation; perspective and facts	129
6.3 Contribution of alveolar type II cells in the metastases; an insight	134
6.4 Putative metastatic initiating cells; contribution of the alveolar lineage	137
7 Critical parameters, troubleshooting and time considerations.....	140
8 Appendix.....	144

9 References.....	147
10 Curriculum Vitae	159
Acknowledgements	163
Affidavit	166

Zusammenfassung

Das nichtkleinzellige Lungenkarzinom („non-small cell lung cancer“, NSCLC) ist die tödlichste Form des Lungenkrebses mit schlechter Prognose aufgrund hoher Metastasierungsneigung. Metastasierung ist eine der häufigsten Todesursachen bei Krebspatienten. Trotz ihrer klinischen Bedeutung sind die zellulären und molekularen Mechanismen der Entstehung, Etablierung und Progression von Metastasen weiterhin unklar. Darüberhinaus basiert das bisherige Wissen über den Metastasierungsprozess überwiegend auf Zellen, die entweder *in vitro* kultiviert oder manipuliert und danach in immundefiziente Mäuse rückübertragen wurden. In der vorliegenden Studie wurde ein Mausmodell mit erblichem Fluoreszenzmarker (DsRed) zur spontanen Metastasierung bei NSCLC entwickelt, der durch den CAG-Promotor („combination of cytomegalovirus early enhancing element and chicken beta actin“) in alveolären Typ II-Zellen (SpC-rtTA/TetO-Cre/LSL-DsRed) exprimiert wird. Aufgrund des Reprogrammierungscharakters des Myc-Onkogens war dieser Ansatz essentiell (Rapp et al, 2009). Die Markierung der Zellpopulation auf genetischem Weg erlaubte uns zum einen, die molekularen und zellulären Veränderungen während der Bildung des Primärtumors zu verfolgen, zum anderen konnte so die Entwicklung von Sekundärtumoren unterschiedlicher Stadien in entfernten Organen identifiziert werden. Bei kombinierter Expression von onkogenem C Raf-BXB und c-Myc (MYC-BXB-DsRed) in Lungenalveolar-Epithelzellen vom Typ II entstanden makroskopische Tumore in der Lunge, die auf zellulärer Ebene sowohl kuboidalen als auch kolumnaren Charakter aufwiesen und Metastasen, vorwiegend in der Leber, ausbildeten. Durch C Raf-BXB (CRAF-DsRed) induzierte Tumore erschienen morphologisch als kuboidal ohne Metastasierungsneigung. Überraschenderweise exprimierten zystische Läsionen in der Leber, obwohl negativ für SpC („surfactant protein C“) und CCSP („Clara cell secretory protein“), als Kennzeichen für deren Ursprung aus Lungenalveolarzellen Typ II stark das DsRed-Protein. Darüberhinaus sind in den frühen zystischen Läsionen Marker für frühe Lungenvorläuferzellen wie GATA4 („GATA-binding protein

4') und TTF1 (thyroid transcription factor 1') weiterhin exprimiert, was auf den Metastasierungsprozess als gestörte Rekapitulation der Ontogenese hindeutet (Rapp et al, 2008). Metastatische Tumore und Mischformen zu zystischen Läsionen enthielten DsRed- und SpC-positive Zellpopulationen. Diese Ergebnisse weisen in Sekundärtumoren den Übergang von zystischer Läsion zur Mischform mit zystischem Anteil und zur malignen Transformation nach. Unsere Resultate werfen ein neues Licht auf Reprogrammierungsprozesse metastasierender Zellen bei der Bildung von Sekundärtumoren. Das vorgestellte fluoreszenzmarkierte und metastasenbildende Mausmodell kann zum einen zur Untersuchung der Migrationsfähigkeit metastasierender Krebszellen in unterschiedliche Organe verwendet werden. Darüberhinaus ermöglicht dieses Mausmodell die Untersuchung des Differenzierungspotenzials markierter Zellen in andere Zelltypen wie Blutgefäße oder Stromazellen im Primärtumor.

Summary

Non-small cell lung cancer (NSCLC) is the deadliest form of lung cancer and has a poor prognosis due to its high rate of metastasis. Notably, metastasis is one of the leading causes of death among cancer patients. Despite the clinical importance, the cellular and molecular mechanisms that govern the initiation, establishment and progression of metastasis remain unclear. Moreover, knowledge gained on metastatic process was largely based on cultured or in vitro manipulated cells that were reintroduced into immune-compromised recipient mice.

In the present study, a spontaneous metastasis mouse model for NSCLC was generated with a heritable fluorescent tag (DsRed) driven by CAG (combination of cytomegalovirus early enhancing element and chicken beta actin) promoter in alveolar type II cells (SpC-rtTA/TetO-Cre/LSL-DsRed). This approach is essential, keeping in mind the reprogramming nature of Myc oncogene (Rapp et al, 2009). Such genetic lineage tracing approach not only allowed us to monitor molecular and cellular changes during development of primary tumor but also led us to identify the different stages of secondary tumor development in distant organs. Upon combined expression of oncogenic C Raf-BXB and c-Myc (MYC-BXB-DsRed) in lung alveolar type II epithelial cells, macroscopic lung tumors arose comprising of both cuboidal and columnar cellular features. C Raf-BXB induced tumors (CRAF-DsRed) exhibit cuboidal morphology and is non-metastatic whereas Myc-BXB induced lung tumors (Myc-BXB-DsRed) present cuboidal-columnar cellular features and is able to undergo metastasis mainly in liver. Surprisingly, cystic lesions which were negative for SpC (Surfactant protein C) and CCSP (Clara cell secretory protein), strongly expressed DsRed proteins indicating its origin from lung alveolar type II cells. Moreover, early lung progenitor markers such as GATA4 (GATA-binding protein 4) and TTF1 (Thyroid Transcription Factor 1) were still expressed in these early cystic lesions suggesting metastasis as a faulty recapitulation of ontogeny (Rapp et al, 2008). Interestingly, mixed cystic lesions and metastatic tumors contained DsRed

and SpC positive cells. These results demonstrate secondary tumor progression from cystic, mixed cystic to malignant transformation.

Our results shed tremendous light on reprogramming of metastasizing cells during secondary tumor development. Moreover, such fluorescent tagged metastatic mice model can also be used to track the migration ability of metastatic cancer cell to different organs and its potential to differentiate into other cell types such as blood vessel or stromal cell within the primary tumor.

1 Introduction

Lung cancer is the leading cause of cancer related deaths throughout the world. (Landis et al, 1999). There are two types of lung cancer based on histology; Small-cell lung carcinoma (SCLC) (Schiller, 2001) and Non-small cell lung carcinoma (NSCLC) (van Zandwijk et al., 1995). NSCLC is the most prevalent type of human lung cancer and has a poor prognosis due to its high rate of metastasis. Metastasis is a process by which cancer cells learn to form satellite tumors in distant organs and represents the principle cause of patient's death with solid tumors (Langley & Fidler, 2007). Metastasis of cancer may cause as many deaths as cancer itself. Amongst other reasons, this is because it is very difficult to know where the new tumour is going to develop. Moreover, the mechanisms of metastasis are still not well understood, although a lot of research into it is taking place and advances are being made. In view of this, the current work is an attempt focused on unraveling the identity of cell type responsible for metastasizing into secondary organs in a murine lung adenocarcinoma model.

1.1 Non small cell lung cancer (NSCLC)

Lung cancer has become the leading cause of cancer deaths in the world, accounting for even more solid tumor deaths than breast, pancreatic, prostate, and colorectal combined (Landis et al, 1999). More than 170,000 new cases are being diagnosed each year in the United States alone, of whom ~160,000 will eventually die, representing 28% of all cancer deaths (Jemal et al, 2004). Lung cancer can be divided into two major histopathological groups: non-small-cell lung cancer (NSCLC) (van Zandwijk et al, 1995) and small-cell lung cancer (SCLC) (Schiller, 2001). About 80% of lung cancers are NSCLC, and they are subdivided into adenocarcinomas, squamous cell, bronchioalveolar, and large-cell carcinomas (Travis, 2011). Squamous cell carcinomas and adenocarcinomas are the most prominent. The remaining 20% of lung cancers show properties of neuroendocrine cells. These

neuroendocrine lung tumors can be further sub-divided into four subgroups based upon their morphological characteristics.

Type	Frequency	5-Year Survival Rate (All stages)
<i>Small cell:</i>	18%	5%
<i>Non-small cell:</i>		
Squamous or epidermoid carcinoma	29%	15%
Adenocarcinoma	32%	17%
Large cell carcinoma	9%	11%

Table 1 Types of Lung cancer with their surveillance rates {Adapted from Dennis (Kaspar et al, 2002)}

1.1.1 The mitogenic cascade and Ras/Raf signaling

In a variety of human tumors, one can find a deregulation of the mitogenic cascade on different levels. Going through the list of hallmarks of cancer defined by Hanahan and Weinberg in 2000 (Hanahan & Weinberg, 2000) the Ras/Raf signaling can contribute to any individual of these criteria (Table 2). The growth factor receptor that triggers the consecutive signaling pathway, the EGF-receptor (EGFR), was found to be mutated in various epithelial tumors (Gschwind et al, 2004) and in 20% of NSCLC a mutation in the EGFR can be observed (Meuwissen & Berns, 2005). Furthermore, the Ras proteins, the transceiver of the receptor signals, are also popular targets for mutations in approx. 30% of human cancers (Karreth & Tuveson, 2009), as for e.g. in 15 to 20% of NSCLC activating KRas mutations are found (Meuwissen & Berns, 2005). Other important targets for mutations in the mitogenic cascade are the Raf-

kinases, which are central players of the MAPKinase signaling pathway, for e.g. B Raf is mutated in 66% of the melanoma patients (Schreck & Rapp, 2006).

Hallmarks of a cancer cell	Corresponding effect of the Ras/Raf signaling pathway
Immortalization	Telomerase Induction
Growth-factor-independent growth	Cell cycle activation
Insensitivity to growth-inhibitory signals	Inactivation of tumor suppressors
Ability to invade and metastasize	Stimulation of motility and extracellular remodelling
Ability to secure nutrients by stimulating angiogenesis	Stimulation of the production of pro-angiogenic factors
Avoidance of apoptosis	BAD inactivation; Caspase inhibition
Resistance to therapeutic measures	Induction of radiation resistance; induction of the multidrug resistance protein MDR 1

Table 2 The Ras/Raf signaling impacts on the hallmarks of cancer defined by Hanahan and Weinberg {Modified from (Kolch et al, 2002)}

1.1.1.1 Ras/Raf signaling

RAF proteins are part of a highly conserved signaling module, the mitogenic cascade, which transduces signals from the cell surface to the nucleus (Fig 1) The upstream regulators of the Raf proteins are members of the Ras-family of small G-proteins (Robbins et al, 1994). Ras is activated by extracellular ligands such as growth factors, cytokines or hormones binding to their receptor leading to the exchange of GDP with GTP, which converts Ras into its active conformation (Boguski & McCormick, 1993). Activated Ras directly interacts with high affinity with Raf and recruits it to the cytoplasmic membrane, where Raf activation via phosphorylation takes place (Avruch et al, 1994). Activated Raf phosphorylates and this triggers the subsequent activation of the kinases MEK1 and MEK 2 on two serine residues on their activation segment. These kinases phosphorylate and

further activate the mitogen activated protein kinases (MAPK) ERK 1 and ERK 2 (extracellular signaling related kinase) on threonine and tyrosine residues within their activation segment. ERK1/2 have both cytosolic (kinases and cytoskeletal proteins) and nuclear (transcription factors) substrates (Flory et al, 1996) and (Marshall, 1999). The activation of this cascade leads to transcriptional activation of proteins possessing cell stimulating, pro-survival and anti-apoptotic properties (Troppmair & Rapp, 2003). In addition to the Raf-kinases, Ras also regulates other proteins, for example the phosphatidylinositol-3 (PI3)kinases, which activates the serine/threonine-specific protein kinase Akt (PKK) via phosphorylation leading to phosphorylation and inactivation of the pro apoptotic protein BAD (Downward, 1998). Raf kinases not only phosphorylate and activates MEK1/2, but also interact with the anti apoptotic protein Bcl-2 and by this blocks the mitochondrial apoptotic pathway. Furthermore they phosphorylate and thereby inactivate the pro apoptotic Bcl-2 family protein BAD (Troppmair & Rapp, 2003).

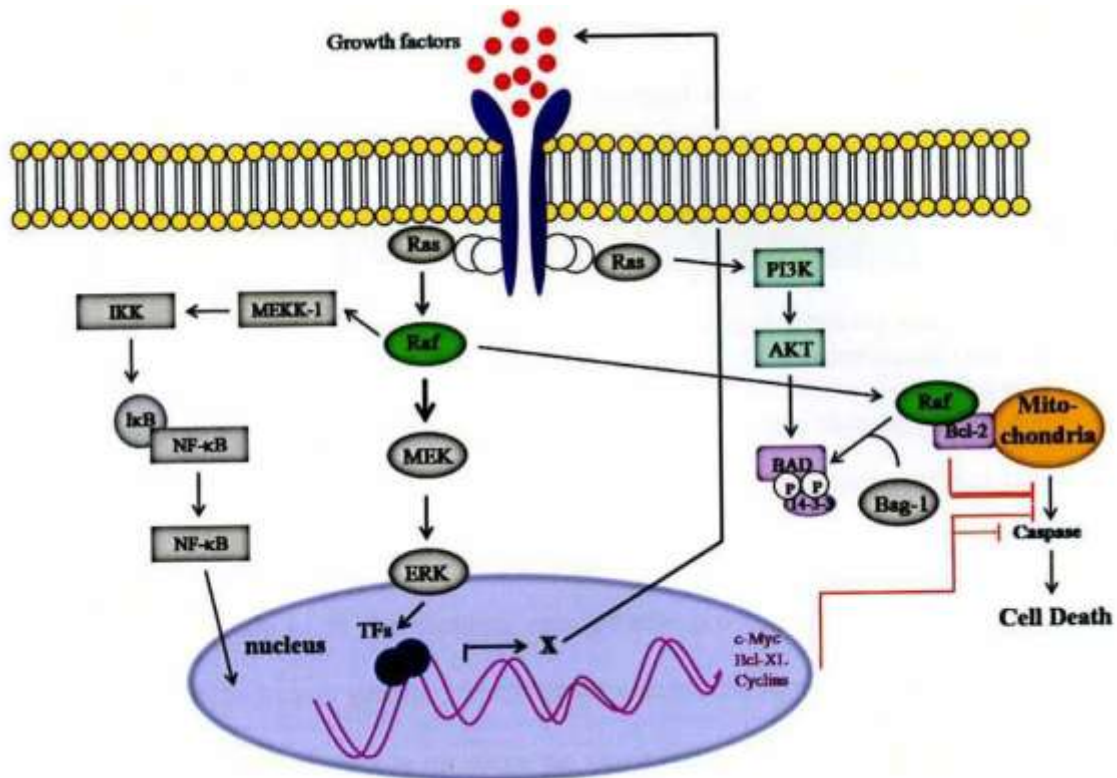


Fig 1 RAF signaling pathway regulating cell growth, differentiation, proliferation and survival {modified from (Troppmair & Rapp, 2003)}.

Molecular abnormality in Human Lung Cancer

Gene/locus	Alteration	NSCLC	SCLC
Myc	Amplification	5-20%	20-35%
Ras	Mutations	15-50%	1%
EGFR	Mutations	20%	--
INK4a	LOH	70%	50%
p16	Mutations	20-50%	5%
p14	Mutations	20%	65%
p53	Mutations	50%	75%
RB	Mutations	15-30%	90%
3p	LOH	70-80%	90-100%
4q	LOH	30%	80%

Table 3 Prominent bio-molecules that are de-regulated in human lung cancer; adapted from (Meuwissen & Berns, 2005).

1.2.1 Raf protein

Raf protein serine/threonine kinases are effectors of Ras signaling and therefore, are likely involved at least in those 30% of lung cancers in which mutated *ras* is detected (Salgia & Skarin, 1998) and (Forgacs et al, 2001). Among Raf proteins; C-Raf has been found to be overexpressed in a large fraction of human lung cancers (Rapp et al, 1988). The basis for increased CRAf protein content in lung tumor cells presumably is translational rather than transcriptional up-regulation (Rapp et al, 1988). Lung targeted expression of normal CRAf kinase in transgenic mice induced development of adenomas at high frequency. Oncogenically activated CRAF (CRAF BXB) caused the same histological type of adenoma to occur more rapidly in 100% of mice (Kerkhoff et al, 2000). CRAF is today a validated target for treatment of a variety of solid tumors (Hotte & Hirte, 2002).

1.2.2 The RAS genes

The Ras genes (*HRAS*, *KRAS*, and *NRAS*) encode GTPase proteins that play a role in transducing growth promoting and survival signals from membrane-bound RTKs. Hydrolysis of bound GTP to GDP abrogates RAS signaling, but oncogenic mutations in *RAS* impair GTP hydrolysis, causing persistent signaling. The *RAS* oncogenes acquire their transforming capacity by point mutations that are detected in 20%–30% of lung adenocarcinomas and ~20% of all NSCLCs (Slebos et al, 1990) . Most point mutations are G–T transversions and are correlated with smoking (Slebos et al, 1990). *KRAS* accounts for 90% of *RAS* mutations in lung adenocarcinomas, and approximately 97% of *KRAS* mutations in NSCLC involve codons 12 or 13 (Forbes et al, 2006). Mouse tumour models carrying oncogenic alleles of *K-ras* that can be activated only on a spontaneous recombination event in the whole animal has been previously described where the mice harbouring these mutations were highly predisposed to a range of tumour types, predominantly early onset lung cancer (Johnson et al, 2001). More recently reports demonstrated an improved mouse lung tumor model that harbours a *loxP*-Stop-*loxP* *Kras*^{G12D} knockin allele and both alleles of *p53* flanked by *loxP* sites (*Kras*^{LSL-G12D/+}; *p53*^{flox/flox} mice). Upon intratracheal administration of lentiviral vectors that express Cre-recombinase (Lenti-Cre)¹⁰, these animals developed between 5 and 20 lung tumors, lived 8–14 months after tumor initiation and developed macroscopic metastases to the draining lymph nodes, pleura, kidneys, heart, adrenal glands and liver (Winslow et al, 2011).

1.2.3 The MYC proto-oncogenes

MYCL, *MYCN*, and *CMYC*, encode transcription factors that regulate the expression of genes involved in DNA synthesis, RNA metabolism, and cell cycle regulation). The family of myc proto-oncogenes encodes basic helix–loop–helix transcription factors (c-, N-, and L-Myc) that regulate cell growth and proliferation and are involved in the etiology of diverse cancers (Oster et al, 2002). Activation of *MYC* genes occurs by amplification or loss of transcriptional control, which results in *MYC* protein overexpression. *MYC* amplification occurs in 15%–30% SCLCs and 5%–

10% NSCLCs (Richardson & Johnson, 1993). Hence *MYC* amplification is an indicative for poor prognosis (Johnson et al, 1996). Over-expression of *myc* genes is also strongly associated with the genesis of diverse cancers in many species (Lutz et al, 2002).

1.2.4 Tumor suppressor genes

Tumor suppressor genes are frequently inactivated in lung cancer. One of the most commonly found aberrations is mutation or deletion of *Tp53*. p53 is critical for maintaining genomic integrity after DNA damage inflicted by gamma and UV irradiation or carcinogen exposure (Hanawalt et al, 2003; Khanna & Jackson, 2001). Cellular stress such as DNA damage or hypoxia causes up-regulation of p53, which then acts as a sequence-specific transcription factor driving expression of a range of genes such as *p21*, controlling G1/S cell cycle transition, or *GADD4*, involved in the G2/M DNA damage checkpoint. Finally apoptosis is induced through p53 by activating *BAX*, *PERP* (Ihrie et al, 2003), and other genes (Mori et al, 2004). Loss of p53 function in lung cancer often occurs through missense mutations and rarely by deletions and is found in 75% and ~50% of SCLCs and NSCLCs, respectively (Toyooka et al, 2003). The *Tp53* mutations in lung tumors, mostly G–T transversions, carry the hallmark of smoking (Lewis & Parry, 2004). Normally, expression levels of p53 are kept low through an autoregulatory feedback loop with *MDM2*, which itself is transcriptionally controlled by p53. MDM2–p53 binding enhances the proteasome-dependent degradation and therefore keeps p53 levels in check. Overexpression of MDM2 is found in 25% of NSCLCs (Higashiyama et al, 1997).

1.3 Metastasis

The spread of cancer from one part of the body to another is called metastasis. Tumors formed from cells that have spread are called "secondary tumors" and contain cells that are like those in the original primary tumors. Tumors are called "malignant" because they have the ability to invade normal tissues (replacing healthy

cells with cancer cells) and to metastasize (spread) to other parts of the body. Death from cancer often comes not from the primary site but from the metastases. It is a multistep process in which metastatic cancer cells invades the surrounding stroma, intravasate, survive in the circulation, arrest, extravasate, invade the matrix, and finally grow in the target organ (Talmadge & Fidler, 2010), Fig 3). The persistence of tumorigenic and migrating cancer progenitor cells in locally invasive and metastatic cancer to current clinical treatments is responsible for the relapse of the disease (Brabletz et al, 2005). NSCLC accounts for about 80% of lung cancers, is the most prevalent, lethal and has poor prognosis due to its high rate of metastasis.

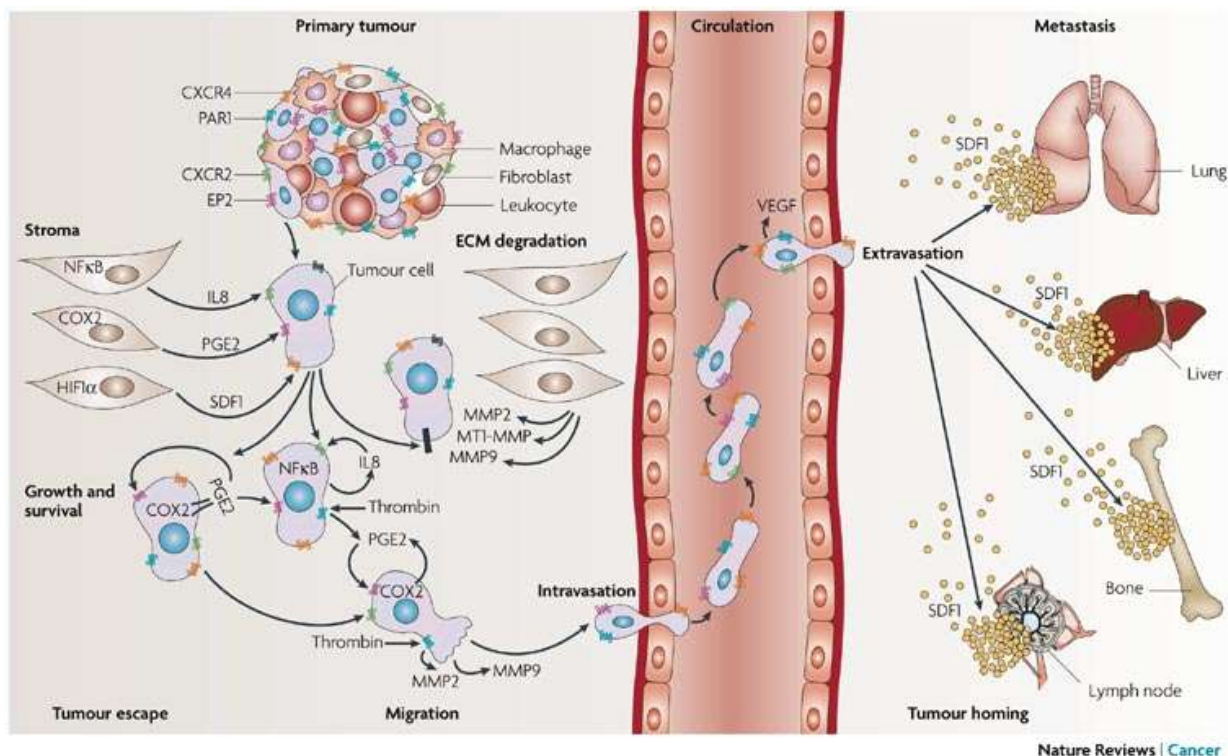


Fig 3 Metastatic progression adapted from (Dorsam & Gutkind, 2007)

1.3.1 Collective migration

Cell migration and invasion are critical parameters in the metastatic dissemination of cancer cells resulting in the formation of metastasis; which represent the major cause of death in cancer patients. Different types of cancer cell migration seem to exist, including single-cell mesenchymal or amoeboid migration and collective cell

migration. Although solitary migrating epithelial cancer cells have mostly undergone epithelial-to-mesenchymal transition (mesenchymal migration), and sometimes even lose their cell-matrix adhesion (amoeboid migration), collective migration of cancer cells in cell sheets, clusters, or streams is also frequently observed (Yilmaz & Christofori, 2010). It is known that collectively migrating cells maintain their cell-cell junctions and migrate in sheets, strands, tubes, and clusters, either still in connection with their originating tissue or as separated, independently migrating clusters (Friedl et al, 2004). There is increasing evidence that collective cell migration is common during invasion and metastasis of malignant tumors (Deisboeck & Couzin, 2009). Hence understanding the biological mechanisms driving cancer cell migration and designing anti-migratory drugs to combat them thus constitute current needs in oncology (Decaestecker et al, 2007).

1.4 Cellular architecture of the lung

Mouse lung development involves four histological stages (Cardoso & Lu, 2006). During the pseudoglandular stage [embryonic day (E) 10.5-16.5] (Au et al, 2004), the bronchiolar tree is laid down by branching morphogenesis (Metzger et al, 2008) and the epithelium begins to differentiate into secretory (Clara), neuroendocrine (NE), or ciliated cells. During the canalicular stage (E16.5-17.5), the undifferentiated distal epithelium continues to branch and gives rise to terminal sacs. These increase in number during the terminal sac stage E17.5- postnatal day (P) 5, and type I and II alveolar epithelial cells begin to differentiate. During the alveolar stage (P5-30), the terminal sacs develop into mature alveoli.

The respiratory system originates from the foregut endoderm, differentiating into many kinds of specialized epithelial cells which include pseudostratified epithelium, columnar epithelium and the alveolar epithelium. The lung develops during embryogenesis from two primary buds that arise in the ventral foregut. These buds undergo extensive branching morphogenesis, directed by reciprocal signaling between the epithelial endoderm and the surrounding mesoderm. During this

branching stage it is thought that the terminal buds contain a population of multipotent epithelial progenitors (Okubo et al, 2005).

The adult lung is composed of two major anatomically distinct regions—the conducting airways and gas-exchanging airspaces. It is functionally and structurally divided into three epithelial domains: the proximal cartilaginous airway (trachea and bronchi), distal bronchioles (bronchioles, terminal bronchioles, and respiratory bronchioles) and gas-exchanging airspaces (alveoli). The conducting airways (including the trachea, bronchi, and bronchioles) constitute a minority of the surface area in the human lung, amounting to approx. 0.25 sq.m whereas the alveolar regions of the lung make up approx. 100 sq.m. In the murine proximal conducting airway and major bronchi; basal, Clara, and ciliated cells are predominant cell types, although less frequent pulmonary neuroendocrine cells (PNECs) also reside in this domain.

In the adult mouse trachea and primary bronchi (cartilaginous airways), the luminal epithelium contains two main columnar cell types: ciliated cells and Clara-like cells. The nonciliated, columnar Clara cells comprise the majority of the distal bronchiolar epithelium in mice. It produces secretoglobins, the most abundant of which is Scgb1a1 (also known as CCSP or CC10). A small number of innervated neuroendocrine (NE) cells are also present.

The alveolar epithelium is lined by squamous alveolar type I pneumocytes (AEC I) and cuboidal type II pneumocytes (AEC II). type I cells have a highly flattened morphology, provided with a thin-walled gas exchange surface and are less differentiated, whereas cuboidal type II cells serve as progenitor cells for type I cells. These alveolar type II cells are important in synthesizing and secreting pulmonary surfactant proteins, a complex mixture of proteins and phospholipids which lower surface tension (Creuwels et al, 1997). They contain numerous secretory vesicles (lamellar bodies) filled with surfactant material, including surfactant-associated protein C or Sftpc. SpC is expressed in the distal epithelium during early lung development, and becomes restricted to alveolar type II cells late in gestation and

postnatally. Apart from SpC, there is also an existence of Nk2 homeobox1 (NKX2.1) (also Thyroid transcription factor 1 (TTF-1), one of the earliest known marker associated with commitment of endodermal cells to pulmonary and thyroid cell lineages and appears before the definitive lung formation (Maeda et al, 2007). During fetal lung development, the level of NKX2.1 decreases with advancing age. At first it is expressed in all pulmonary epithelial cells, later it becomes restricted to distal alveolar type II cells and proximal Clara Cells (Yuan et al, 2000).

1.4.1 Cell populations involved in the homeostasis and injury repair of the distal lung

In a normal steady state airway, epithelial cell proliferation in the adult lung is much lower compared with highly proliferative compartments in the gut, skin, and hematopoietic system (Liu et al, 2006). It shows both slow turnover and rapid repair. Since the cell turnover in the lung is normally very low, so a conveyor belt type mechanism for constantly and rapidly renewing the epithelium is not required. However, when injury to the epithelium of the lung does occur it has to be repaired as quickly as possible. In this case, a situation in which multiple cell types can proliferate and function as progenitors for repair is probably the only scenario.

Over the years, several experimental protocols have been developed in mice that mimic the injuries and rapid repair processes elicited in the lung by environmental challenges. The picture that is emerging from these models is that different regions of the respiratory system – the trachea and large airways, and the distal bronchioles and alveoli – use different kinds of stem cells and strategies for maintenance and repair.

According to their position within the pulmonary tree, several cell types in the lung (Fig 4) have been suggested to act as stem/progenitor cells in response to injury, and to serve to effect local repair (Emura, 2002; Engelhardt, 2001; Otto, 2002). Lung injury modeling in rodents has suggested that adult lung stem or progenitor cells exist, yet there has been a paucity of lineage relationship analysis in the pulmonary

system and little demonstration that lung cells exhibit stem cell properties (Rawlins & Hogan, 2006), (Sutherland & Berns, 2010).

Basal cells, Clara cells, and cells that reside in submucosal glands have been shown to function as progenitors or stem cells in the conducting airway of mice (Borges et al, 1997; Borthwick et al, 2001; Engelhardt, 2001; Engelhardt et al, 1995; Hong et al, 2004a). In the proximal airways, columnar epithelial cells give rise to basal cells (McDowell et al, 1985). Once formed, basal cells can self-renew and contribute to other lineages, but differentiated ciliated cells do not appear to divide (Otani et al, 1986).

Bronchiolar progenitor cells are thought to be Clara cells, particularly the ones residing within neuroepithelial bodies or bronchoalveolar duct junctions (Hong et al, 2001). In addition, a subset of variant Clara cells residing within neuroepithelial bodies (NEBs) (Hong et al, 2001; Peake et al, 2000; Reynolds et al, 2000) or bronchoalveolar duct junctions (Giangreco et al, 2002; Kim et al, 2005) has been considered stem cells in bronchioles. More recent studies have also found, in another region in the terminal bronchioles, that is, the bronchioalveolar duct junctions, bronchioalveolar stem cells (BASCs) that accumulate label-retaining cells. BASCs were previously termed DPCs (double-positive cells that express both SpC and CCSP) (Giangreco et al, 2002; Kim et al, 2005). These cells appear to be resistant to bronchiolar and alveolar damage, proliferate during epithelial cell renewal *in vivo*, and are thought to function to maintain the bronchiolar Clara cell and alveolar cell populations of the distal lung. BASCs also possess characteristics of regional stem cells, such as self-renewal and multipotency in clonal assays. More recently investigators reported a model in which the trachea, bronchioles, and alveoli are maintained by distinct populations of epithelial progenitor cells (Rawlins et al, 2009b)

Pulmonary neuroendocrine cells and bodies (PNECs/NEBs) have been suggested to be capable of dividing, although further research is needed to confirm this notion (Giangreco et al, 2002).

In the gas-exchanging regions of the lung, alveolar type II cells have been considered the stem/progenitor cell of the alveolar epithelium, based on their ability to repopulate/replenish both type II and terminally differentiated type I cells after injury (Giangreco et al, 2002; Kim et al, 2005). Studies using a rat lung injury model have suggested that there may be four alveolar type II groups, based on their expression of markers. The subpopulation of alveolar type II that is E-cadherin negative, proliferative, and expresses high levels of telomerase activity was considered a stem cell candidate for alveolar epithelium (Reddy et al, 2004).

In the adult lung, candidate stem cell populations have been identified that are restricted to the tracheal submucosal gland ducts, neuroepithelial bodies (NEBs) of the bronchi and bronchioles, and bronchoalveolar duct junction (BADJ) of the terminal bronchioles, suggesting distinct regional stem cell niches in the adult lung (Borthwick et al, 2001; Engelhardt, 2001; Engelhardt et al, 1995; Giangreco et al, 2002; Hong et al, 2001; Kim et al, 2005).

Stem cells can produce daughter cells or transient-amplifying (TA) cells, which often have a limited proliferation capacity and a distinct marker profile before they enter a terminal differentiation state. Clara and alveolar type II cells meet this TA cell phenotype since both do proliferate but finally differentiate into ciliated and alveolar type I cells, respectively. At this moment one cannot fully rule out that transient amplifying cells like Clara and alveolar type II cells are the precursors of lung tumors although these cells, unlike the multipotent pulmonary stem cells, do not have the ability to trans-differentiate. Identification of lung tumor precursor cells will ultimately not only be of great use for understanding basic lung tumor biology but will also enable the characterization of the consecutive steps early in SCLC and NSCLC development.

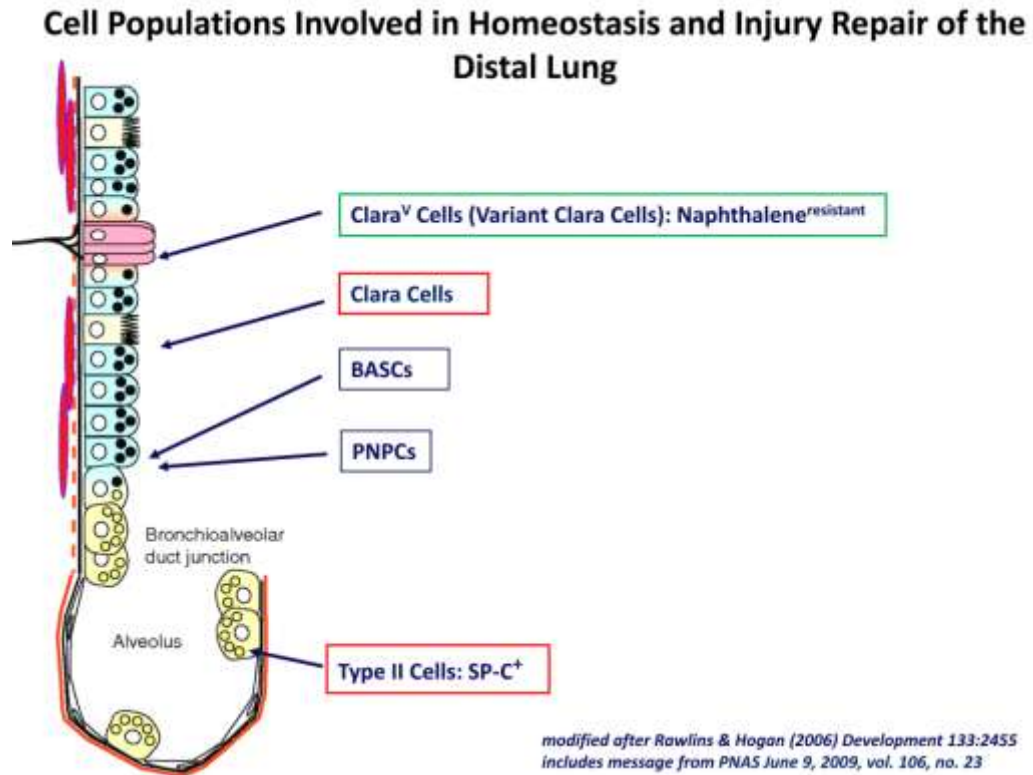


Fig 4 Cell populations involved in the Homeostasis and Injury repair of the distal lung

1.5 Genetic lineage tracing

1.5.1 What is lineage tracing?

Clonal marking methods represent one of the most powerful tools available for identifying stem/progenitor cells and analyzing their function. Ideally, a single cell is marked in such a manner that the mark is faithfully transmitted to all daughters of the initial cell, resulting in a labeled clone. By analyzing the number, location and phenotype of clonally derived cells at increasingly greater times after marking, the types of cells generated by the progenitor, their movements and their lifetimes can all be deduced. Moreover, a cell's clonal profile reveals information about its state of differentiation. This methodology is widely accepted by investigators across the

globe and has contributed to outstanding findings. (Hoffman, 2005; Rock et al, 2009).

1.5.2 Need of lineage tracing strategy in pulmonary/oncology research

Because cellular turnover in airways is relatively slow, methods for analysis of stem cells or progenitor cells *in vivo* have required prior injury to the lung. In contrast, *ex vivo* and *in vitro* models for analysis of airway stem cells have used genetic markers to track lineage relationships together with reconstitution systems that mimic airway biology. One way to follow cell fate during lung development, homeostasis, and repair is to use genetic lineage-labeling techniques to indelibly mark the descendants of specific cell types. In this way, the daughter cells express the lineage marker whatever phenotype they acquire. There are at least five distinct epithelial cell types in the lung that all derive from a common progenitor in the foregut endoderm. In contrast with our detailed understanding of cell lineage relationships in the hematopoietic system, the number of lineages and the relationship of cell types within a lineage of lung epithelial cells are poorly understood. Earlier studies were carried out to circumvent the limitations of cell enrichment approaches; retrovirus-mediated gene transfer has been used to genetically tag epithelial stem/ progenitor cells and to follow lineage relationships, using histochemical markers (Engelhardt et al, 1995; Engelhardt et al, 1992). Histochemical staining for marker transgenes such as β -galactosidase and/or alkaline phosphatase or other reporter proteins can then be used to visualize clonal expansion of stem/progenitor cells in the reconstituted airway epithelium.

This genetic lineage labeling approach can serve an important advantage as well. It can be used to isolate progenitor cells and their daughters for gene expression analysis to investigate the mechanisms of cell fate specification and differentiation, and they can be exploited for functional studies based on gene inactivation and overexpression. Such tools have so far only been applied in a very limited way to the lung. Moreover, they have sometimes been used in the absence of a completely cell type-specific promoter, making interpretation difficult (Belteki et al, 2005; Hong et al,

2004b; Kim et al, 2006; Perl et al, 2002b). Therefore a long-term goal in this field is thus to engineer mice for efficient lineage labeling of each of the different airway epithelial cell types.

1.5.3 Reporter molecules employed for lineage labeling experiments

1.5.3.1 Fluorescent reporter proteins

Non-invasive auto-fluorescent reporters have revolutionized lineage labeling in an array of different organisms. Naturally occurring fluorescent proteins have revolutionized biology by enabling what was formerly invisible to be seen clearly. These proteins have allowed the researchers to visualize, in real time, cancer dynamics in living animals, including tumor growth, metastasis, cell mobility, invasion and angiogenesis. Visualization of many aspects of cancer initiation and progression in vivo are now possible, even at the subcellular level, with fluorescent proteins. (Yamamoto et al, 2003). In recent years green fluorescent protein (GFP) from the bioluminescent jellyfish *Aequoria Victoria* has gained popularity in mouse transgenic and gene targeting regimes (Chalfie et al, 1994). In murine system, enhanced green (EGFP) (Okabe et al, 1997), yellow (EYFP) (Hadjantonakis & Nagy, 2000) and cyan (ECFP) (Srinivas et al, 2001) fluorescent proteins have served as invaluable tools.

1.5.3.2 Advantage of fluorescent reporters over conventional marking systems

The application of fluorescent proteins as expression markers and protein fusion partners has proved immensely valuable for resolving the organization of biological events in living cells, tissues, and organisms (Hadjantonakis et al, 2003; Lippincott-Schwartz & Patterson, 2003; Verkhusha & Lukyanov, 2004). One area of recent progress concerns the development of optical marking methods used to differentially highlight cells, organelles, and fusion proteins for tracking purposes. Such methods have found utility for studying organelle dynamics, protein trafficking, and cell lineage, as well as for selective retrieval of marked cells from within a population. It offers several advantages over conventional gene-based reporters, such as lacZ and alkaline phosphatase, in that its visualization does not require a chromogenic

substrate and can be realized *in vivo*. Fluorescence can be monitored in real-time *in vivo* and *in situ*, and has the added advantage in that it can be quantified.

The development of new models of human and animal cancer by transfer of the fluorescent protein gene to tumor cells enables visualization of fluorescent tumors and metastases. Fluorescent labels have proven to be a highly versatile means with which to image tumors in mice, as in addition to providing an opportunity to observe tumor biology *in vivo*, labeled cells are particularly well suited to *ex vivo* analyses (eg fluorescence microscopy or FACS analysis) once experimental end-points have been reached (Schmitt et al, 2002).

1.5.3.3 Red Fluorescent protein (DsRed)

DsRed, a red-emitting fluorescent protein (RFP) is a 25.7-kDa protein and a variant of naturally occurring chromoproteins found in colored body parts of corals and anemones; *Discosoma* sp. (Mizuno et al, 2001), with the excitation and emission maxima at 558 and 583 nm, respectively (Matz et al, 1999). DsRed is homologous to green fluorescent protein (GFP), which forms an 11-strand β barrel and a chromophore embedded inside the barrel (Wall et al, 2000). It has a much higher extinction coefficient and fluorescent quantum yield compared to GFP, and it quite resists to photo bleaching with a wider pH tolerance range. The protein exhibits a bright red, autocatalytic fluorescence emission easily separable from of residual green emission (Terskikh et al, 2002; Verkhusha et al, 2001). These advantages attracted tremendous interests for applications in live-cell imaging (Matz et al, 1999). The longer wavelength of the emitted light minimizes problems associated with light scattering and autofluorescence of the cells (Tsien). The long-wavelength emission of RFP enables high sensitivity and resolution of microscopic tumor growth using appropriate imaging techniques. DsRed provides an opportunity to generate useful Imaging tools. The serendipitous discovery that multiphoton excitation (760 nm) rapidly bleaches the red species, dequenching the intrinsic FRET to result in a red-to-green color change, allows exploitation of DsRed as an optical highlighter to track cell lineage and fusion protein dynamics or to retrieve marked cells from a larger population (Marchant et al, 2001). DsRed has shown to be very enabling for whole-

body imaging and has been used to non-invasively follow cancer metastasis in real time (Katz et al, 2003) in nude mice as well as whole-body image dual-color models of tumors expressing DsRed-2 growing in transgenic GFP nude mice as hosts (Yang et al, 2003).

Higher wavelength emissions (such as red) are preferred due to the lower background- autofluorescence in tissues (Miyawaki et al, 2003). Red fluorescent wavelength has a superior tissue penetrance compared with spectral variants of lower wavelength.

1.6 In vivo imaging

Significant progress has been made recently in the variety of ways that cancer can be noninvasively imaged in murine tumor models. Other tumor imaging strategies have been developed that rely upon the detection of reporter transgene expression *in vivo*, and these too have made a significant impact on both the versatility and the specificity of tumor imaging in living mice. The use of fluorescent proteins for imaging is revolutionizing *in vivo* biology (Hoffman, 2005; Hoffman, 2008). Fluorescent protein imaging has been particularly useful to study tumor progression (Hoffman, 2005). Whole-body imaging with fluorescent proteins has been shown to be able to quantitatively track tumor growth and metastasis, gene expression, angiogenesis, and bacterial infection (Hoffman, 2005; Zhao et al, 2001).

Recent developments in the field of small animal imaging have advanced our understanding of *in vivo* tumor biology. The technology comprises of magnetic resonance imaging (MRI), positron emission tomography (PET), single photon emission computed tomography (SPECT), bioluminescence imaging (BLI), and fluorescence imaging and these approaches have had the most significant impact on mouse tumor model research.

Tumors in mice can be imaged *in vivo* by fluorescence imaging techniques when labeled with fluorescent proteins, dyes or nano sized photonic crystals termed 'quantum dots'. Light emission from labeled cells first requires excitation of the fluorescent marker with relatively shorter wavelengths of light. The imaging sensitivity of far-red and near-infrared materials is further enhanced by the fact that

their excitation results in significantly reduced levels of autofluorescence from normal non-labeled tissues. Populations of tumor cells labeled with either GFP or RFP have also been imaged together to investigate the clonal nature of metastasis (Yamamoto et al, 2003).

A major advantage of fluorescent proteins expressing tumor cells is that imaging requires no preparative procedures, substrate, or contrast agents and is, therefore, uniquely suited for visualizing cells and tissues *in vivo*. The very bright fluorescence enables internal tumors and metastases to be externally observed in critical organs such as colon, liver, bone, brain, pancreas, breast, lymph nodes, prostate, etc.

1.7 Mouse models for studying tumor progression and metastasis

One of the most frequent malignancies in humans is lung adenocarcinoma. To develop novel diagnostic and therapeutic approaches for the management of this disease, animal models are required. With the possibility to introduce genetic insults (mutations, abnormalities) identical to those commonly found in human cancer into the endogenous murine gene locus; has served as a valuable tool not only for understanding the basics of tumor biology but also for the development and validation of new tumor intervention strategies as well as for the identification of markers for early diagnosis.

For over two decades, transgenic mice have permitted the study of biological functions of numerous genes during normal organogenesis. In addition, the first generation of transgenic mice that were purposely made to induce neoplasia in a variety of tissues provided valuable insight into cellular processes that are crucial for the initiation of cancer (Brinster et al, 1984; Stewart et al, 1984). Hence, mouse models have provided an essential means with which to elucidate the involvement and *in vivo* effects of various genetic lesions in tumorigenesis, tumor progression, and metastasis. Here I briefly describe the two important and basic strategy of conditional gene activation exploited in the current research work.

1.7.1 Tetracycline-controlled transcriptional activation

The scientific challenge of determining whether a multistage cancer process is reversible fueled the development of mouse models that overexpress oncogenes in a temporally and spatially controlled manner. One of the most powerful transgenic approaches that have been developed is the tetracycline (Tet)-dependent system, which permits temporal as well as tissue-specific control of transgene expression (Furth et al, 1994; Gossen & Bujard, 1992).

Tetracycline-Controlled Transcriptional Activation is a method of inducible expression where transcription is reversibly turned on or off in the presence of the antibiotic tetracycline or one of its derivatives (e.g. doxycycline). In nature, the P_{tet} promoter expresses TetR, the repressor, and TetA, the protein that pumps tetracycline antibiotic out of the cell.

The two most commonly used inducible expression systems for research of eukaryote cell biology are named Tet-Off and Tet-On. This system consists of a fusion of the Tet repressor and a VP16 activation domain to create a transcriptional activator protein (transactivator) rather than a repressor. Gene expression is activated as a result of binding of the Tet-Off or Tet-On protein to tetracycline response elements (TREs) located within an inducible promoter. The difference between Tet-On and Tet-Off is not whether the transactivator turns a gene on or off as the name might suggest; rather, both proteins activate expression. The difference relates to their respective response to doxycycline (Dox, a more stable tetracycline analogue); Tet-Off activates expression in the absence of Dox, whereas Tet-On activates in the presence of Dox.

1.7.1.1 Tet Off

The Tet-Off system for controlling expression of genes of interest in mammalian cells was developed by Professors Hermann Bujard and Manfred Gossen at the University of Heidelberg (1992). This system makes use of the tetracycline transactivator (tTA) protein created by fusing one protein, TetR (tetracycline repressor), found in *Escherichia coli* bacteria with another protein, VP16, produced by the Herpes Simplex Virus. The tTA protein binds on DNA at a 'tet'O operator.

Once bound the 'tet'O operator will activate a promoter coupled to the 'tet'O operator, activating the transcription of nearby gene. Tetracycline derivatives bind tTA and render it incapable of binding to TRE sequences, thereby preventing transactivation of target genes. This expression system is also used in generation of transgenic mice, which conditionally express gene of interest.

1.7.1.2 Tet On

The Tet-On system works in the opposite fashion. In this system, the rtTA protein is capable of binding the operator only when bound by doxycycline. Thus, the introduction of doxycycline to the system initiates the transcription of the genetic product. The Tet-On system is sometimes preferred for the faster responsiveness.

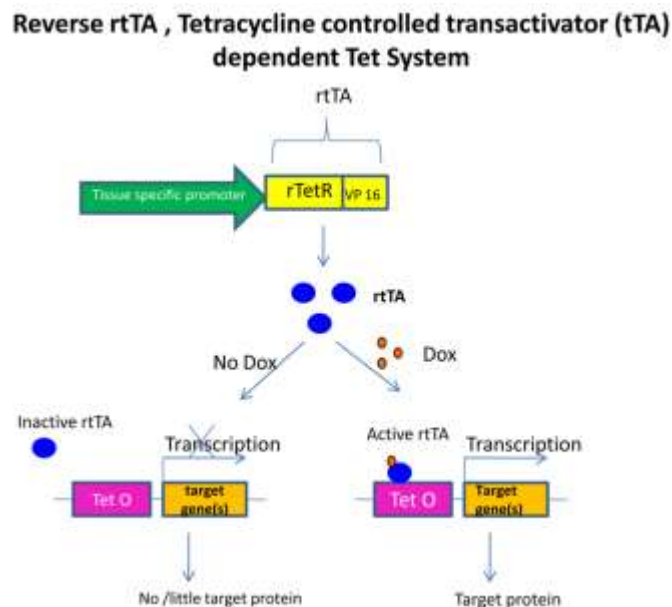


Fig 5 Reverse Tetracycline controlled transactivator (tTA) dependent Tet System for conditional gene activation

Recent advances in the development of mouse strains that express the reverse tetracycline-responsive transactivator (rtTA, Tet-ON) under the ubiquitously active Rosa26 locus are very valuable for studying the full spectrum of functions of particular genes in many cell types (Yu et al, 2005) and (Belteki et al, 2005). A tissue specific expression of the rtTA as well as the Tet controlled activation of transgenes can be achieved in these strains through Cre-mediated deletion of a selectable marker cassette that acts as a transcriptional Stop sequence located between the

Rosa26 promoter and the rtTA coding sequence. A sustained activation of the TetO-driven transgenes requires a constant administration of doxycycline. Freshly prepared Dox in drinking water appears to be the safest and most effective way to activate transgenes. In contrast, feeding commercially available chow containing Dox is less expensive in the long-term. The rtTA-mediated transactivation of Tet operator-driven responder genes can be rapidly and completely blocked by withdrawing the doxycycline, and administration of the ligand lifts the transcriptional block from the Tet-regulatable promoter.

1.7.2 The Cre-loxP technology

One approach for inducing tightly restricted gene modification in mice is with the Cre/loxP system (Sauer & Henderson, 1988). The Cre-lox technology is a binary system, where the Cre recombinase catalyzes the deletion of a DNA fragment between two directly orientated *loxP* sites (Hoess & Abremski, 1984). LoxP recognition sites are inserted around the regions to be deleted using homologous recombination, thus creating an allele, which is flanked by *loxP* sites (a floxed allele). The temporal and spatial excision of the floxed allele is achieved by expressing the Cre enzyme under a tissue-specific promoter in the same mouse (Nagy, 2000). The details of this technology have been elaborated below.

The Cre-lox system is used as a genetic tool to control site-specific recombination events in genomic DNA. This system has allowed researchers to manipulate a variety of genetically modified organisms to control gene expression, delete undesired DNA sequences and modify chromosome architecture. Cre-Lox recombination is a special type of site-specific recombination developed by Dr. Brian Sauer initially for use in activating gene expression in mammalian cell lines and transgenic mice (Sauer & Henderson, 1988). The Cre protein is a site-specific DNA recombinase, and can catalyse the recombination of DNA between specific sites in a DNA molecule. These sites, known as *loxP* sequences, contain specific binding sites for Cre that surround a directional core sequence where recombination can occur.

Lox P (locus of X-over P1) is a site on the Bacteriophage P1 consisting of 34 bp. There exists an asymmetric 8 bp sequence in between with two sets of palindromic, 13 bp sequences flanking it. The detailed structure is given below (Fig 6a)

13bp **8bp** **13bp**
 ATAACTTCGTATA - GCATACAT - TATACGAAGTTAT

Fig 6a *Lox P* sequence

When cells that have *loxP* sites in their genome express Cre, a recombination event can occur between the *loxP* sites. The double stranded DNA is cut at both *loxP* sites by the Cre protein. The strands are then rejoined with DNA ligase in a quick and efficient process. The result of recombination depends on the orientation of the *loxP* sites.

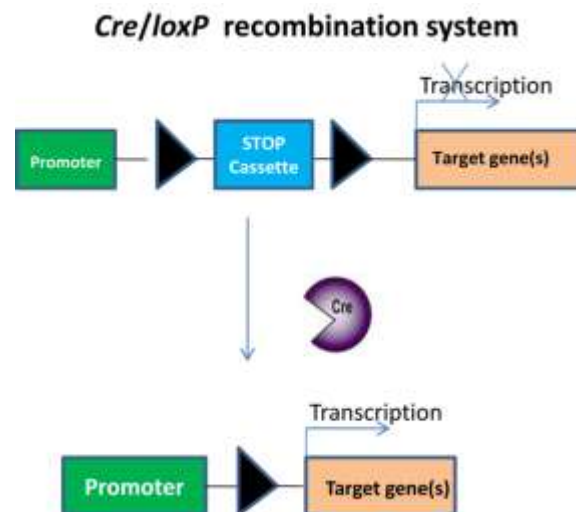


Fig 6b Cre *Lox P* system for gene expression

LoxP sites can be inserted into the mouse genome such that they flank important coding sequences of a particular gene of interest (gene “floxing”). Genes modified to contain *loxP* sites within introns function normally in the absence of Cre, but are rendered nonfunctional in the presence of Cre due to excision of the floxed segment (Sauer & Henderson, 1988). Since the floxed gene is found in every cell of the mouse, the specificity of the gene excision arises from tissue- or cell-selective

delivery of Cre recombinase (Fig 6b). This can be accomplished through breeding of the mouse containing the floxed allele with a second transgenic mouse that expresses Cre only in the cells/tissue of interest through the use of a highly specific promoter (Kilby et al, 1993). However, in cases where such promoters are not available, recombinant viral vectors provide an important alternative for selective delivery of Cre (Brooks et al, 2000; Kaspar et al, 2002; Stec et al, 1999).

2 Experimental design and goals of the project

The research work is focused on studying Non-small cell lung cancer (NSCLC) metastasis by genetic lineage tracing approach.

In the primary neoplasm, the tumor initiation at host distant tissues/organs may result from the division of the tumorigenic and migrating cancer progenitor cells or their early progeny from primary neoplasm that give rise to further differentiated cell subpopulations. Non small-cell lung cancer is lethal due to its high rate of metastasis. Identifying the cell type that is capable of metastasizing to secondary tissues is of great importance which would help us in developing therapeutics targeting the identified cell type. Lack of suitable animal model has so far hampered the analysis of metastatic progression. Recently investigators have generated the first conditional model for metastasis of NSCLC and have declared the ability of c Myc in successfully executing metastasis in a C-RAF driven mouse model for NSCLC (Rapp et al, 2009). In view of this, the present study aims at incorporating a heritable tag to the alveolar type II cells and following its fate invivo during the process of tumor progression culminating into metastasis thereby investigating the contribution of type II cells in metastasis. The advantage of genetic lineage labeling of type II cells with a marker will eventually reflect the record of the previous status acquired by the type II cells. Thereafter during the course of tumorigenesis and metastatic progression; loss of differentiation markers (SpC in this case), will no longer pose a threat in identifying the previous fate of the cell type, since the lineage tag would still retain in the current status of the cell type once it has been initially marked by the reporter molecule; inspite of whatever phenotype a cell acquires during the later stages in the process of neoplastic transformation and in malignant progression.

2.1 Goals of the project

1. Generation of transgenic mouse model to label alveolar type II cells with the reporter gene, driven by a combination of oncogenes.
2. To investigate whether we can follow the track of the labeled cells and detect them in the metastatic sites.
3. To unravel the identity of the cell type responsible for initiating metastasis in the NSCLC murine model.

2.2 Transgenic mice used for the study

1. DsRed transgenic reporter mouse (Tg(CAG-Bgeo,-DsRed*MST)1Nagy/J)

These Lac Z/RED transgenic mice express beta-galactosidase (*lacZ*) under the control of the chicken beta actin promoter coupled with the cytomegalovirus (CMV) immediate early enhancer (Nagy, 2000). When crossed with a Cre recombinase-expressing strain, *lacZ* expression is replaced with red fluorescent protein (DsRed*MST) expression in tissues expressing Cre recombinase. This double reporter system makes it possible to distinguish a lack of reporter expression from a lack of Cre recombinase expression while providing a means to assess Cre excision activity in live animals and cells. A transgenic construct containing a Red Fluorescent Protein variant (DsRed.MST) gene under the control of the a chicken beta actin promoter coupled with the cytomegalovirus (CMV) immediate early enhancer upstream of a *loxP* site flanked beta-geo gene, was introduced into 129S6B6F1 derived G4 embryonic stem (ES) cells. ES cell clone containing one copy of the transgene and expressing LacZ was aggregated with ICR outbred tetraploid embryos to generate chimeric mice. The resulting chimeric male animal was bred with an ICR outbred female. Progeny from this cross, that were hemizygous for the transgene, were bred to ICR outbred mice. While mice hemizygous for this Z/RED transgene are reported to be viable and fertile, but hemizygous animals are often smaller than littermates and subject to postnatal mortality. Delayed weaning greatly enhances the survival. Although homozygous animals are born, animals have not survived past five weeks of age (Fig 7).

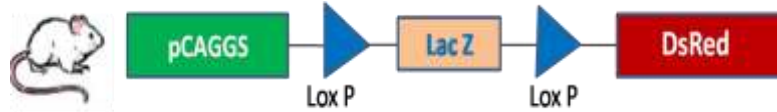


Fig 7 Lac Z (Floxed) /DsRed mouse

2. SP-C-rtTA mice

This mouse line was obtained from Dr. Whitsett Lab.

This mouse line is being used to target alveolar type II cells of the lung in a conditional manner. Crossing these mice with other transgenic mice that have the Tet-regulated genes will lead to type II cell specific expression.

Plasmid construction: The rtTA construct was a gift of Dr. Herman Bujard (ZMBH, Heidelberg). The 1 kb rtTA coding sequence was placed under the control of the 3.7 kb human SP-C promoter (Glasser et al., 1991) or the 2.3 kb rat CCSP promoter (Stripp et al., 1992) that direct expression of transgenes in respiratory epithelial cells of the lung. Polyadenylation sequences from SV40 (SP-C-rtTA) and the human growth hormone gene (CCSP-rtTA) were used to ensure transcript termination (Perl et al, 2002a).

3. Tet O Cre (LC-1)

This mouse line was obtained from other Dr. Bujard Lab.

This is a conditional transgenic mouse system in which Cre will be expressed in desired organs only when these mice are crossed with another transgenic mouse line (inducer line). The purpose of using these mice is to employ them to inactivate specific genes in certain cell types in an inducible manner. The bidirectional transcription unit encoding the *cre* and the luciferase (*luc*) gene under the control of the promoter Ptetbi-1 was derived as described previously. The PLAP rtTA2s-S2 transcription unit was obtained by first replacing the SV40 poly (A) site in pUHRt61-1 by the β -globin intron/poly (A) sequence. Subsequently, the PCMV sequence was exchanged for the sequence encoding the promoter of the liver enriched activator protein derived from plasmid pUHG15-30. LC transgenic mice were obtained by pronuclear injection of a purified 6.8 kb *NotI* fragment containing the bidirectional transcription unit into fertilized F2 (C57Bl/6X BALB/c) eggs. Similarly, rTALAP mice were generated by transferring the 5.1 kb *XmnI*-*AsnI* fragment of p UHRt61-30 into

fertilized F2 (C57Bl/6X DBA) eggs, following standard techniques (Schonig et al, 2002).

4. Tet-O C-RAF BXB

This mouse was generated in Ulf R.Rapp's Lab.

To generate mice conditionally expressing C-RAF BXB, Tet-O C-RAF ha-BXB fragment (6.0 kb) was isolated by gel electrophoresis and injected into the pronucleus of fertilized mouse eggs. To generate mice conditionally expressing C-RAF BXB, pcDNA3 plasmid harboring ha-tagged oncogenic C-RAF, here after C-RAF ha-BxB, was digested with Hind III and Xba I and cloned into pTS4 vector. The resulting pTS4-C-RAF ha-BxB plasmid was subsequently cut with Sma I and Xba I to clone a 1.3 kb C-RAF ha-BxB fragment into pBI5 vector (containing a tet operator) using Pvu II (compatible with Sma I site) and Xba I sites. The final PBI5 C-RAF ha-BxB plasmid was cut with Ase I to remove the vector backbone and the Tet-O C-RAF ha-BxB fragment (6.0 kb) was isolated by gel electrophoresis and injected into the pronucleus of fertilized mouse eggs. Eight potential founders were generated and five of them showed germ line transmission after PCR genotyping. All positive founders were mated with either SP-C rtTA or CCSP rtTA transgenic activator lines to obtain double transgenic progeny. These compound mice were induced with doxycycline (DOX) (Sigma) containing food (500 mg/kg, Sniff) for different periods and analyzed for phenotypes of lung pathology. All mice were kept on FVB/n background.

5. SPC c Myc

This mouse line was obtained from Dr. Halter's Lab.

This mouse line express the murine oncogene *c-myc* under the control of lung-specific surfactant protein C promoter, to study the bronchiolo-alveolar adenocarcinomas derived from alveolar type II pneumocytes. The transgenic mice were produced as follows: The *Apal-HindIII* mouse *c-myc* DNA fragment from the plasmid pTG2948 (Dalemans et al, 1990) was subcloned into the corresponding restriction sites in pBSKS II (+/-) (Stratagene). *Apal* was converted into a *SalI* restriction site. The 2.7 kb *SalI/EcoRI* *c-myc* DNA fragment was ligated to the *SalI/EcoRI* site of the vector pUC18/3.7SP-C downstream of the human SP-C

Experimental design and goals of the project

promoter 5'-flanking region (Wikenheiser et al, 1992). The *Bam*HI site of the *Bam*HI–*Sa*II IgEGF fragment (nucleotides 0 to 360, including the Ig signal sequence and a synthetic EGF gene) derived from the plasmid alb-DS4 (Tönjes et al, 1995) was converted to a *Sa*II restriction site. The new IgEGF *Sa*II fragment was cloned into the *Sa*II restriction site 3' of the promoter of the human SP-C gene of pUC18/3.7SP-C. Both gene constructs were cleaved with *Nde*I and *Not*I and the fusion gene fragments were purified by the Qiagen gel extraction kit and microinjected into male pronuclei of fertilized oocytes from hybrid CD2/F1 (DBA/2 × Balb/C) mice (Hogan et al, 1994). Viable oocytes were transferred into the oviduct of pseudopregnant CD2F1 recipient mice. Transgenic founder mice were mated with CD2F1 for propagation as hemizygous transgenics (Ehrhardt et al, 2001).

3 Materials

3.1 Instruments

Hardware/General materials

Autoclave
 Blotting Chamber
 Bacterial shaker
 Cell Culture Hood
 Cell culture Incubator
 Cell culture dish (6, 12, 24, 96 well)
 Cell culture dish (6, 10 cm)
 100/40/20 um cell strainer
 Conical tubes (15, 50 ml)
 Cover slips
 Cooling centrifuge
 Cryo Microtome
 Dissection Microscope
 Desktop centrifuge
 Electrophoresis power supply
 Electrophoresis unit, small
 Embedding cassettes
 Exposure cassettes
 Electrophoresis unit for Agarose Gels
 Electrophoresis unit for Agarose Gels
 Earmarks
 Fluorescence Microscope (CCD)
 FACS Calibur
 Filter paper
 Freezer -20 degree
 Freezer -80 degree
 Fridge 4degree

Manufacturer

Webeco
 Bio-Rad
 New Brunswick Scientific innova 4330
 Heraeus Instruments
 Heraeus Instruments
 Nunc Brand Products
 Corning
 BD Falcon
 BD Falcon
 Menzel-Glaser
 OMNILAB
 Leica
 Leica
 OMNILAB/EPPENDORF
 Bio-Rad
 Bio-Rad Mini-Protean II
 Simport
 Dr.Gross-Suprema
 BioRad
 BioRad
 Harlan
 Leica
 Becton Dickinson
 Schleicher & Schuell
 Liebherr
 Liebherr
 Nunc

FUJI Medical X –Ray films	Hartenstein
Glass plates for SDS gels	BioRad
Glass coverslips	Leica
Heating block	Gebr.Liebisch
Heating Block with shaker	GFL 1083, Amersham-Buchler
Homogenizer	Ultra-Turrax
Inverted Microscope	Olympus
Incubator	Heraeus Instruments
Ice Machine	Scotsman
Microtome	Leitz,Wetzlar
Microscope slides	Super frost ®Plus
MicroAmp® Fast Optical 96-Well	Applied Biosystems
Reaction Plate	
Nanodrop	Thermo Scientific
Neubauer chamber	Hartenstein
PCR Machine	Bio-Metra
Ph meter	Inolab
Pipettes	Eppendorf Research
Power supply	Bio-Rad
Parafilm™M™ ®	Verschlußfolie Josef Peske GmbH & Co.KG
Scale	A.Hartenstein
Shakers	BellcoBiot, Heidolph,Unimax 2010
Spectrophotometer	Ultraspec 3000, Pharmacia Biotech
Sonicator	Sono Plus HD
Scalpel	Hartenstein
Triple-Timer weiß 100 stunden	Hartenstein
Thermocycler	PE 9600, Perkin Elmer; T3, Biometra®
Timer	Roth
0.2 ml Thermo-Strip PCR tubes and caps DNA/RNA/RNase free ab-0266	Thermo SCIENTIFIC

Vortex	Scientific Industries Genie-2
Water Bath	GFL 1083, Amersham-Buchler
Whatman paper	Hartenstein

3.2 Chemical Reagents

Chemical	Manufacturer
1kb DNA Ladder	Fermentas
100 bp DNA Ladder	Fermentas
Acetone	Applichem
Acrylamide (30%) /Bisacrylamide (0.8%)	Roth
Agarose, ultra pure	Invitrogen
Ammoniumpersulphate (APS)	Sigma
Butylated Hydroxy toluene (BHT)	Sigma
Beta-Mercaptoethanol	Roth
Bovine serum albumin (BSA)	Sigma
Bromophenol blue	Sigma
Beetle Luciferin, Potassium Salt	Promega
Brain extract type II from bovine brain	Sigma
Bromodeoxyuridine (BrdU)	Sigma
Chloroform	Roth
Citric Acid	Roth
Corn oil	Mazola
DAPI	Sigma
Diethyl pyrocarbonate (DEPC)	Merck
Diaminobenzidine(DAB)	Sigma
Dimethylformide	Roth
Dimethylsulfoxide (DMSO)	Sigma
Doxycycline	Sigma
dNTPs	Fermentas

EDTA	Sigma
Entellan	Merck
Eosin	Merck
Ethanol	Sigma Aldrich
Ethidiumbromide	Applichem
Fetal Calf Serum	Invitrogen
Fetal Bovine Serum, charcoal stripped	Sigma
Formaldehyde	Roth
Formamide	Roth
Glacial acetic acid	Roth
Glucose	Sigma
Glycerol	Sigma
Glutaraldehyde, 25%	Alfa Aesar GmbH
HCl	Roth
Heparin	Roth
HEPES	Roth
Hydrogen peroxide	Sigma
Isopropanol	Merck
Ketamin (10 %)	Bela-pharm
Lipofectamine	Invitrogen
Low melting agarose	Biozyme
Mayers's Hematoxylin	AppliChem
Methanol	Hartenstein
MgCl ₂	Sigma
Mowiol	Calbiochem
Na ₂ EDTA	Sigma
NaOH	Sigma
n-butanol	Roth
Normal Goat Serum	MILLIPORE
Normal Donkey Serum	MILLIPORE
Paraformaldehyde(PFA)	Sigma

Paraffin wax	Merck
Phenol	Roth
Phosphate.buffered saline (PBS)	Roth
Prestained protein ladder	Fermentas
Polybrene	Sigma
Polyvinil Pyrolidine (PVP- 40)	Roth
Ponceau S	Sigma
Ribose ATP	Fermentas
Rompun	Bayer
Rabbit Serum	Chemicon
Sodium Chloride	Roth
Sodiumdodecylsulphate (SDS)	Roth
TEMED	Sigma
TissueTEK (OCT)	Chemicon
Tris	Roth
triSodium dehydrate	Roth
Triton X-100	Sigma
Trizol Reagent	Invitrogen
Tween 20	Roth
Potassium Ferrocyanide 99% , P-9387	Sigma
Potassium Ferricyanide 99% P-8131	Sigma
X- Gal	Fermentas
Xylene, 0.25 %	Cyanole
Xylol	Fisher Scientific

3.3 Antibodies

3.3.1 Primary antibodies

Primary Antibody	Firma
Rabbit anti DsRed monoclonal	Clonetech
Mouse anti-beta-Galactosidase, purified monoclonal , Z3781	Promega
Anti-ki-67 Antigen, clone: MM1, Isotype Mouse IgG1 Cat.No IMG-80159	IMGENEX
CC10 (S-20) sc-9773 goat polyclonal IgG	Santa Cruz
Vimentin (C-20) sc-7557, goat polyclonal IgG	Santa Cruz
c-Myc (N-262) sc-764 rabbit polyclonal IgG	Santa Cruz
GATA-4 (C-20) sc-1237 goat polyclonal IgG	Santacruz
Rabbit Anti-Human Protein Gene Product 9.5 (50 µl) 78-504 AbD	Serotec
DsRed (L-18) sc-33353 goat polyclonal IgG	Santa Cruz
Anti-TTF-1 Cat .No.IMG-80195 Clone: 8G7G3/1 Isotype: Mouse IgG1	IMGENEX
Actin (I-19) sc-1616-R rabbit polyclonal IgG	Santacruz
Purified anti-human PCNA Cat. No. 555566	Becton Dickinson Co.
pro SPC , Rabbit	Gift from J. Whitsett
P-p44/42 MAPK (T202/Y204) (20G11) # 4376S Rabbit monoclonal antibody (Phospho Erk)	Cell Signaling
p44/42 MAPK (Erk 1/2) (137F5) # 4695S Rabbit monoclonal antibody (Total Erk)	Cell Signaling

3.3.2 Secondary antibodies

Secondary antibody	Firma
Polyclonal Rabbit Anti-Cow Cytokeratin Wide Spectrum Screening (WSS) , Ref Z0622	DAKO North America , Inc. 6392 Via Real Carpinteria , CA 93013 USA
Polyclonal Rabbit Anti-Mouse Immunoglobulins/Biotinylated Ref. E0354	DAKO Denmark A/S Produktionsvej 42 DK-2600 Glostrup, Denmark
Polyclonal Rabbit Anti-Goat Immunoglobulins/Biotinylated Ref. E0466	DAKO Denmark A/S Produktionsvej 42 DK-2600 Glostrup, Denmark
Polyclonal Goat Anti-Rabbit Immunoglobulins/Biotinylated Ref. E0432	DAKO Denmark A/S Produktionsvej 42 DK-2600 Glostrup , Denmark
Polyclonal Goat Anti-Mouse Immunoglobulins/Biotinylated Ref. E0433	DAKO Denmark A/S Produktionsvej 42 DK-2600 Glostrup, Denmark
Biotinylated Rabbit Anti-Rat IgG(H+L) Affinity Purified	Vector Laboratories, Inc. Burlingame, CA 94010
DyLight tm 488-conjugated AffiniPure Donkey Anti-Rat IgG (H+L)	Jackson ImmunoResearch Code No. 712-485-150
DyLight tm 488-conjugated AffiniPure Donkey Anti-Rabbit IgG (H+L)	Jackson ImmunoResearch Code No. 711-485-152
DyLight tm 488-conjugated AffiniPure Donkey Anti-Goat IgG (H+L)	Jackson ImmunoResearch Code No. 705-485-147
Cy TM 5-conjugated AffiniPure Donkey Anti-Rat-IgG (H+L)	Jackson ImmunoResearch Code No. 712-175-153
Cy TM 3-conjugated AffiniPure Donkey Anti-Rat-	Jackson ImmunoResearch Code No.

IgG (H+L)	712-165-153
Cy TM 5-conjugated AffiniPure Donkey Anti-Mouse -IgG (H+L)	Jackson ImmunoResearch Code No. 715-175-113
Cy TM 3-conjugated AffiniPure Donkey Anti-Rabbit -IgG (H+L)	Jackson ImmunoResearch Code No. 711-165-152
Cy TM 5-conjugated AffiniPure Donkey Anti-Goat-IgG (H+L)	Jackson ImmunoResearch Code No. 705-175-147
Cy TM 3-conjugated AffiniPure Goat Anti-Mouse -IgG (H+L)	Jackson ImmunoResearch Code No. 115-165-166
Cy TM 5-conjugated AffiniPure Donkey Anti-Rabbit -IgG (H+L)	Jackson ImmunoResearch Code No. 711-175-152

3.3.3 Antibodies for immunoblotting

- ECLTM Anti-Rat IgG, Horseradish Peroxidase-linked F(ab')₂ fragment (from goat) NA9350V : GE Healthcare UK Limited
- ECLTM Anti-Rabbit IgG, Horseradish Peroxidase-linked F(ab')₂ fragment (from donkey) NA9340V : GE Healthcare UK Limited

3.4 Enzymes

Enzyme	Firma
Proteinase K (for Genotyping), 500 mg Art. 7528-3	ROTH
Proteinase K from Tritirachium album, P5568-1MI > 500 units/MI ie. 22.2mg protein/ml (Biuret); 974 units/mL	Sigma Alrich GmbH
Dispase® from Bacillus Polymyxa 1.82 units/mg Cat.No.17105-041	GIBCO TM
DNase I Ref: 11 284 932 001 100 mg from	Roche Diagnostics GmbH

Bovine pancreas	
Collagenase, from <i>Clostridium histolyticum</i> C0130-100 mg	Sigma-Aldrich Chemie GmbH
Collagenase /Dispase (collagenase from <i>Vibrio alginolyticus</i> &Dispase from <i>Bacillus polymyxa</i>)	Roche
Restriction Endonucleases	Fermentas
Taq Polymerase	Genecraft

3.5 Kits

Kit	Firma
BCA- Kit	Thermo Scientific Pierce
First Strand cDNA Synthesis Kit # K1612 (for 100 Reactions)	Fermentas Life Sciences
Fast SYBR® Green Master Mix, Part No. 4385612, Qty 5 mL	Applied Biosystems
AVIDIN/BIOTIN Blocking Kit SP-2001	Vector Laboratories, Inc. Burlingame, CA 94010
Elite® PK-6100 Standard VECTASTAIN ABC Kit	BIOZOL Diagnostica Vertrieb GmbH
Pierce ECL Western Blotting Substrate Prod 32106	Thermo SCIENTIFIC
QIAGEN DNeasy tissue kit	Qiagen
BEGM® Bronchiolar Epithelial Cell Growth Medium Bullet kit (CC -3171 & CC-4175)	Lonza
RT2 Profiler PCR Arrays for mouse Tumor Metastasis , PAMM- 028C -2	Qiagen
RED Taq®ReadyMix™ PCR Reaction Mix R2523-100RXN 080M6110 GmbH ; omponents: Water, PCR Reagent W1754-1VL ReadyMix™ redtaq™ PCR reaction mix with MgCl ₂ R2648- 20RXN	Sigma Aldrich Chemie

3.6 Oligonucleotides

Mouse Line	Sequence	PCR Conditions
SPC rtTA (USA) 400 bp	5' gac aca tat aag acc ctg gtc 3' 5' aaa atc ttg cca gct ttc ccc 3'	95 °C for 3 minutes 95 °C for 30 seconds 58 °C for 30 seconds 72 °C for 60 sec; 35cycles 72 °C for 10 minutes 4 °C hold
Tet O Cre	cre 3: tcg ctg cat tac cgg tcg atg c cre 4: cca tga gtg aac gaa cct ggt cg	95 °C for 3 minutes 94°C for 25 seconds 63 °C for 30 seconds 72 °C for 1minutes 15 sec; 35 cycles 72 for 10 minutes 4 °C hold
SPC c Myc (Mouse) 500 bp	spc-c myc aag gac ttg gct ggc aga cag c myc tgt tgg tga agt tca cgt tga gg	94 °C for 3 minutes 94 °C for 30 seconds 60 °C for 30 seconds 72 °C for 1minutes 15 sec; 35 cycles 72 °C for 10 minutes 4 °C hold
Tet O C Raf BXB	tetnew : tag aag aca ccg gga ccg atc cag bxb : aca tct ccg tgc cat tta ccc	95 °C for 3 minutes 94 °C for 30 seconds 62 °C for 30 seconds 72 °C for 1minutes 35 cycles 72 °C for 10 minutes 4 °C hold

SPC C Raf BXB 23 400 bp	SPC S1 gag gag agg aga gca tag cac c BXB aca tct ccg tgc cat tta ccc	94 °C for 3 minutes 94 °C for 30 seconds 60 °C for 30 seconds 72 °C for 1minutes 35 cycles 72 for 10 minutes 4 °C hold
DsRed 208 bp	IMR 3846 5' ccc cgt aat gca gaa gaa ga IMR 3847 5' ggt gat gtc cag ctt gga gt	95 °C for 3 minutes 95 °C for 30 seconds 61 °C for 60 seconds 72 °C for 1minutes 35 cycle 72 for 10 minutes 4 °C hold
Lac Z 410 bp	Lac 7 5' ccc att acg gtc aat ccg ccg Lac 8 5' gcc tcc agt aca gcg cgg ctg	95 °C for 3 minutes 95°C for 30 seconds 60°C for 30 seconds 72 °C for 1minutes 35 cycle 72 °C for 10 minutes 4 °C hold

3.7 Oligos for expression analysis

Primers used for expression analysis. All primers were designed using the program AIO (Karreman, 2002)

Gene	Sequence and Annealing temperature
Axin 2	5'ccacttcaaggagcagctcagca 3' and 5'- taccaggctcctggagactga-3'. 55 °C
CD 133	5'-gga gct gac ttg aat tga gg-3' and 5'-acc aac acc aag aac aag gc-3' 51 °C

CD 24	5'-gac aaa atg ggt ctc cat tcc gca c-3' and 5'-taa agg acg cgt gaa agg ttt ga-3' 58 °C
CD 34	5'-ctg tcc tga tag atc aag tag -3' and 5'-atg cag gtc cac agg gac acg -3' 59 °C
CD 44	5'-cgc tgc tga cat cgt cat c-3' and 5'-aat tcc gag gat tca tcc ca-3' 53 °C
Lef-1	5'-tgg aca tgc ctt gct tgg agt t-3'and 5'-aca gcg acc cgt aca tgt caa a-3' 57 °C
LGR 5	5'-cttccgaatcgtcgatcttc -3' and 5- aacgatcgtctcaggctaa-3' 62 °C
SYK	5'-tcc atg gca aca tct cca g-3' and 5'- gac atg gta ccg tga gga-3' 60 °C
Sca 1	5'-tca gag caa ggt ctg cag gag gac tg-3' and 5'-atg gac act tct cac act aca aag -3' 64 °C
TCF -1	5'-gtg gac tgc tga aat gtt cg-3'and 5'-agc aca ctt cgc aga gac ttt -3' 51 °C
TERT	5'-ttc aac cgc aag acc gac ag-3' and 5'-atg gcg ttc ctg agt atg -3' 56 °C
c Kit	5'-tgg ttt gag cat ctt cac gg-3' and 5'-gac gca act tcc tta tga tc-3' 53 °C
Vimentin	5'-gtg cgc cag cag tat gaa ag-3' and 5'-gca tcg ttg ttc cgg ttg g-3' 58 °C
TTF-1	5' ttg ctc acg tcc ccc agc g 3' and 5' cct tac cag gac acc atg gc 3' 60 °C
SpC	5' gca gag ccc cta caa tca cc 3' and 5' gca aag agg tcc tga tgg ag 3' 61 °C
DsRed	5 'ctt cgc ctg gga cat cct g 3 ' and 5' tgg gtc acg gtc gcc acg cc 3' 62 °C
Human C RAF BXB	5' ttt ccc cag atc ctg tct tcc at 3' and 5'aca tgt gtt ctg cct ctg gaga 3' 61 °C
CCSP	5'gaa gat cgc cat cac aat cac t 3' and 5' cag ggt tga aag gct tca gg 3'

3.8 Solutions and buffers

1. For RNA Isolation

- BCP Phase separation reagent: cat. No. BP- 151 molecular biology grade from Roth
- TRIzol® Reagent Cat. No. 15596-018 from Invitrogen™

2. For Protein Isolation

- PhosSTOP Phosphatase Inhibitor Cocktail Tablets (10 tablets).04 906 845 001 Roche Diagnostics GmbH Mannheim, Germany
- Complete Mini, EDTA-free Protease inhibitor cocktail tablets (25 tablets) Ref 11 836 170 001 Roche Diagnostics GmbH Mannheim, Germany

Solutions/Buffers's formulations

Nonidet P40 Lysis buffer	3X Laemmli Buffer
10 Mm Hepes, pH 7.4	100 mM Tris/HCl pH 6.8
145 mM KCl	3% SDS
5 mM MgCl ₂	45% Glycerol
1 mM EGTA	0.01 % Bromophenol blue
0.2% IGEPAL(NP 40)	7.5 % beta-Mercaptoethanol
1 Mm Sodium Vanadate	
1x Net Gelatin	SD-transblot buffer
50mMTris/HCl pH 7.4	50 mM Tris/HCl pH 7.5
5mM EDTA	40mM Glycine
0.05% Triton X-100	20% Methanol
150 mM NaCl	0.004 % SDS
0.25% Gelatine	
Tail lysis buffer	Stripping Buffer
50 mM EDTA	62.5mM Tris/HCl , pH 6.8
50 mM Tris/HCl	2% SDS
0.5% SDS	100 mM Beta-Mercaptoethanol
pH 8.0	50 X TAE Buffer
For 5 ml Anesthesia solution	Tris-base: 242 g
Ketamine from Bela-pharma	Glacial acetic acid, 57.1 ml
Rompun ®2% Injektionslösung from Bayer	0.5 M Na ₂ EDTA (pH 8.0), 100 ml

HealthCare	
Ketamine: 500 µl + Rompun 250µl + Rest 0.9%NaCl	Distilled water,upto 100 ml
10 X TBS	TBST
0.5% SDS	1X TBS
500 mM Tris- HCL pH 7.4	000.05 % Tween-20
1.5 M NaCl	Distilled water
Distilled water	Loading Buffer (6X)
TE Buffer	30%Glycerol (make 25 ml with H2O)
50 mM Tris Base (pH 8.0)	0.25%Bromophenol blue
1 mM EDTA	Antigen Retrieval solution
0.5% Triton X-100	10 mM Citrate buffer (pH 6)
4% PFA in PBS	Stock solutions
Weigh 37 g PFA in 850 ml of Water	Solution A= 0.1 M Citric Acid solution (21.01 g Citric Acid monohydrate in 1 litre of water)
Add 2 to 3 drops of 1 N NaOH	Solution B= 0.1 M Sodium Citrate (29.49 g trisodium citrate dehydrate in 1 litre of water)
Heat to 60 °C and mix until the PFA is completely dissolved.	Working solution (pH 6)
Add 100 ml of 10X PBS and adjust the pH to 7.4	18 ml of Solution A
Bring the final volume to 1 litre with water.	82 ml of Solution B
	Make the volume till 1 litre with ddH ₂ O

18. FACS Buffer: 10% Fetal Bovine Serum in sterile cell culture grade PBS

19. Proteinase K Buffer: 10 mM Tris-HCl (pH 8.0), 1 mM EDTA and 1% Tween

20. 1% Low Melting Point (LMP) Agarose: Weigh 1 g of LMP Agarose and dissolve in 100 ml of Millipore water using a microwave. Autoclave the solution. Warmify (Liquefy) before using by keeping the vial immersed in a water bath at 45 °C.

4 Methods

4.1 Molecular Biology Methods

4.1.1 Measurement of DNA concentration

The concentration of DNA was determined by measuring the absorbance at 260 nm on a NanoDrop ND 1000 spectrophotometer (Thermo Scientific). The DNA purity was controlled by the ratio of absorbance values at 260 nm and 280 nm (A₂₆₀/A₂₈₀) which should lie between 1.8 and 2. The ratio of A₂₆₀/A₂₈₀ lower than 1.8 indicates protein contamination in the given sample.

Isolation of DNA from tissue : For isolation of DNA from murine tissue, the QIAGEN DNeasy tissue kit was used according to the included manual.

4.1.2 Polymerase Chain Reaction (PCR)

The Polymerase Chain Reaction (PCR) is used for amplification of specific regions of a DNA-target. PCR was performed in a 30 µl reaction mix containing 3 µl of 10X Taq-Polymerase buffer, 1 µl of 2mM dNTP-mix, 0.5 µl of 20pmol forward and reverse primer and 0.3 µl Taq-Polymerase, filled up with Milli Q water. The PCR reaction typically consisted of 20 to 40 repeated temperature changes called cycles. After an initiation step for 10 minutes at 95 degree centigrade follows a cycling of the denaturation step (usually for 30 seconds at 95 degree centigrade), the annealing step (temperature for this stage depends on the type of primers that are used) and the elongation step (30 sec to 1 minute at 72 °C). Finally before cooling down the reaction mix, there is an additional elongation step at 72 °C for 10 minutes. All PCR reactions were performed as described above and the details of the individual PCR type has been already mentioned in the materials section.

4.1.3 Agarose-gel electrophoresis of DNA molecules

Double stranded DNA fragments with a length between 50 bp and 10kbp can be separated according to their length on an agarose gel. For this purpose a suspension of agarose (0.8-2%) in 1x TAE –buffer was cooked until the agarose was completely dissolved. After cooling to about 50 °C, 0.5 µg/ml Ethidiumbromidum was

added before the solution was poured into the gel apparatus. When the gel was solidified, the DNA mixed with loading dye was applied on the gel and electrophoresis was performed in 1X TAE buffer at 120 V for 30 min. The DNA bands then could be visualized under UV-light.

4.1.4 Isolation of RNA

RNA isolation from cells and tissue

RNA isolation from cells or tissues was performed using TRIzol Reagent (Invitrogen) according to the manufacturer's instructions. Briefly approx. 100 mg frozen tissue was homogenized in 1 ml TRIzol solution with an Ultra-Turrax (IKA) in cold environment. Phase separation was carried out by adding either 100 μ l of BCP reagent (MCP) or 200 μ l of Chloroform. Subsequently, probes were vortexed for 15 seconds, incubated at room temperature for 2 to 5 minutes and then centrifuged for 5 minutes at full speed at 4 °C. RNA contained in the upper aqueous phase was precipitated by adding 500 μ l isopropanol and centrifuged for 10 minutes at full speed at 4 °C. Pellet containing RNA was washed with 70% ethanol, air dried and dissolved in DEPC water and was stored at -80 °C.

Quantification and determination of the Quality of RNA (RNA yield)

The concentration of the isolated RNA was determined by measuring the absorbance at 260 nm (A_{260}) using a spectrophotometer. An absorbance of 1 unit at 260 nm equals 44 μ g of RNA per ml. The ratio between the absorbance values at 260 nm and 280 nm, which should be between 1.7 and 2.1, gives an estimate of the RNA purity.

4.1.5 cDNA synthesis

Total RNA obtained from eukaryotic cells or tissue, was treated with RNase-free DNaseI to remove the genomic DNA contamination from the RNA sample. For this purpose 1 μ g RNA was filled up to a volume of 9 μ l with RNase free water and 1 μ l DNaseI buffer was added to the reaction mix. After pipetting 1 μ l of DNase I to the sample, the mix was incubated for 30 minutes at 37°C. The reaction was stopped by the addition of 1 μ l of 25 mM EDTA and heated to 65 °C for 10 minutes. The first

strand synthesis was performed , using the sample directly from the DNaseI-treatment with the fermentas first strand synthesis kit and random hexamer primers as described in the instruction manual. The cDNA was used as a template for RT-PCR and qPCR respectively.

4.1.6 Real-time PCR

Depending on the cDNA quality, 0.5 to 2 μ l of cDNA obtained from cDNA-synthesis described above was used as a template for real time PCR analysis. 10 μ l of Finnzymes SYBR Green master-mix, the template cDNA, 0.5 μ M of the primers specific for the gene of interest or for the house keeping gene, respectively, and 0.4 μ l of the dye ROX as an internal control were used in a 20 μ l reaction. To calculate the relative amount of the transcript of the gene of interest , the amplification efficiency was raised to the power of the threshold cycle (Ct –value). This gives the number of cycles necessary for the product to be detectable. The resulting value was normalized to the level of the house keeping gene for all samples in the same experiment. Assays were performed in triplicates following the manufacturer's instructions in an Applied Biosystem set up.

4.2 Biochemistry methods

4.2.1 Preparation of whole protein lysates from cells and tissues

Tissues were lysed in ice-cold NP40 buffer with protease and phosphatase inhibitor cocktails (Roche) using an Ultra-Turrax (IKA) homogenizer in a cold environment. After centrifugation for 10 minutes at full speed at 4 degrees, supernatant containing proteins was transferred into a new eppendorf tube to measure the protein concentration.

4.2.2 Measurement of protein concentration

Protein concentration was measured by using the BCA protein assay kit (23225, Thermo Scientific) according to the supplier's instructions and using Bovine Serum Albumin (BSA) as standard control. 20 to 30 μ g of proteins were denatured by

mixing with 3x laemmli buffer with beta-Mercaptoethnaol and heated for 10 minutes at 95 °C. Protein lysates were stored at -20 °C prior to SDS –PAGE and immunoblot analysis.

4.2.3 SDS PAGE

SDS PAGE was carried out using the Mini-PROTEAN Tetra Cell system from Bio-Rad (Catalog number 165-8000). Glass cassettes and electrophoresis modules were assembled according to the manufacturer's instructions. A resolving gel of 8-15 % acrylamide was prepared and poured between the two glass cassettes, leaving a gap of about 1cm for accomodating the stacking gel. Isopropanol was added on top of the solution. After the gel was polymerized , isopropanol was removed off. A stacking gel of 5 % acrylamide was prepared and poured over the resolving gel. Immediately, a comb with either 10 or 15 wells was inserted and the gel was allowed to polymerize. After polymerization the comb was removed and the wells were rinsed with water. The gel was placed in the electrophoresis module and the tank was filled with 1x SDS-PAGE running buffer. Protein samples were incubated at 95 °C for 5 minutes and shortly centrifuged . Protein marker (6.5 µl /well) and protein samples (20-30 µl /well) were loaded on gel and the electrophoresis was run at 100 V by using a power pack supply (Bio-Rad) for about 1.5 hour. After electrophoresis the gel was removed from the glass cassttes and subjected to western blotting.

Resolving gel

Tris 1M pH 8.8	1.25 ml
10 % SDS.....	50 µl
10% APS.....	50 µl
30% Acrylamide/Bisacrylamide..	1.33-2.5 ml
Temed.....	3 µl
Milipore water.....	upto 5ml

Stacking gel

Tris 1M pH 6.8	0.3125 ml
10% SDS.....	25 µl
10% APS.....	25 µl
30 % Acrylamide/Bisacrylamide.....	0.425 ml

Temed.....2.5 μ l
Milipore water.....upto 2.5ml

4.2.4 Immunoblotting

After SDS –Gelelectrophoresis , the proteins were transferred by electroblotting from the gel to a nitrocellulose membrane. This was carried out using the Mini Trans-Blot Electrophoretic Transfer Cell system from BIO-RAD (Catalog no. 170-3930) according to the manufacturer’s instructions. The gel sandwich was prepared by placing the materials in the following order: Fiber pad, two to three Whattman filter paper , Gel, Nitrocellulose membrane , then two to three Whattman filter paper and finally the Fiber pad again. All were soaked and rinsed with the SD Transblot buffer while carrying out this preparation. The sandwich gel was placed in the blotting cassette and subsequently submerged in the blotting tank filled with the SD Transblot buffer with a cold pack. SDS gels were transferred at 400mA in a blotting buffer for 1 hour. After the transfer, the membrane was incubated with blocking buffer containing 5% skimmed milk in 1X NET Gelatin for 1 hour at room temperature or overnight at 4 °C. To detect the protein of interest , after blocking , the membrane was incubated with the primary antibody diluted in 1X NET Gelatin (1:50 to 1:10000 concentration, depending on the type of antibody) for 2 hours at room temperature or overnight at 4 °C. Before applying the secondary antibody , the membrane was washed at least three times for 10 minutes each with 1X NET Gelatin. The appropriate peroxide –conjugated secondary antibody was diluted in PBS (1:100 to 1:10000 depending upon the type of antibody) and incubated with the membrane for 45 minutes at room temperature. An additional washing step was performed before the membrane was incubated for 1 minute at room temperature with a 1:1 mixture of the ECL-solutions I and II. The incubation of the peroxide bound to the secondary antibody with the ECL-solutions leads to the emission of light photons , which can be detected on an X Ray film.

4.2.5 Membrane stripping

To reprobe the same nitrocellulose membrane with the bound proteins with another antibody, it is possible to remove the primary and secondary antibodies using

stripping buffer and incubating the membrane for 30 min at 54°C. Stripping was carried out by incubating the nitrocellulose membrane with stripping buffer in a shaking incubator. The membrane was then washed 3x for 10 minutes with Net Gelatin, blocked with 5% milk in Net Gelatin for 1 hour at room temperature and subsequently re-probed with other primary antibody as described before.

4.2.6 Eukaryotic cell culture technique

All handling of cell cultures was performed using a clean and sterile bench and under a laminar air flow hood. To the media used for the cell lines used, 10 % Fetal calf serum was added and 1% Penicillin/Streptomycin was used to avoid the contamination. To passage the adherent cell lines, the cells were washed with PBS, treated with Trypsin-EDTA for 3 to 5 minutes, and then splitted in the desired ratio. The cultures were kept in an incubator at 37 °C in a humidified atmosphere with 5 % CO₂. Type II cells are cultured in a special medium from clonetics® ie the BEGM medium supplemented with growth factors and other additives that includes Insulin, Hydrocortisone, Transferrin, Retinoic Acid, Epinephrine, and Triiodothyronine.

4.2.7 Freezing cell lines

By addition of an anti-freezing compound like DMSO, eukaryotic cell lines can be stored in liquid nitrogen for several years. For this purpose, the trypsinized cells were spun down in a centrifuge (1000 rpm, 5 minutes, room temperature), the pellet was washed with PBS, counted using a Neubauer chamber and diluted in ice cold medium containing 20 % FCS and 10% DMSO to obtain at least 1-2x 10⁶ cells per ml. 1 ml of this suspension was then transferred into a cryotube and stored at -80 °C for at least 24 hrs. For prolonged storage the cryotubes were then transferred to liquid nitrogen.

For reculturing of the frozen cells, the cell suspension was defrosted at 37°C and immediately put into prewarmed medium. To remove the toxic DMSO, the cells were spun down (1000 rpm, 5 min, 37°C) and the pellet was resuspended in warm medium and cultured at 37 °C as described before.

4.2.8 Analysis of cultured cells via immunocytochemistry

For immunocytochemical staining of cultured cells, the cells were grown on sterile coverslips, washed three times with PBS and fixed for 15 minutes at room temperature using 4% PFA-PBS. After fixation, the cells were washed three times for 5 minutes with PBS and permeabilized with 0.5% Triton X-100 in PBS for 15 minutes at room temperature and then washed two times with PBS. Thereafter the cells were blocked with blocking solution containing the blocking reagent (consisting of 5% donkey serum, 0.2% Triton X-100 in PBS) for 2 hours at room temperature. The primary antibody (Goat polyclonal anti DsRed, Santacruz (1:50) and Rabbit polyclonal anti-human proSpC (1:500) was diluted in the blocking solution and the cells were incubated at 4°C overnight. Next day the cells were washed three times for 5 minutes each with PBS. Secondary antibody (Donkey anti-goat Cy 5 and Donkey anti-rabbit Cy 3) was diluted (1:200) in the blocking solution and the cells were incubated for 2 hours at room temperature. After secondary antibody incubation, the cells were again washed with PBS, three times for 5 minutes each. The cells were then counterstained with DAPI diluted to 1:200 in PBS at room temperature for 15 minutes. After washing with millipore water, the cells were mounted with mowiol and stored at 4 °C until analysed under a Fluorescent Microscope.

4.3 Histological methods

4.3.1 Paraffin-embedding and sectioning of tissue

Animals were sacrificed and lungs were fixed under 25 cm water pressure with 4 % buffered paraformaldehyde and paraffin embedded. Tissue was placed in proper embedding cassettes and paraffin embedding was carried out as follow. Paraffinization requires essentially three steps: dehydration, clearing and embedding. Dehydration process was achieved by passing the tissue through a series of increasing alcohol concentrations, the detailed steps were: 1 hour in 50% ethanol, 1 hour in 70% ethanol, 1 hour in 80% ethanol, 1 hour in 90% ethanol and 2

times for 1 hour in 100% ethanol. Clearing refers to the use of an intermediate fluid that is miscible with ethanol and paraffin since these two substances are immiscible. This step was carried out by passing the tissue, twice for 30 minutes, through a 1:1 mixture of xylol and ethanol and subsequently 2 times for 30 minutes in xylol only. All these steps were performed at room temperature in an automated tissue processor (Shandon Citadel 2000). For embedding procedure the tissue was transferred into melted paraffin and incubated for 1 hour at 65°C and then in fresh paraffin for 2 hours or overnight at 65°C. Finally, the tissue was placed into an embedding mold and melted paraffin was poured into the mold to form a block. After cooling down the blocks were ready for sectioning. Tissue blocks were sectioned in 6 µm sections by using a manual rotary microtome (Leica RM2235). Embedding of mouse embryos was essentially carried out as already described except that chloroform was used instead of xylol and that the last step of paraffin incubation was prolonged to 5-7 days. Embryos tissue blocks were sectioned in 10 µm microsections.

4.3.2 Optimal cutting temperature (O.C.T.) - embedding and cryosectioning of tissue

The fresh tissue was washed with PBS and fixed in 4% PFA in PBS at 4°C overnight. After washing with PBS, the tissue was transferred into 30% sucrose in PBS and incubated at 4°C until the tissue had fallen to the bottom of the tube owing to density. Before embedding on dry ice with OCT (Tissue-Tek), the tissue was washed with PBS. The blocks were sectioned into 6-10 µm micro-sections and used for further histological analysis. The blocks and the sections were stored at -80 °C until use.

4.3.3 Haematoxylin and Eosin Staining

For histological analysis of paraffin embedded sections, the tissue was stained with H&E. As indicated in first the paraffin has to be removed from the sections, then the tissue is stained with H&E, dehydrated and mounted with Entellan.

Reagent	Incubation time
Xylol	10 minues each two times
100 % Ethanol	5 minutes each three times
70 % Ethanol	10 minutes
Millipore water	5 minutes
Hematoxylin	30 seconds
Tap water	5 minutes
Millipore water	5 minutes
Eosin	20 seconds
Millipore water	5 minutes
70 % Ethanol	10 minutes
100 % Ethanol	5 minutes each three times
Xylol	10 minutes each two times

4.3.4 Immunohistochemical stainings (Enzymatic based detection)

After deparaffinization of the slides , apart from H&E staining , the paraffin sections can be stained immunohistochemically using a specific antibody inorder to detect an antigen/protein of interest. For this purpose, an antigen retrieval step was performed using 10mM Sodium citrate buffer, pH 6.0 and cooking the tissue in the microwave for few minutes ranging from 6 minutes to 30 minutes. After cooling down at room temperature for at least 30 to 45 minutes, the sections were washed with tap water and three times for five minutes each with PBS. Before incubation with the primary antibody , the sections were blocked for few hours (from 30 minutes to 2 hours) at room temperature with the appropriate serums and Triton X-100 in PBS. The primary antibody is diluted in the blocking solution in appropriate concentrations and was incubated at 4°C overnight. Next day the sections were washed three times for five minutes each with PBS. The secondary antibody (biotynlated) was diluted 1:200 in blocking solution and the sections were incubated for 1 to 2 hours. The A+B reagent was mixed at 1:1 ratio and 30 minutes later applied on the sections for 40 minutes at

room temperature. Before that the sections has been washed again three times with PBS. After incubation, the sections were washed again three times for five minutes each with PBS and incubated with DAB (1ml DAB + 0.8ul of 30% H₂O₂, Hydrogen peroxide) until the appearance of brown colour. The reaction was stopped with tap water for 5 minutes and afterwards the tissue was counterstained shortly with hematoxylin , washed with tap water, dehydrated and mounted with Entellan. The sections were then air dried until visualized under a Bright field Microscopy system.

Antigen	Antigen retrieval	Blocking solution	Primary antibody	Secondary antibody
DsRed	Citrate buffer, 15 min.	5% Rabbit serum, 0.2% TritonX-100 in PBS	Goat polyclonal anti-DsRed Santa Cruz (1:100)	Rabbit anti goat biotinylated
Cre	Citrate buffer, 15 min.	10% Goat serum, 0.2% Tween 20 in PBS	Rabbit anti Cre Novagen (1:5000)	Goat anti rabbit biotinylated
pro SpC	Citrate buffer, 10 min.	5% Goat serum, 0.2% Triton X-100 in PBS	Rabbit anti-pro SpC Whitsett (1:5000)	Goat anti rabbit biotinylated
c-Myc	Citrate buffer, 15 min.	4% Goat serum, 0.2% Triton X-100 in PBS	Rabbit anti- c Myc (SC- 764) Santa Cruz (1:100)	Goat anti rabbit biotinylated
pERK	Citrate buffer, 10min.	5% Goat serum, 0.2% Triton X-100 in PBS	Rabbit monoclonal anti-pERK Cell signalling (1:100)	Goat anti rabbit biotinylated
C Raf	Citrate buffer, 10min.	5% Rabbit serum, 0.2% Triton X-100 in PBS	Mouse monoclonal anti-Raf 1(E 10) Santa Cruz (1:100)	Rabbit anti mouse biotinylated
Aquaporin 5	Citrate buffer, 6 min.	4% Goat serum, 0.2% Triton X-100 in PBS	Rabbit polyclonal anti-Aquaporin 5 Alomene Aqp-005 (1:1000)	Goat anti rabbit biotinylated
Ki 67	Citrate buffer, 15 min.	5% Goat serum in PBS	Mouse anti-Ki67, MM1 Vector lab (1:50)	Goat anti mouse biotinylated
PGP 9.5	Citrate buffer, 12 min.	4% Goat serum, 0.2% Triton X-100 in PBS	Rabbit anti-human PGP 9.5 Serotec (1:6000)	Goat anti rabbit biotinylated

HA Tag	Citrate buffer, 15 min.	5% Rabbit serum, 0.2% Triton X -100 in PBS	Rat monoclonal (clone 3F10) anti-HA Roche (1:500)	Rabbit anti-Rat biotinylated
TTF-1	Tris EDTA Buffer, 20 min.	5% Rabbit serum, 0.1% Triton X-100 in PBS followed by Streptavidin/Biotin Blocking	Mouse monoclonal anti-rat TTF-1 (1:100)	Goat anti mouse biotinylated
Pecam-1	Proteinase K buffer, 12 min.	2% Rabbit serum, 0.2% Triton X -100in PBS	Rat anti-Pecam 1 BD Pharmingen (1:200)	Rabbit anti-Rat biotinylated
E Cadherin	Citrate buffer, 15 min.	10% Goat serum in PBS	Rabbit polyclonal E Cadherin Cell signalling (1:500)	Goat anti rabbit biotinylated
Cytokeratin	Citrate buffer, 15 min.	5% Goat serum, 0.2% Triton X-100 in PBS	Polyclonal rabbit anti-cow Cytokeratin (1:400)	Goat anti rabbit biotinylated
Cleaved Caspase 3	Citrate buffer, 20 min.	5% Goat serum, 0.1% Tween-20	Rabbit monoclonal anti-Caspase 3 Cell Signaling (1:200)	Goat anti rabbit biotinylated
p53	Citrate buffer, 12 min.	5% Goat serum in PBS	Rabbit p53 (CM5) Vector (1:200)	Goat anti rabbit biotinylated
CCSP	Citrate buffer, 12 min.	4% Rabbit serum, 0.1% Triton X-100 in PBS	Goat anti-CCSP (sc-9773) Santa Cruz (1:2000)	Rabbit anti goat biotinylated
GATA4	Citrate buffer, 20min.	4% Rabbit serum, 0.2% Triton X-100 in PBS	Goat polyclonal GATA-4 (C-20) sc-1237 Santa Cruz (1:200)	Rabbit anti goat biotinylated

4.3.5 Alcian Blue Staining

Reagents needed

3% Acetic acid solution	Alcian blue solution, pH 2.5
Acetic acid, 3 ml	Alcian blue, 8GX, 1gram
Distilled water, 97 ml	Acetic acid, 3 % solution, 100 ml

Mix well and adjust the pH to 2.5 using Acetic acid.

0.1% Nuclear Fast Red solution
Nuclear Fast , 0.1gram
Aluminium sulphate, 5 gram
Distilled water, 100 ml

Dissolve aluminium sulphate in water. Add Nuclear Fast Red and slowly heat to boil and then cool. Filter Alcian blue and Nuclear Fast Red before use.

Procedure:

Deparaffinization of the section was carried out like other staining procedures. The slides were then kept in millipore water. The slides were then incubated with Alcian Blue 2.5 solution for 30 minutes at room temperature. After that the slides were washed under tap water to get rid of the excess stain. The slides were then incubated with Nuclear Fast Red solution for 3 to 5 minutes. Again they were rinsed under tap water, subsequently dehydrated with a graded series of alcohols and xylol and then finally mounted with Entellan.

4.3.6 Immunofluorescence stainings

Antigen/Staining type	Blocking solution	Primary antibody	Secondary antibody
DsRed	5% donkey serum, 0.1% Triton X-100 in PBS	Rabbit polyclonal anti DsRed, Clonotech, 1:500	Donkey anti Rabbit Cy5
DsRed/SpC	5% donkey serum, 0.2% Triton-X 100 in PBS	Goat polyclonal anti-DsRed, Santa Cruz (1:50) Rabbit polyclonal anti human-Pro SpC (1:500)	Donkey anti goat Cy5 Donkey anti rabbit Cy3
CCSP/DsRed	4% donkey serum, 0.1% Triton X-100 in PBS	Rabbit polyclonal anti DsRed, Clonotech, 1:500 goat polyclonal CC10 (S-20), Santa Cruz (1:500)	Donkey anti rabbit Cy3 Donkey anti goat Cy5
SpC/CCSP	4% donkey serum, 0.2% Triton X-100 in PBS	Rabbit anti-pro SpC , Whitsett(1:4000) goat polyclonal CC10 (S-20), Santa Cruz (1:2000)	Donkey anti rabbit Cy3 Donkey anti goat Cy5

4.3.7 X Gal staining on frozen sections

Reagents

1. Fixation solution

0.5% Glutaraldehyde

100mM EGTA , pH7.3

1 M MgCl₂

0.1M Sodium Phosphate buffer, pH 7.3

2. Wash Buffer

1M MgCl₂

1% Deoxycholate

2% NP40

0.1M Sodium Phosphate buffer, pH 7.3

3.X Gal staining solution (to be freshly prepared and stored in dark)

X Gal stock @ 1mg/ml

Potassium Ferrocyanide

Potassium Ferricyanide

Wash buffer

Procedure:

Air dry the frozen tissue section for about 30 minutes at room temperature. Incubate the slides with the fixative solution for 15 to 20 minutes in 4°C. Wash three times for five minutes each with the wash buffer. Incubate the slides in the staining solution at 37°C /humidified chamber in dark for as long as 4 to 18 hours. Observe the appearance of blue colour in the tissue sections. Subsequently wash the sections three times with wash buffer. Counter-stain with Nuclear Fast Red staining solution for 30 seconds. Rinse with tap water to get rid off the excess stain. Dehydrate in a graded series of alcohol and then Xylol. Mount the sections with Entellan and store the sections at 4 °C for better retention of the signal.

4.3.8 X Gal staining of FACS sorted DsRed cells

The left over cells obtained after sorting for DsRed were stained with X Gal to detect the presence of the Lac Z transgene. The cells were cultured on a coverslip. Media was removed and the cells were gently washed with sterile PBS. The cells were then incubated with fixative solution for 10 minutes at 4 °C. After fixation the cells were rinsed gently with wash buffer. Subsequently the cells were incubated with the X Gal staining solution at 37 °C in a humidified chamber in dark for about 4 hours to 18 hours. Later the cells were washed with wash buffer for 10 minutes at room temperature , and then the coverslips were removed from the cell culture plate and were mounted with Entellan and stored at 4 °C.

4.3.9 X-Gal : Whole mount tissue preparation

Reagents required:

1.FIX Solution (for 50 ml)

25% Glutaraldehyde.....0.4 ml

100 mM EGTA, pH 7.3.....2.5ml

1M MgCl₂.....01ml
 0.1 M Sodium Phosphate buffer, pH 7.3.....47 ml

2.Wash buffer (for 200 ml)

1 M MgCl₂.....0.4 ml
 1%Deoxycholate.....2ml
 2%Nonidet-P 40.....2ml
 0.1 M Sodium Phosphate buffer, pH 7.3.....195.6ml

3.X Gal staining solution (for 50 ml)

Potassium ferrocyanide.....0.016g
 Potassium ferricyanide.....0.082 g
 Wash buffer.....48ml
 X Gal @ 1mg/ml.....1.25 ml from a stock of 40mg/ml

Prepare a 40 mg/ml X-gal (5-bromo-4-chloro-3-indolyl- β -galactosidase stock in dimethylformamide. Dispense into 5-ml aliquots, and store at -20 °C.

Procedure

The organs were dissected and fixed in the fixative solution for 1 hour at 4 °C. After fixation, they were rinsed three times with the wash buffer by gentle shaking. Then the organs were incubated overnight with the X Gal staining solution at 37 °C in dark. Next day they were again post fixed with 4%PFA for 1 hour in dark. Subsequently tissues were washed with PBS, three times for 5 minutes each, transferred to 70 % Ethanol at 4 °C, and finally subjected to normal paraffin embedding procedures.

4.3.10 FACS sorting of DsRed cells from triple transgenic reporter mice

Procedure:

Anesthetize the mice with Ketamin/Rompun formulation. The mice were sprayed with 70% alcohol. An incision was made over the rib cage. After that 10 ml of cold saline solution was injected through the right ventricle until the lungs were cleared off from blood. The trachea was exposed using a forcep placing beneath it. Tip of the needle was inserted, all the way into the trachea and was tied securely with a thread to keep the trachea and the needle intact in the right position. 5 ml of Dispase

was injected via the trachea followed by warm 1% LMP Agarose (approx. 0.5 to 1 ml). The animal was immediately covered with ice for 2 minutes to let the agarose harden. The lung was dissected out and placed in a 50 ml falcom tube containing 6 ml of PBS (sterile cell culture grade) in cold. Enzymatic digestion of the lung was carried out by the addition of collagenase/dispase, agitated for 45 minutes at 37 °C on a shaker. After the incubation, the lung was squeezed gently like a tea bag using a forcep until it was turned into a mass of suspension, leaving behind only connective tissue. At this stage, DNase I was added. The digested tissue was placed on ice for 5 minutes. Subsequently the digested tissue suspension was filtered through 100 µm and then via 40 µm cell strainer to obtain a clear single cell suspension. The suspension was collected in a 50 ml falcom tube, centrifuged at 800 rpm for 8 minutes in 4°C. A soft pellet was obtained. The supernatant was discarded. The pellet was resuspended in 2 ml of FACS buffer and was proceeded for FACS sorting (DsRed sorting was carried out in FLH-2 channel of the BD FACS, caliber). The sorted cells were collected in a special BEGM medium and cultured on matrigel coated plates.

4.4 Animal Experiments

4.4.1 Generation of reporter transgenic mouse lines for lineage tracing experiments

To begin with the experiments; required the generation of transgenic mice with the reporter line (DsRed). This was carried out by breeding of single transgenic mice with several others in combination to obtain the final mice which can be utilized for the preliminary and future experiments. The details of the mating schemes has been described in the results section (5.1.2).

4.4.2 Breeding of mice

Mating was started when female and male mice were at least 4 and 6 weeks old, respectively. Often two females were bred together with one male. Matings were stopped by separating the males from the pregnant female after approx. 2 weeks. New born pups were weaned from the mother at the age of 3 to 4 weeks. At this

point of separation, individual mouse was marked by an earmark (clip) and a tail biopsy was taken for genotyping.

Animals

All animal experiments were performed according to the regulations of the Bavarian State authorities. Mice were maintained as a specific pathogen-free in-house colony. Mice were allowed food and water *ad libitum* and maintained on a 12-hour/day light/dark cycle. Animals used in this study were from two to 24 months old. Animals were sacrificed via cervical dislocation unless described differently.

Mice harboring the Lac Z floxed -DsRed recombination substrate (RS) transgene on a C57BL/6J background were purchased from The Jackson Laboratory and maintained by mating hemizygous individuals. Transgene positive mice were identified by PCR analysis of tail DNA using primers specific for the *LacZ* and the DsRed coding sequences. Bitransgenic SpCrtTA/ Tet O Cre mice were generated by breeding homozygous or hemizygous SpC rtTA with the Tet O Cre founder lines. Triple transgenic SpC rtTA/Tet O Cre/DsRed mice were generated by breeding hemizygous DsRed reporter transgenic mice with hemizygous bitransgenic SpCrtTA/Tet O Cre mice and the progeny were genotyped for the presence of individual transgenes. The details of the compound reporter transgenic animals generated are described in the results section.

4.4.3 Genotyping of transgenic mice

For obtaining DNA for genotyping, the mouse tails were cut (less than 1 cm) during the age of 3 to 4 weeks and the mice were marked by earclips. The tails were lysed by the addition of 190 μ l of tail lysis buffer and 12 μ l of 0.4 mg/ml Proteinase K and incubated overnight at 54 °C. The resulting lysate was then centrifuged at 10000 rpm for 15 minutes and the resulting supernatant was diluted 1:10 or 1:40 with distilled/autoclaved water. This was used as a template for a PCR reaction as described above with primers for genotyping in the material section. In some cases a preliminary step of DNA isolation followed by PCR detection was necessary. DNA isolation was carried out by adding to tail lysates 250 μ l lysis buffer and 250 μ l of saturated NaCl (approx. 5 M NaCl). The mixture was mixed by inversion approx. 10

times, incubated for 5 minutes at room temperature and centrifuged at full speed for 10 minutes. The supernatant was transferred into new 1.5 ml tube and DNA was precipitated by adding 600 μ l of Isopropanol. The sample was thoroughly mixed by inverting the tube several times, then incubated for 5 minutes at room temperature and centrifuged at full speed for 10 minutes. Supernatant was discarded and the pellet containing DNA was washed by adding 1 ml of 100% ethanol and centrifugation at full speed for 5 minutes. Finally, the pellet was air-dried for 10-15 minutes at room temperature and resuspended with 50 -100 μ l of sterile water. This DNA solution was diluted 1:10 or 1:40 with sterile water and used as a template for PCR reaction as described in materials section using the genotyping primers reported in section (3.1.6).

4.4.4 Sacrification of mice

Mice were euthanized with a lethal intraperitoneal injection of Ketamin and Rompun in 0.9% NaCl. After the loss of righting reflex, mice were perfused by intra-cardiac injection of PBS into the left ventricle of the beating heart to get rid off the excess blood, and the organs were then dissected out. For isolation of organs for RNA and protein purposes, the animals were not perfused and the organs were directly removed out and were immediately snap frozen in liquid nitrogen and stored at -80 °C until use.

4.4.5 Transplantation – experiments

For subcutaneous injection of the DsRed tumor cells, the cells were washed two times with sterile PBS after trypsinization and were counted. 10^6 cells were subcutaneously injected in 100 μ l of sterile Matrigel solution into Rag^{-/-} mice. The appearance of tumor and tumor size was measured weekly and the animals were sacrificed when the first tumors in the different groups were close to 2 cm of diameter. Under anaesthetic conditions the animals were perfused using 4 % PFA – PBS and the primary tumors, lungs, livers and lymph nodes were collected for histology.

4.5 Statistical Analysis

Statistical analysis of data sets were performed using the Graphpad Prism version 4.0 software. Differences among the groups were compared with Students's t test. Results are presented as means +/- SE. All P values were two tailed. For all test, the statistical significance was considered to be at $P < 0.005$. Survival graphs were generated by Kaplan-Meier method. The statistical significance between proportions was determined by the log rank test.

5 Results

5.1 Transgenic reporter mice for lineage labeling studies in a murine NSCLC model

The ability to introduce lineage tags within selective progenitor cell populations *in vivo* provides tools to unambiguously define the contribution that differential progenitor cell utilization makes toward altered epithelial cell function and its involvement in malignant progression. Towards this context, the goal of this project was to select a suitable tag that can be monitored easily in live cells, in tissues and which can be exploited for imaging purpose. Once such tag was confirmed for its feasible detection, we can utilize it for the generation of transgenic compound reporter mice for lineage tracing studies. For this purpose several reporter mice were tested for the suitability in the detection of the reporter molecule in the organs of the transgenic mice (data not shown). The preliminary results strongly indicated that DsRed would be the best choice to label cells, since it displays no signs of auto-fluorescence in the tissues observed and can be exploited for imaging studies. Hence, LacZ/DsRed reporter mice were decided to be utilized for all our future experiments.

5.1.1 The Red Fluorescent protein (RFP) mice

The Lac Z/Red transgenic mice express beta-galactosidase (*lacZ*) under the control of the chicken beta actin promoter coupled with the cytomegalovirus (CMV) immediate early enhancer. When crossed with a Cre recombinase-expressing strain, *lacZ* expression is replaced with red fluorescent protein (DsRed*MST) expression in tissues expressing Cre recombinase.

5.1.2 Generation of compound transgenic reporter mice for lineage tracing experiments

Once the reporter mice are validated; next begins the generation of compound transgenic mice with a combination of oncogenes under a DsRed reporter background for lineage tracing studies.

For lineage tracing of mouse alveolar type II cells we chose to use the Cre-loxP system, which is an effective method for expressing or deleting a target gene in Cre-expressing cells. We introduced a mouse line in which a 37 kb human Surfactant Protein C (SpC) promoter drives the expression of Cre. We used this allele, in combination with the *lacZ/DsRed reporter*, to lineage trace type II cells in adult mice. With this strategy, we generated a series of compound mouse lines expressing Cre recombinase from specific lung alveolar epithelial type II cell promoter, SpC in combination with an inducible form of oncogenic C RAF (Tet O C RAF BXB) and a mouse line where SpC drives the expression of c Myc (Fig 8.1 and Fig 8.2).

Beginning from one single transgenic mouse, via successive and continuous rounds of multiple breeding schemes, we were successful in obtaining more than 100 compound reporter animals for our experiments in a span of 1 year. Once the compound animals were ready, Doxycycline was administered orally via food; (occasionally with water when the animals were being transported in a different animal facility) and targeted cells were identified by a series of experimental procedures that will be described in the following pages.

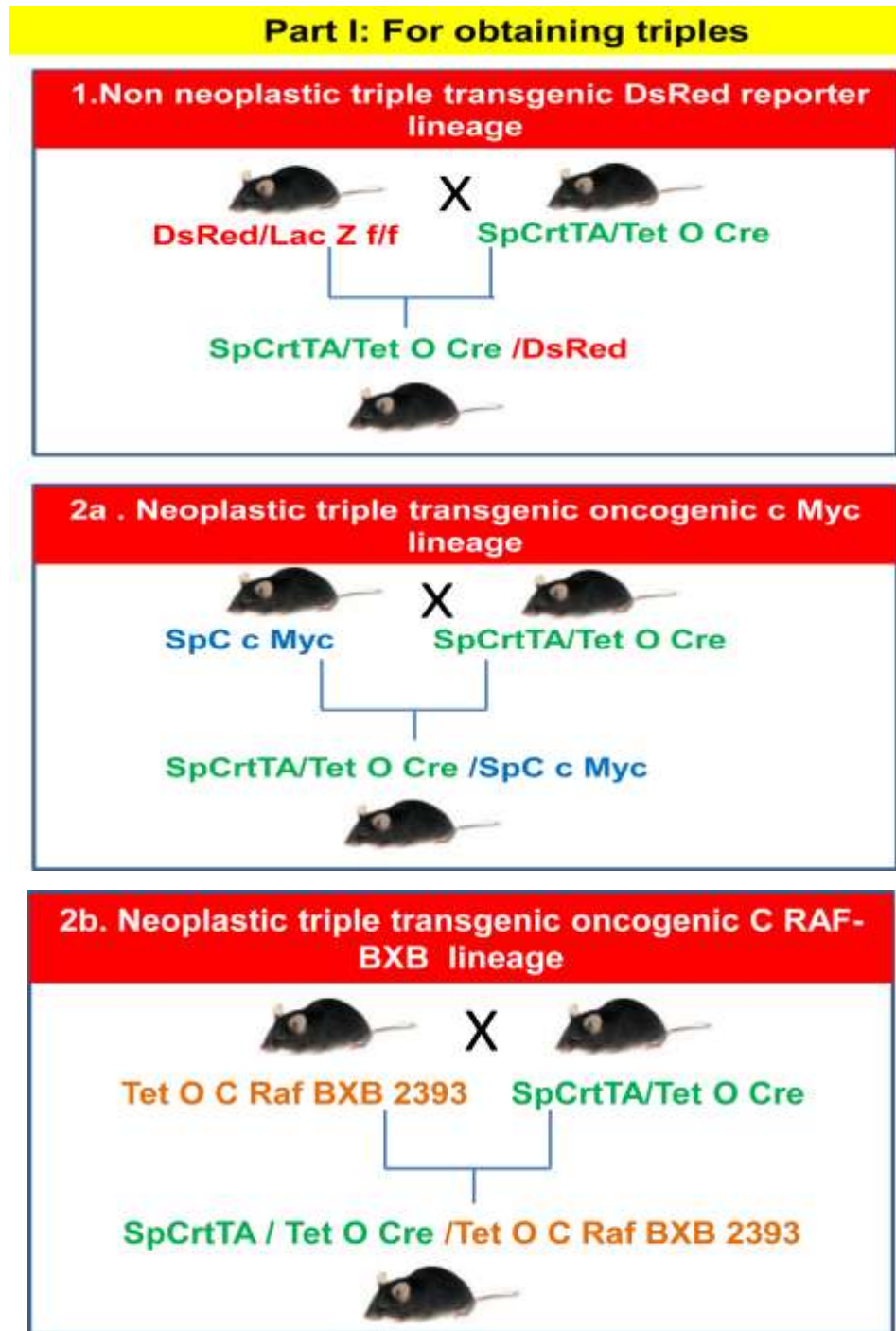


Fig 8.1 Mating scheme of the transgenic animals to obtain the basic lineage of compound mice with an integration of the reporter gene (1) and the oncogenes that includes c Myc (2a) and an inducible C RAF BXB (2b). The resulting progeny obtained is the triple transgenic compound mice that have a common backbone of the promoter/transactivator elements (SpC rtTA/Tet O Cre).

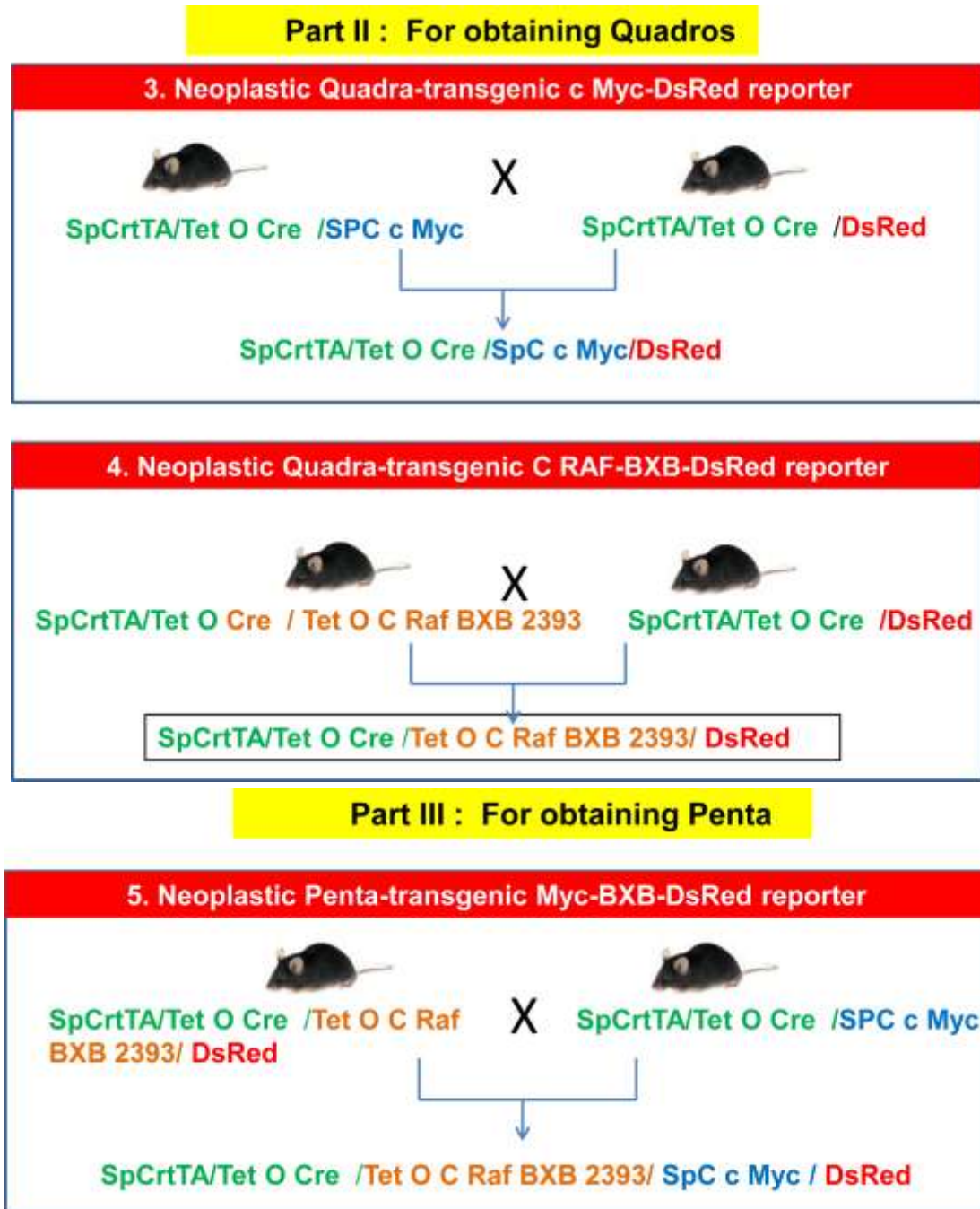


Fig 8.2 Mating schemes of the triple transgenic reporter mice to obtain a quadra transgenic reporter mice incorporating c Myc (3) and Tet O C RAF BXB (4). A final breeding was performed to obtain penta transgenic reporter mice with the intergration of both the oncogenes c Myc and Tet O C RAF BXB with a reporter line of DsRed (5).

In the present study, we utilized transgenic mice in which the human SpC gene promoter is used to express the reverse tetracycline transactivator (rtTA) thus

placing the expression of Cre-recombinase (CRE) under conditional control of doxycycline. Expression of Cre was used to permanently label cells with Red fluorescent protein (DsRed) in subsets of respiratory epithelial cells in the conducting airways. Distinct lines of transgenic mice that expresses rtTA under the control of the human SpC gene promoter were bred to Tet O Cre mice and reporter mice (LacZ/DsRed) creating triple transgenic mice as SpCrtTA/Tet O Cre /DsRed (here in designated as DsRed) in which respiratory alveolar epithelial cells permanently expressed DsRed after doxycycline induced recombination (Fig 9.1 and 9.2). Once we obtained triple transgenic reporter mice, multiple rounds of successive breeding with the oncogenic mice gave rise to Quadra as SpCrtTA/Tet O Cre /SpC c Myc/ DsRed (Fig 8.2-3 here in designated as Myc-DsRed) and SpCrtTA/Tet O Cre /Tet O C RAF BXB/ DsRed (Fig 8.2-4 here in designated as C RAF BXB-DsRed) and penta transgenic as SpCrtTA/Tet O Cre /Tet O C RAF BXB/SpC c Myc/ DsRed (Fig 8.2-5 (here in designated as Myc-BXB-DsRed) were obtained.

5.1.3 Testing of the compound reporter transgenic mice generated for the expression of the reporter gene

To validate the specificity of our targeting strategy; we first began to analyze the triple transgenic reporter mice i.e. DsRed. Adult mice lungs were harvested 2 weeks following Dox induction and were processed for paraffin embedding and Cryo fixation. Sections of lung tissue were stained for X Gal and DsRed was visualized via immunohistochemical and Immunofluorescence staining procedures.

5.1.3.1 Lung targeted expression of the reporter gene in the DsRed mice.

A Lac Z and DsRed expression in the lung

Lungs from the DsRed mice were analysed for the expression of the reporter molecules that includes lac Z and DsRed. The X gal staining revealed the presence of Lac Z +ve cells in the bronchiolar region of the lung (where Clara cells are predominant) including areas that were devoid of type II cells. Whereas the lung section from the whole mount tissue processed for Lac Z activity, displayed those regions which were negative for the blue colour (Lac Z) in the form of a pink colour stain due to Nuclear fast Red stain. Rest region of the lung parenchyma is

completely blue (Fig 9.1). Subsequently, DsRed staining was performed on an X Gal whole mount lung section. The lac Z negative cells are indeed DsRed cells as depicted from the staining results (Fig 9.1 lower panels). Histochemical detection for the DsRed was carried using an anti-DsRed antibody via standard immunohistochemical and Immunofluorescence staining procedures as described in the methods section. Lungs were harvested, processed for paraffin and cryo embedding; sections were stained and were visualized using bright field and fluorescent microscope. DsRed staining on frozen sections revealed many distinct cells positive for DsRed (Fig 9.2) whereas staining on a paraffin-embedded section also displayed the same pattern of DsRed expression, which morphologically resembles a type II cell. DsRed was exclusively observed in cells lining the alveolar epithelium (Fig 9.2).

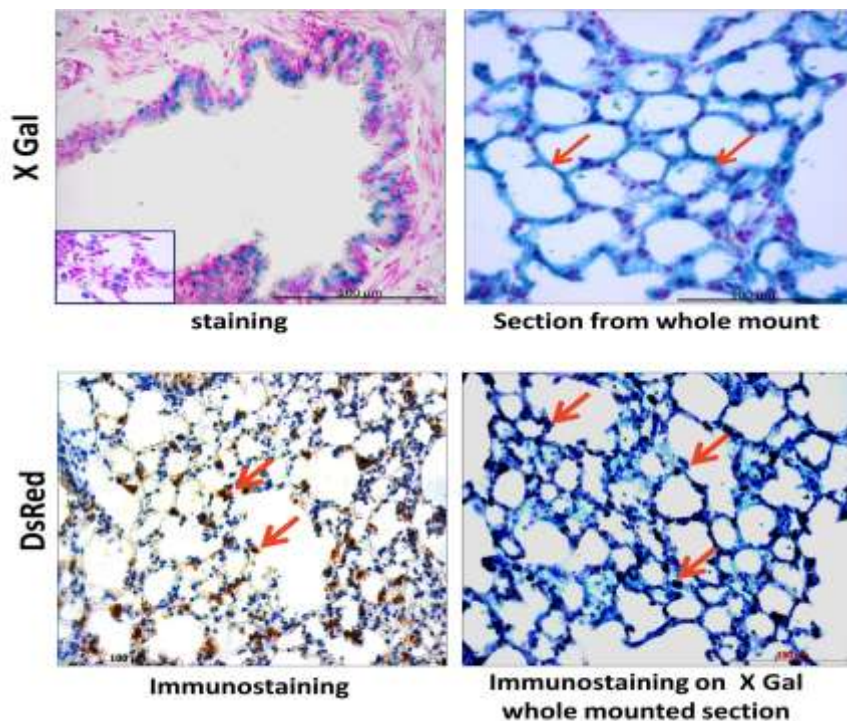


Fig 9.1 Lung targeted expression of the reporter gene (DsRed and Lac Z). X gal staining on frozen lung sections shows the bronchiolar Clara cells positive for Lac Z (in blue). Lung section derived from a whole mount tissue for X Gal shows the region that express lac Z (in blue colour; arrows indicated) and the cells negative for the lac Z expression (in pink). DsRed immunostaining depicts the DsRed positive cells (in arrows) in the alveolar distribution pattern. DsRed immunostaining on the X Gal mounted lung sections shows DsRed positive cells (in brown) on a lac Z background (in blue). Scale bar = 100 μ m

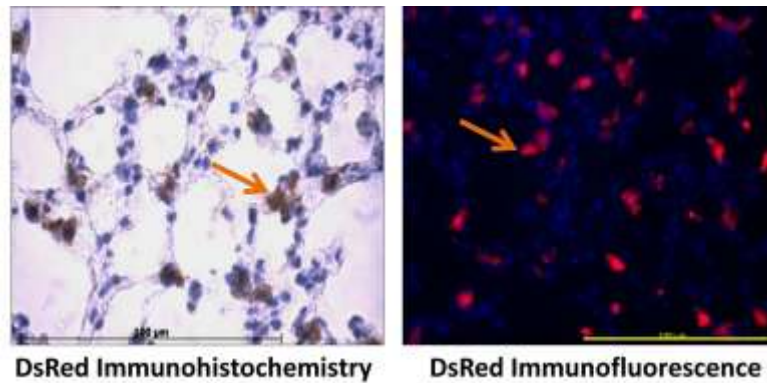


Fig 9.2 DsRed expression in lungs of the induced DsRed transgenic mice. Formalin fixed lung sections depicting DsRed cells (brown). Frozen lung section depicting DsRed cells (red). Scale bar = 100 μ m

B DsRed and Lac Z co-immunofluorescence staining of the lung

With the findings that many lineage tagged cells (DsRed +ve) were detected in the alveolar epithelium, there comes another interesting aspect of our labeling pattern. We were not able to detect any DsRed +ve cells in the bronchioles (Fig 9.3 A). This suggests that we are specifically able to mark only type II cells whereas the Clara cells are rendered negative for the lineage tag. Double immunofluorescence staining on the cryo-embedded lung sections with an antibody for beta Galactosidase and DsRed , revealed that those cells which are positive for DsRed showed the absence of Lac Z and vice versa (Fig 9.3 B).

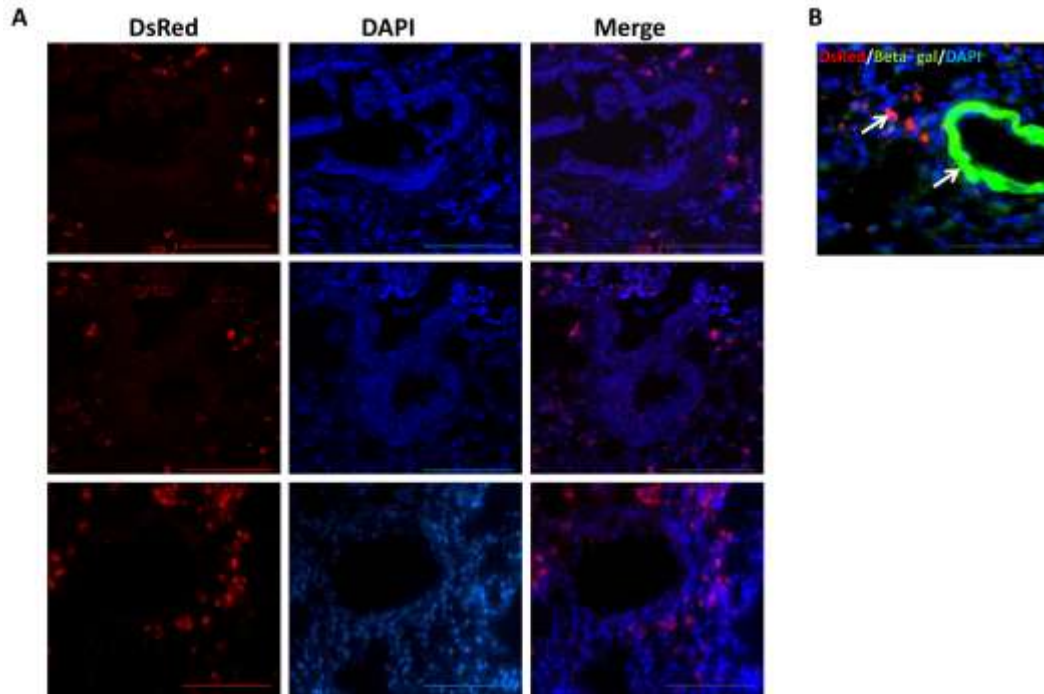


Fig 9.3 Reporter gene is expressed in the type II cell specific fashion. Representative immunofluorescence staining images for DsRed (A) and DsRed/ β -gal (B) on cryoembedded lung section from a non neo-plastic DsRed mouse shows the region displaying the bronchiolar epithelium. Note that the Clara cells in the bronchioles are negative for the DsRed expression (A) whereas expressed lac Z in the same (B). Scale bar = 100 μ m

C Alveolar type II cells are selectively targeted by cell type-restricted Cre

To confirm that the SpCrtTA/Tet O Cre/DsRed - switched cells are in fact type II cells, it becomes important to analyze for the Cre expression via induction. In addition, to be sure that the cells that we are targeting are type II, one has to evaluate the expression of SpC, a potent marker for type II cells of the lung. Lungs from induced and non-induced triple transgenic mice were viewed unstained for the detection of any DsRed positive cells, under a confocal laser-scanning microscope. As expected, the induced mice displayed many DsRed positive cells whereas the uninduced ones lacked the expression (Fig 10.1). This suggests that the Cre is not leaky in our transgenic system.

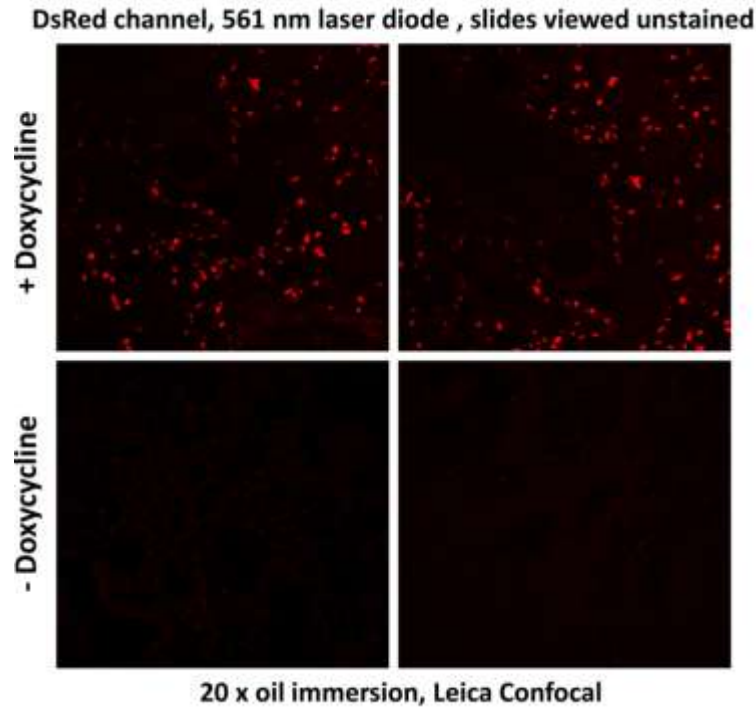


Fig 10.1 Unstained lung sections from the DsRed mice viewed under the RFP channel. The induced mice showed many DsRed +ve cell whereas the uninduced one lacks the expression.

Furthermore to find out the tissue specificity for the expression of lineage marker; protein lysates from the different organs (Kidney, brain and liver) of the induced animals were analysed for the DsRed expression. As shown in the immunoblot, DsRed is expressed only in the lung whereas the rest organs were found to be negative for the expression (Fig 10.2). This data suggest that with our labeling strategy, we were able to target the pulmonary cells only, which says that the labeling system is tightly regulated.

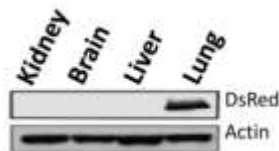


Fig 10.2 Lung targeted expression of the DsRed reporter. Immunoblot for DsRed protein expression in the tissue obtained from the induced DsRed mice

D SpC and DsRed co-localization in the lung

To further confirm that the SpC rtTA/Tet O Cre/DsRed switched cells are alveolar type II cells, we stained 10 mm thick cryosections with an anti-DsRed and a proSpC antibody. As expected, DsRed cells colocalized with SpC+ve cells in the airway epithelium (Fig 10.3 C). The same sections were stained with pro SpC, DsRed and with an anti-Cre antibody individually. The lung displayed abundant SpC (Fig 10.3 A), and Cre (Fig 10.3 B) in almost similar fashion. Taken together these results confirm that Cre-mediated recombination is confined to a specific cell population as dictated by the promoter utilized.

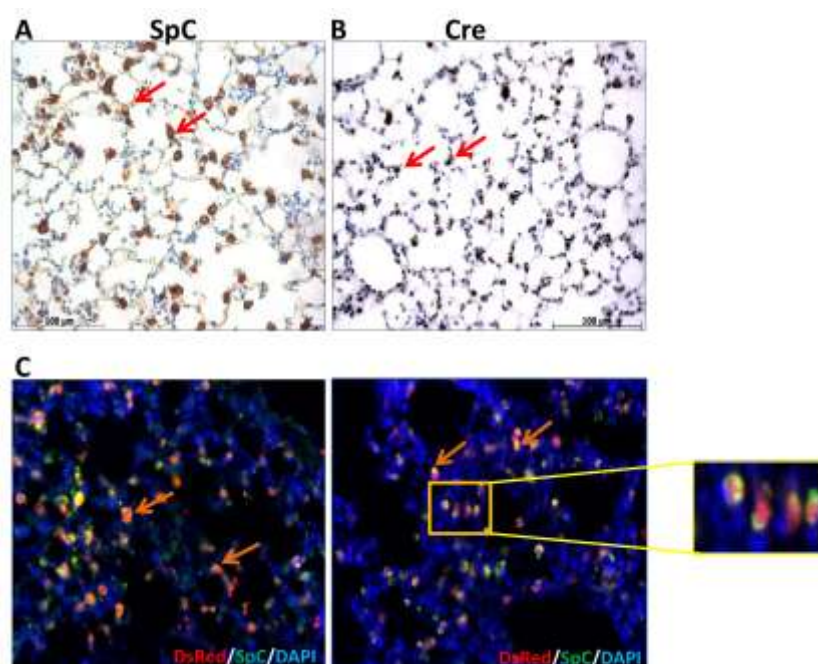


Fig 10.3 DsRed reporter gene is expressed in the alveolar type II cell compartment. Immunostaining for (A) SpC and (B) Cre on paraffin embedded lung sections. Double immunofluorescence staining for SpC and DsRed on cryo embedded lung sections display the colocalization of SpC cells with DsRed. Inset shows it in high magnification. Scale bar = 100 μ m

5.1.3.2 FACS sorted DsRed cells cultured on matrigel

One of the advantages of lineage tagging is that it provides an opportunity to obtain a purified population of cell enriched with the reporter tag. The cells obtained can be processed for vital experiments which can decipher their properties in detail, multilineage differentiation potential and transplantation experiments. Flow cytometry

has allowed to obtain pure cells based on the marker that is expressed by the desired cell of interest. Utilizing this strategy, we have sorted type II cells based on DsRed expression in the FLH 2 channel of the BD FACS Calibur. Lungs from the non-neoplastic DsRed mice were dissected, enzymatically digested and filtered to obtain a single cell suspension that was subjected for sorting via FACS.

The DsRed+ve cells were cultured on a matrigel layer in a special BEGM medium. The cells appeared round in shape and were always found to retain the lineage marker, DsRed (Fig 11.1 A).

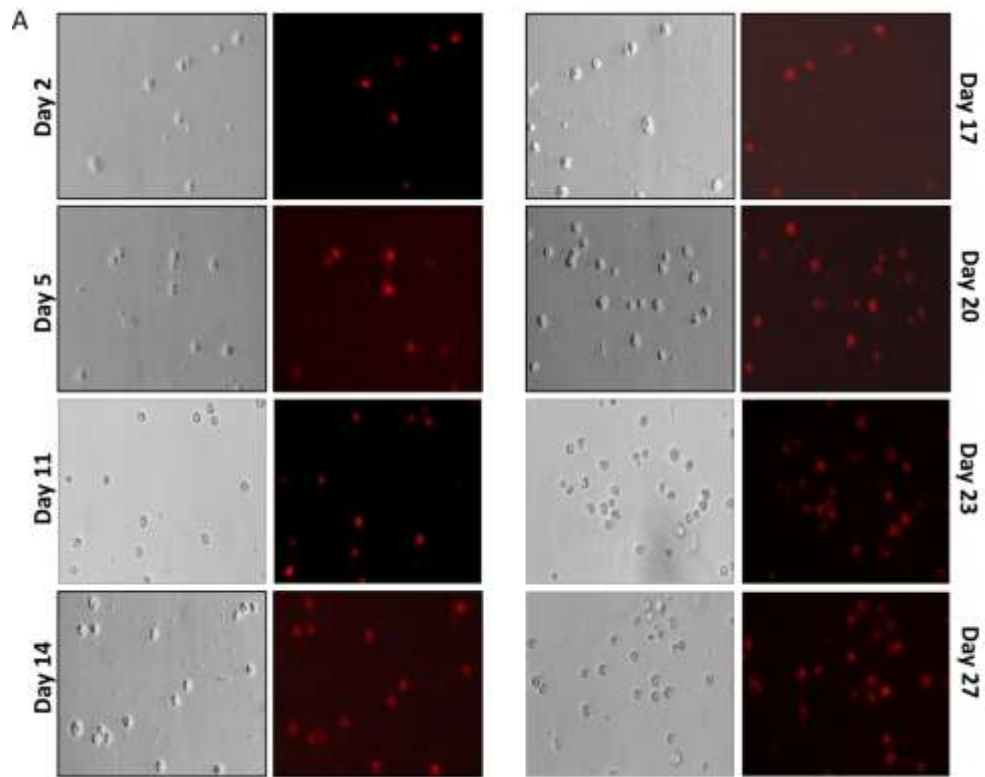


Fig 11.1 (A) DsRed sorted cells from induced DsRed mice; cultured on matrigel.

The DsRed-ve population obtained was also cultured under similar conditions. Initially they appeared round, but within one week, gained fibroblast like structures. They did not show any DsRed expression when observed under the RFP channel (Fig 11.2 B); but were stained positive for the Lac Z via an X Gal staining (Fig 11.2 C). Finally, to make sure that the cells that we sorted were from alveolar type II lineage, cultured cells were cytopspined and double immunofluorescence staining

was performed using a pro SpC and a DsRed antibody. The cells were found to be positive for both SpC and DsRed marker and visualized under high magnification confocal microscope (Fig 11.2 D)

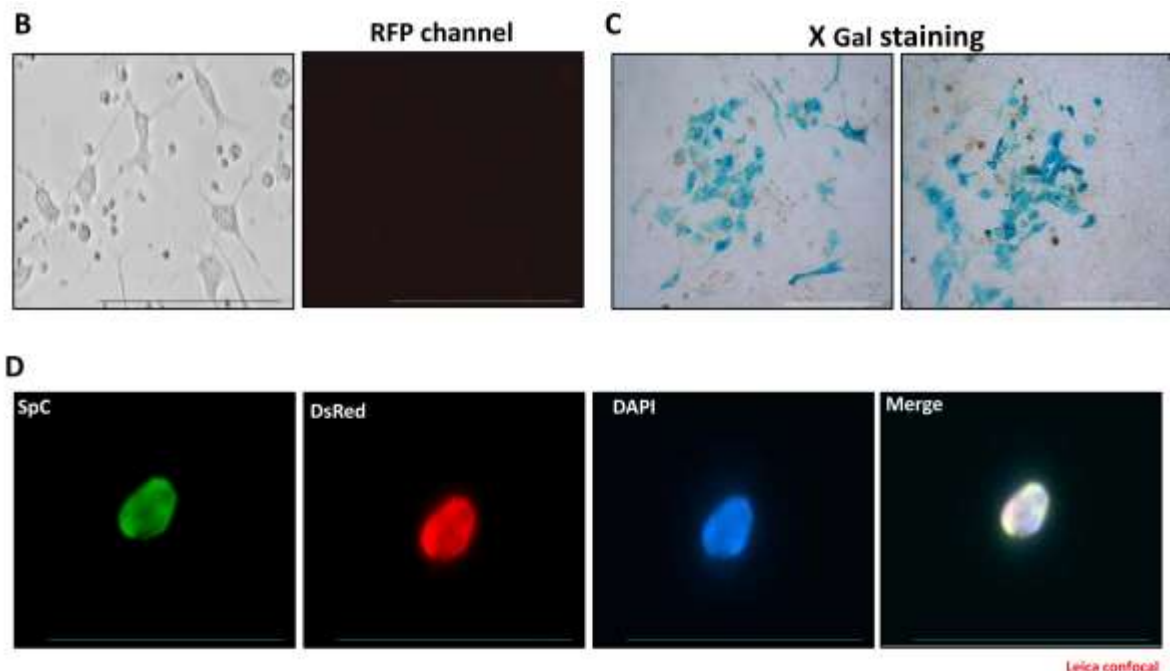


Fig 11.2 DsRed negative sorted population of cells from induced DsRed mice are negative for the DsRed expression (B) and are stained positive for the lac Z expression (C). Co-immunofluorescence staining of the DsRed sorted cells with SpC and DsRed antibodies shows the co-localization of the indicated markers (D). Scale bar = 100 μ m

Thus validating with a series of immunohistochemical staining, cell sorting and culturing the lineage tagged cells; we confirm that the strategy applied for lineage tracing by restricted Cre expression is technically sound which can be used to address the lineage specific and cell of origin in murine lung cancer (NSCLC) thereby elucidating the identity of putative cells contributing towards metastasis in our murine NSCLC model.

5.1.4 Labeling tumor cells induced by oncogenic C RAF

Once we were able to genetically tag the type II cells with DsRed in non-neoplastic cells, the next goal was to label the tumor cells with the lineage tag. For this purpose, Quadra C RAF BXB-DsRed transgenic reporter mice were generated. The cell of origin of lung adenocarcinomas remains unknown, and candidates include

multipotent stem cells, Clara cells, and alveolar type II cells (Dermer, 1982). Oral administration of Doxycycline induces the expression of Cre that rapidly mediates excision of the transcriptional roadblock by catalyzing recombination across the flanking *LoxP* sites. With induction there occurs the expression of both the C RAF BXB oncogene and at the same time deletion of the stop cassette (*lac Z*) in front of the *DsRed* allele. The *DsRed* reporter gene is thereby activated in the SpC positive cells and subsequently transmitted to their progeny as they repopulate the tissue during normal homeostasis and in tumor formation.

5.1.4.1 Lung tumor formation in C RAF BXB-DsRed induced mice exhibiting cuboidal tumor cell phenotype

Quadra compound reporter animals were under doxycycline induction which gave rise to tumor nodules in the lung (Fig 12.1 A). Histological examination of the tumor nodules displayed the cellular structure of the tumor. The cuboidal shaped cells comprised the tumor mass as depicted by an H&E staining (Fig 12.1B).

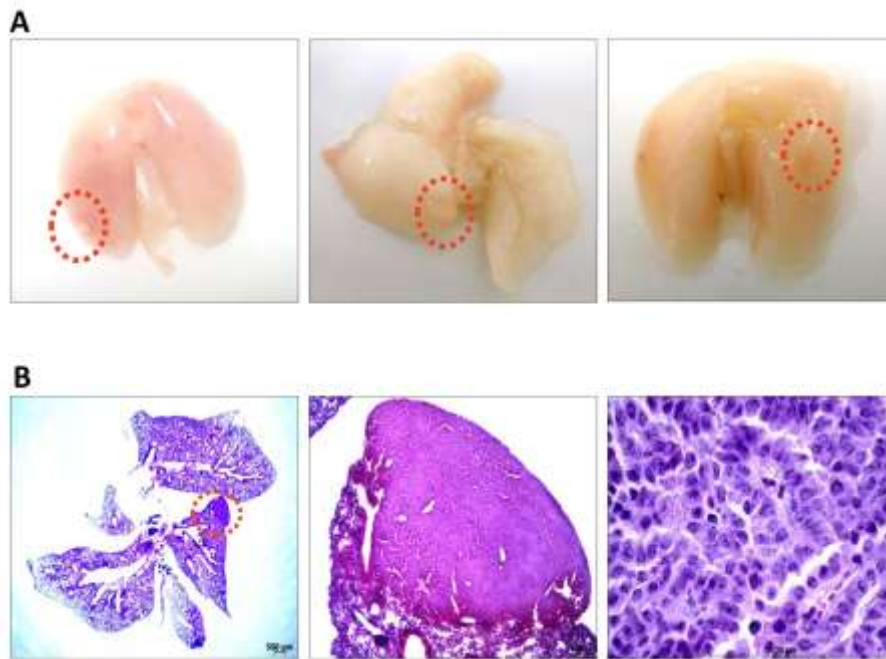


Fig 12.1 Lung tumor formation in C RAF BXB-DsRed transgenic mice. (A) Whole lung photographs of 9 to 12 months induced transgenic mice shows visible adenomas (in red circles). (B) Paraffin embedded H&E stained lung sections shows a tumor (in red circle, scale bar = 500 μ m). A closer view of the adenoma shows the presence of cuboidal shaped tumor cells. Scale bar = 100 μ m

5.1.4.2 Evaluation of the tumor for the expression of the lineage marker and the transgene

Histological sections of the tumor bearing lungs were processed for immuno-staining to find out whether we were able to mark the tumor cells with the lineage tag of DsRed. The tumor cells were composed of type II cells as evident by the expression of SpC (Fig 12.2). The consecutive tumor sections were then stained for Ha tag, which serves as a read out for the Tet O C RAF BXB transgene. Lastly, the sections were stained for DsRed. To our surprise, all the cells comprising the tumor were found to be positive for DsRed (Fig 12.2). These results indicate that these tumor have been initiated by a population of cell type that expresses SpC and thus has an alveolar type II phenotype.

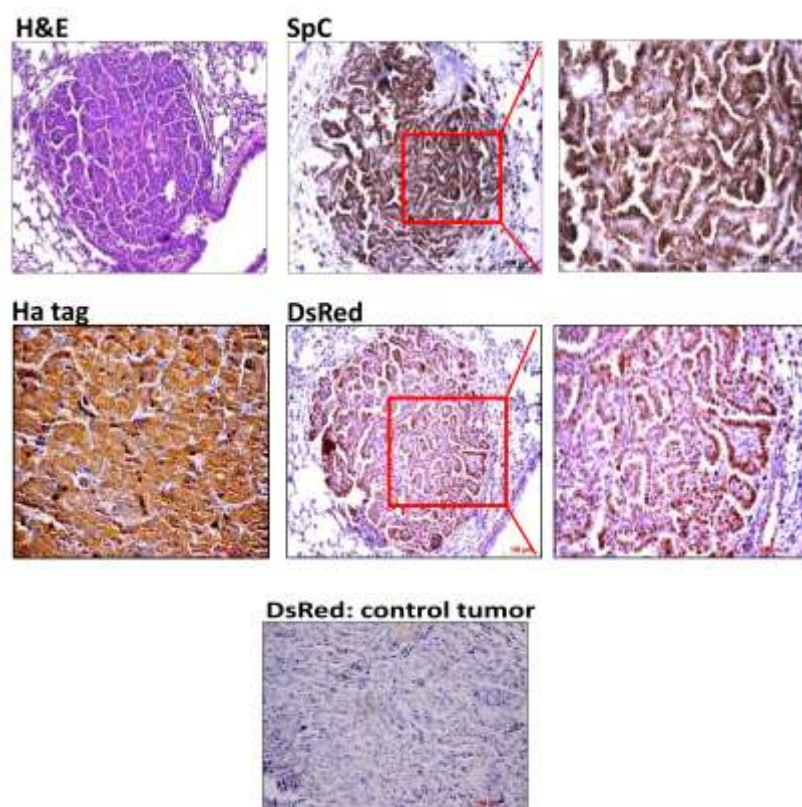


Fig 12.2 Lung tumor generated from C RAF BXB-DsRed transgenic mice (9 month) are labeled with the lineage marker DsRed and are positive for the alveolar type II cell marker, SpC and the tumor driving transgene Ha tag, which is a read out for the Tet O C RAF BXB expression. Paraffin embedded lung sections were immunostained for the indicated markers. Tumor stained with DsRed, derived from a control mouse displayed the negative expression of DsRed. Scale bar = 100 μ m

The lung tumor section was then processed for double-immunofluorescence staining to ascertain the identity of the tumor cells. The tumor cells exhibited double positive cells, claiming them to be derived from alveolar type II cells (Fig 12.3 A). Along with this the tumor were sustained by an active MAPKinase signaling as observed from the western blots for total ERK and phospho ERK. Actin served as a loading control (Fig 12.3B).

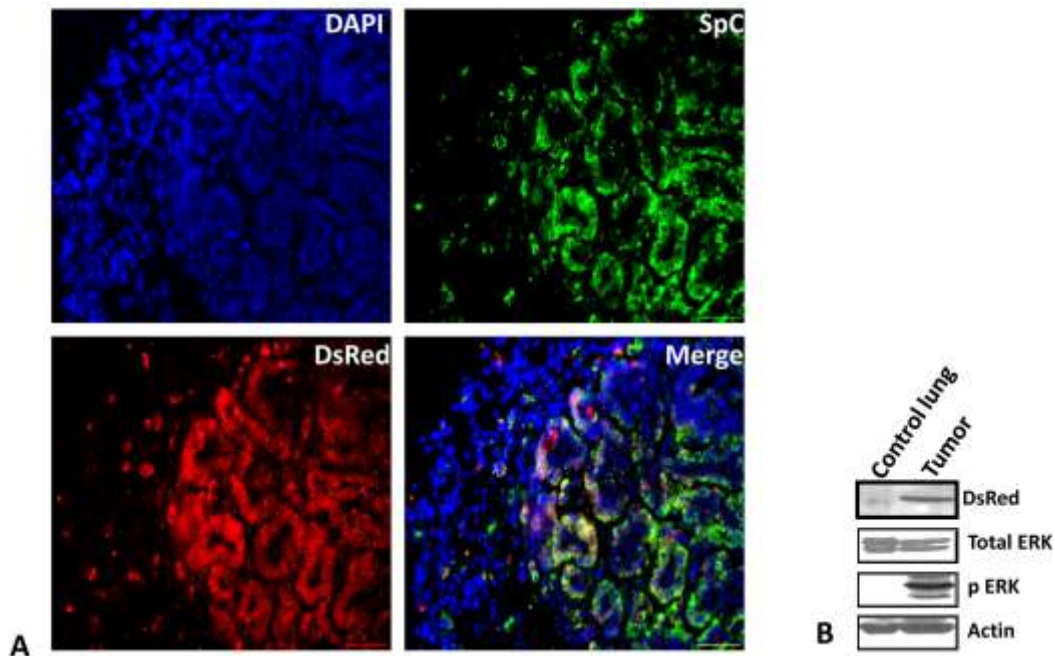


Fig 12.3 Co-localization of SpC and DsRed cells in the tumors generated from C RAF BXB-DsRed transgenic mice. (A) Double immunofluorescence staining for SpC and DsRed on the cryo embedded lung sections. Scale bar = 100 μ m (B) Analysis of the mitogenic cascade in the tumors. Immuno-blot showing the expression of DsRed, total ERK and phospho ERK in the tumor.

5.1.4.3 Labeling small cryptic lesions at earlier time points

Analyzing lungs from induced C RAF BXB-DsRed mice at earlier time points (between 6 to 8 months) shows small cryptic tumor like lesions whose size varies from few cell clusters to many cells comprising a mass. This early tumor like lesions expressed DsRed (Fig 12.4). This indicates that the type II cells are in the process of tumor formation and these lesions would eventually progress to macroscopic visible adenoma in the lung at later stages.

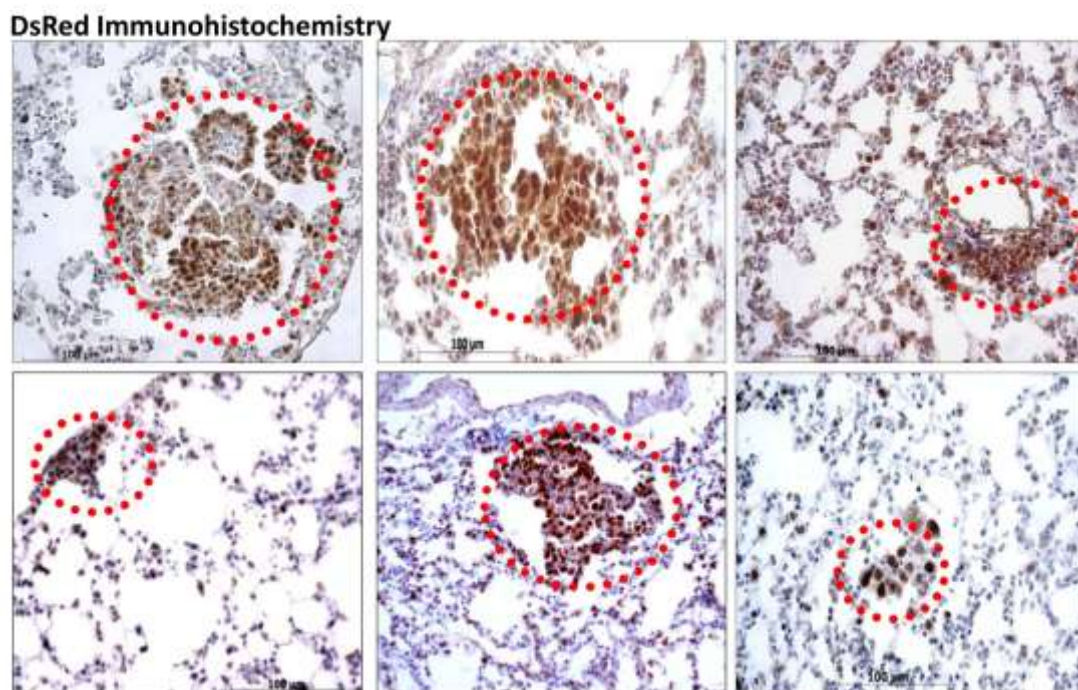


Fig 12.4 Labeling adenoma like lesions with DsRed from C RAF BXB-DsRed transgenic mice harvested at earlier time points (6 to 8 months). Paraffin embedded lung sections stained with DsRed. Small tumor like lesions positive for DsRed is indicated within red circles. Scale bar = 100 μ m

5.1.4.4 C RAF BXB-DsRed transgenic mice exhibit proliferating bronchiolar hyperplasia

Another striking feature observed in the compound reporter mice, was the presence of abundant bronchiolar hyperplastic regions. These hyperplasias were often continuous with the alveolar space adjacent to the respiratory bronchioles (Fig 12.5 H&E). To investigate the histogenesis of the hyperplasias, immunohistochemistry was performed using antibodies against Clara cell antigen (CCSP) and the surfactant protein-C (SpC), commonly used markers that distinguish between Clara cells and alveolar type II cells, respectively. The isolated hyperplastic lesions were found to be positive for CCSP (Fig 12.5) suggesting that these lesions arose from Clara cells or their precursors but the adenomas were found to be positive for SpC, suggesting that they arise from type II cells. Few cells within the lesions were positive for SpC and were proliferating as depicted by the Ki67 positive cells within this zone (Fig 12.5).

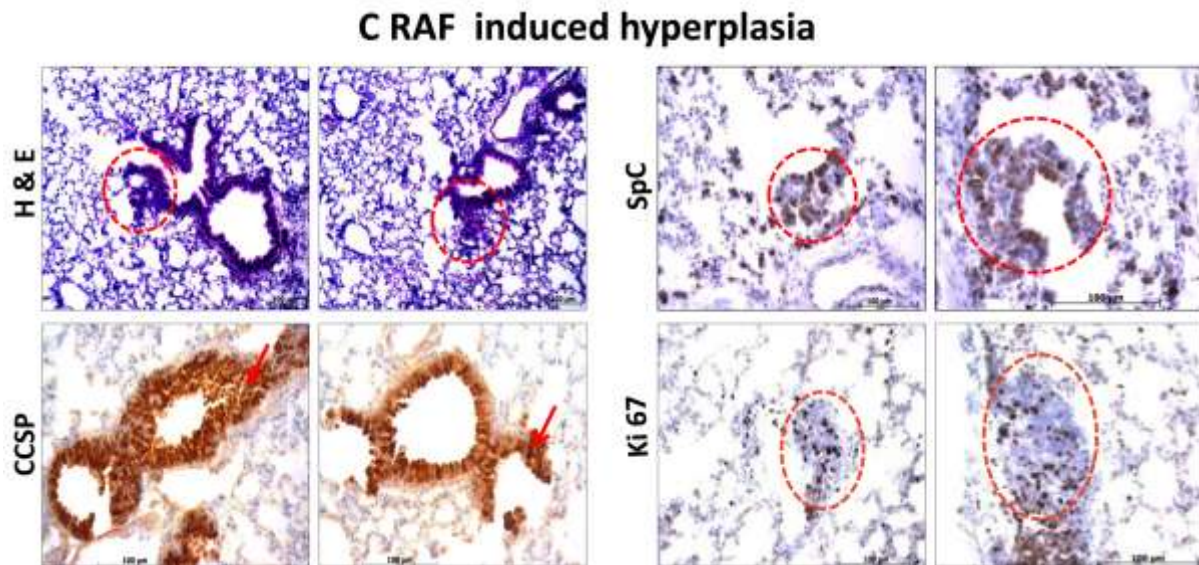


Fig 12.5 C RAF BXB-DsRed lungs displayed abundant bronchiolar hyperplasias that are proliferating and express the markers of type II cell, SpC. Paraffin embedded lung sections stained with H&E, CCSP, SpC and Ki 67. Red circles indicate the hyperplastic regions. CCSP staining showing the massive expression of Clara cells in the hyperplasias (in red arrows). Scale bar = 100 μ m

Furthermore, double immunofluorescence staining was performed to determine whether individual cells in the hyperplastic structures were expressing both SpC and CCSP. Usually cells expressing both SpC and CCSP are observed at the junction of bronchiolar and alveolar epithelium in the respiratory bronchioles, called as bronchio-alveolar duct junction (BADJ) and in rare cases extended into the center of the adenoma. These cells are designated as bronchio-alveolar stem cells (BASCs). We did not find any double positive cells in these lesions (Fig 12.6).

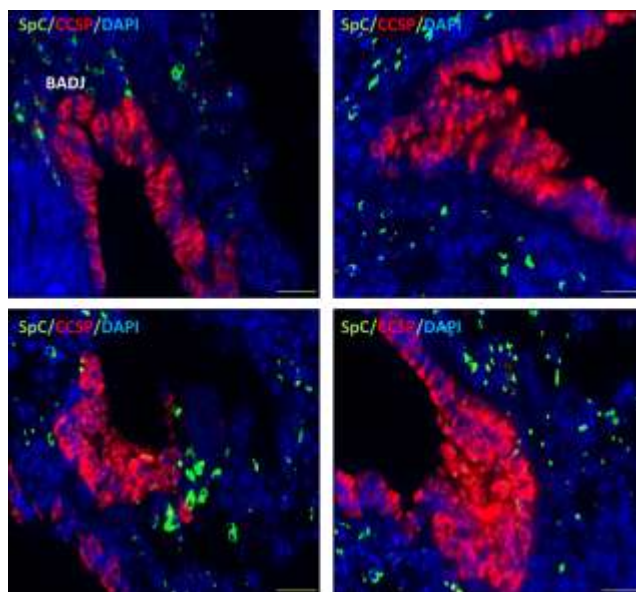


Fig 12.6 Hyperplasias generated in the C RAF BXB-DsRed transgenic mice displayed the absence of BASCs. Co-immunofluorescence staining for SpC and CCSP on the paraffin embedded lung sections showed no double positive cells. (BADJ = Bronchio-alveolar duct junction). Scale bar = 100 μ m

5.1.5 Labeling tumor cells generated in a reporter metastatic NSCLC model

Since c Myc is known to be a metastatic gene for NSCLC and induced macrometastasis in liver (Rapp et al, 2009); we were interested to study the involvement of type II cells and its fate in malignant progression. For this purpose, Myc-DsRed and Myc-BXB-DsRed transgenic mice were generated.

Transgenic mice were induced with doxycycline food and were harvested after a period of 1 year. Multiple macroscopic lung tumors were formed in Myc -DsRed mice (Fig 13.1 A) and Myc-BXB-DsRed (Fig 13.2 A). Whereas tumors derived from the Myc-DsRed mice exhibited columnar cell phenotype (Fig 13.1B); tumors obtained from the Myc-BXB-DsRed mice displayed a mixed phenotype comprising both cuboidal and columnar structure (Fig 13.2 C). This suggests that introduction of c Myc induces the tumor cells to gain a new phenotype-the columnar structure, which is thought to be more malignant and hence a signature for the appearance of papillary carcinomas in the advanced stages of tumor progression.

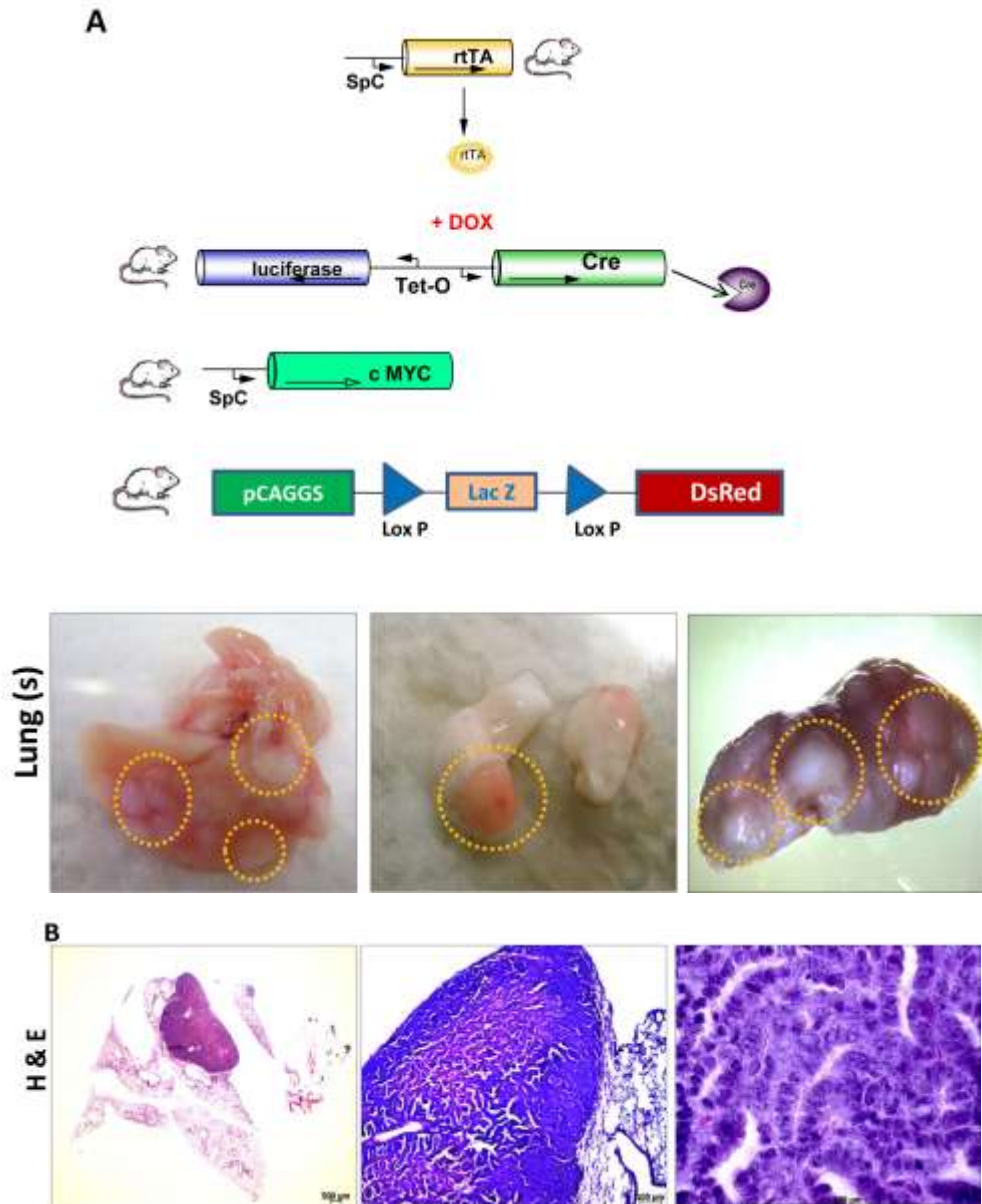


Fig 13.1 Macroscopic lung tumors are formed in Myc-DsRed transgenic mice and are made up of columnar cells. (A) Experimental strategy for conditional expression of DsRed in SpC c Myc mediated lung tumors. Whole lung photographs of 12 to 15 months induced transgenic mice shows visible tumor nodules (in yellow circles). (B) Paraffin embedded H&E stained lung sections show tumor (left panel, scale bar = 500 μ m) which on closer examination depicts the presence of columnar cells (right panel). Scale bar = 100 μ m

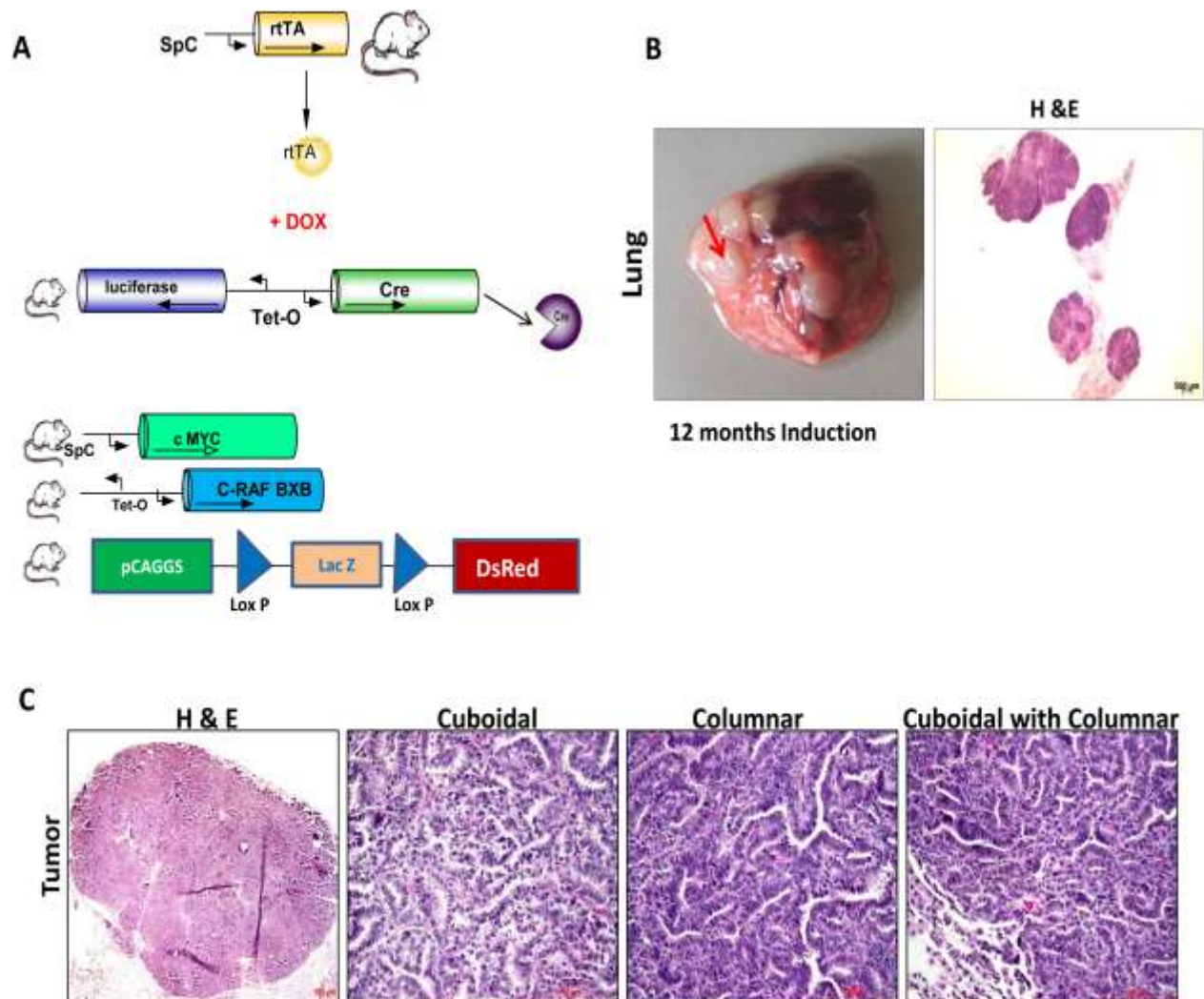


Fig 13.2 Macroscopic lung tumors are formed in Myc-BXB-DsRed transgenic mice and are composed of cuboidal and columnar tumor cells. (A) Experimental strategy for conditional expression of DsRed in SpC c Myc and C RAF BXB induced lung tumor. (B) Whole lung photograph of 12 months induced transgenic mice shows macroscopic tumor nodules. (C) Paraffin embedded H&E stained lung section shows tumor which consist of both cuboidal and columnar tumor cells. Right panel images (scale bar = 100 μ m) are the higher magnifications of randomly selected regions from the tumor (left most panel, scale bar = 500 μ m)

5.1.6 Introduction of Myc induces a new phenotype: premalignant lesions

Clusters of pleomorphic cells are detected in the lungs that are speculated to be the potential sources for metastasis initiating cells (MICs) (Fig 13.3 A H&E); (Rapp et al, 2009) In order to characterize these potential premalignant lesions, and their lineage, expression of genes regulating proliferation and apoptosis were analyzed. Paraffin embedded lung sections from Myc-DsRed and Myc-BXB-DsRed transgenic mice (> 12 months) were immunostained with c-Myc, Cleaved caspase 3, Ki 67 and DsRed antibodies. These pleomorphic clusters exhibited strong nuclear c-Myc (Fig 13.3 A). Pleomorphic cells proliferate as seen by the Ki 67 staining (Fig 13.3 B) and simultaneously exhibit cells undergoing apoptosis as observed by the presence of cleaved-caspase 3 positive cells (Fig 13.3B). Lineage marker for type II pneumocytes are maintained in the c-Myc positive foci as depicted by the expression of DsRed (Fig 13.3 B).

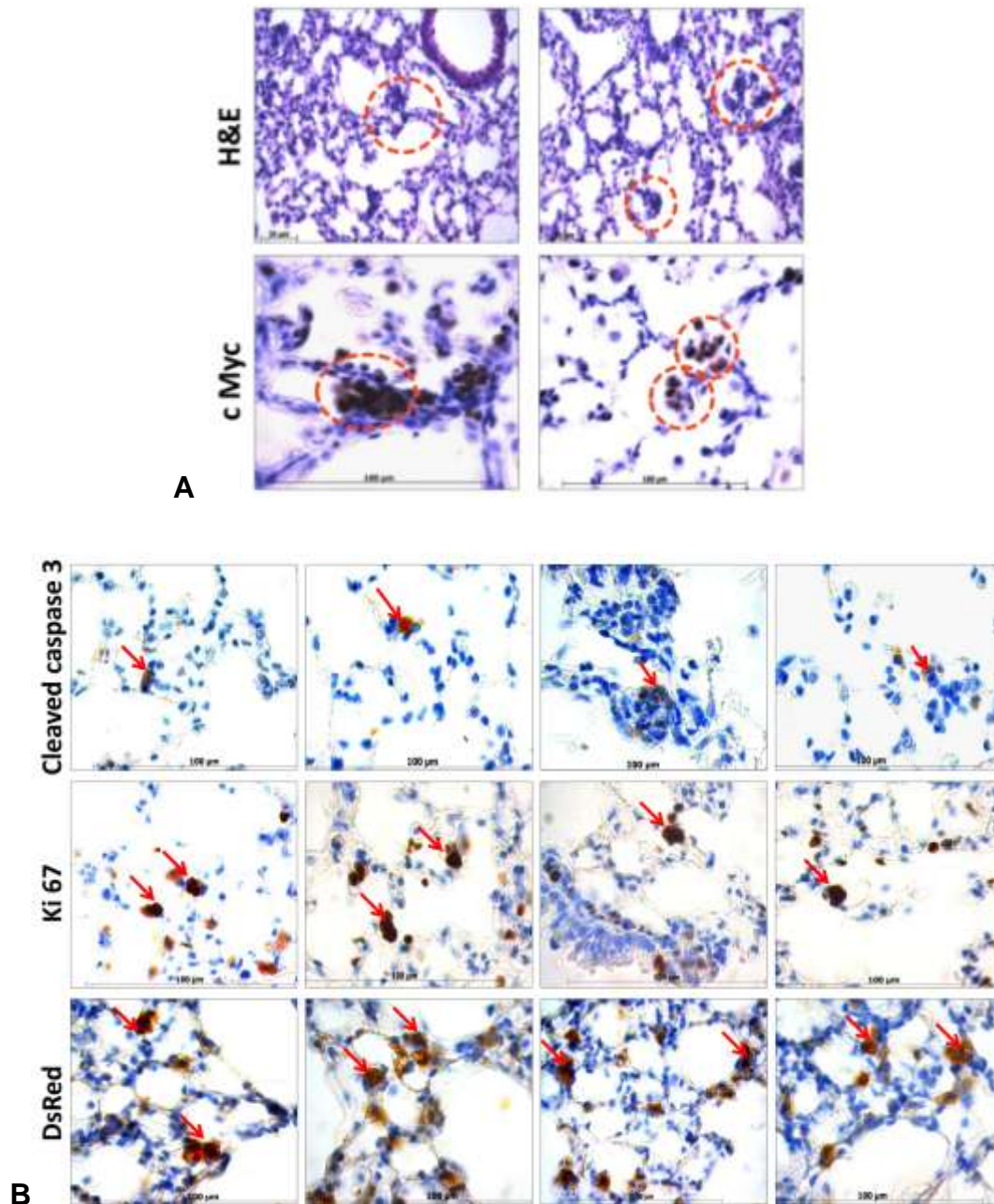


Fig 13.3 Representative images from Myc-DsRed and Myc-BXB-DsRed transgenic lungs (>12 months) displayed the presence of unique premalignant lesions composed of pleomorphic cluster of cells that are labeled with DsRed and express c Myc which are in a constant status of proliferation and apoptosis. (A) Paraffin embedded lung sections stained with H&E shows the pleomorphic clusters (in red circles) which are immunopositive for c Myc (brown cells within red circles). (B) Immunostaining of the pleomorphic clusters for the indicated markers. Scale bar = 100 µm

5.1.7 Evaluation and characterization of the primary tumor

Adenocarcinoma of the lung is the most common form of lung cancer, but the cell of origin and the stages of progression of this tumor type are not well understood. Tumor might arise from Clara cells, alveolar type II cells, multipotent stem cell, or from derivative lineages from these cells (Beer & Malkinson, 1985; Jackson et al, 2001; Magdaleno et al, 1998; Mason et al, 2000; Rehm et al, 1991; Thaete & Malkinson, 1991). In an attempt to get closer to identifying candidate precursors, tumor cells were analyzed by immunohistochemistry. Paraffin embedded tumor bearing lung sections from Myc-BXB-DsRed mice (>12 months) were analysed for the expression of the cell type specific markers. Heterogeneous expression of the lineage tag; DsRed persisted within the tumors in abundance (Fig 14.1A) which was subsequently confirmed by the similar SpC expression pattern observed (Fig 14.1A). Tumor also displayed a fair expression of the driving oncogenes. Membranous C RAF and Ha tag along with strong nuclear c Myc were detected in the tumor cells (Fig 14.1B). Marker of alveolar type I cell lineage, Aquaporin 5 was also expressed in these tumors (Fig 14.1B). In accordance with the immunoblot results, tumor cells displayed heterogeneous expression of nuclear pERK (Fig14.1B). In addition novel marker like PGP 9.5 was expressed, which represents an endothelial cell lineage. Previously PGP 9.5 was known to be a marker for immature neuroendocrine cells (Rawlins, 2008) and as a candidate tumor marker for NSCLC (Hibi et al, 1999).

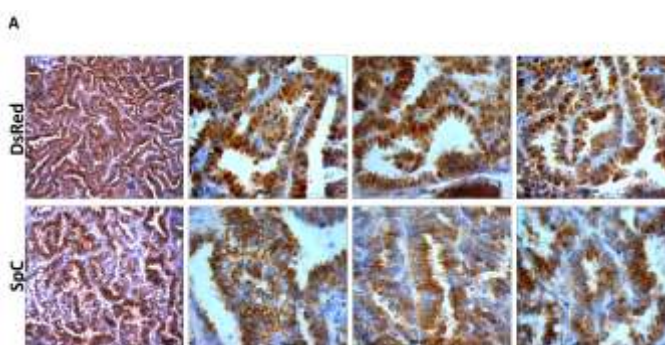


Fig 14.1A Lung tumors from Myc-BXB-DsRed mice (>12 months) were labeled with the lineage tag DsRed and express alveolar type II cell marker, SpC. Immunohistochemical staining of the paraffin embedded lung sections displayed nucleo-cytoplasmic expression of DsRed and membranous localization of SpC. Right panel images display the higher magnification of the randomly selected regions of the left panel image. Scale bar = 100 μ m

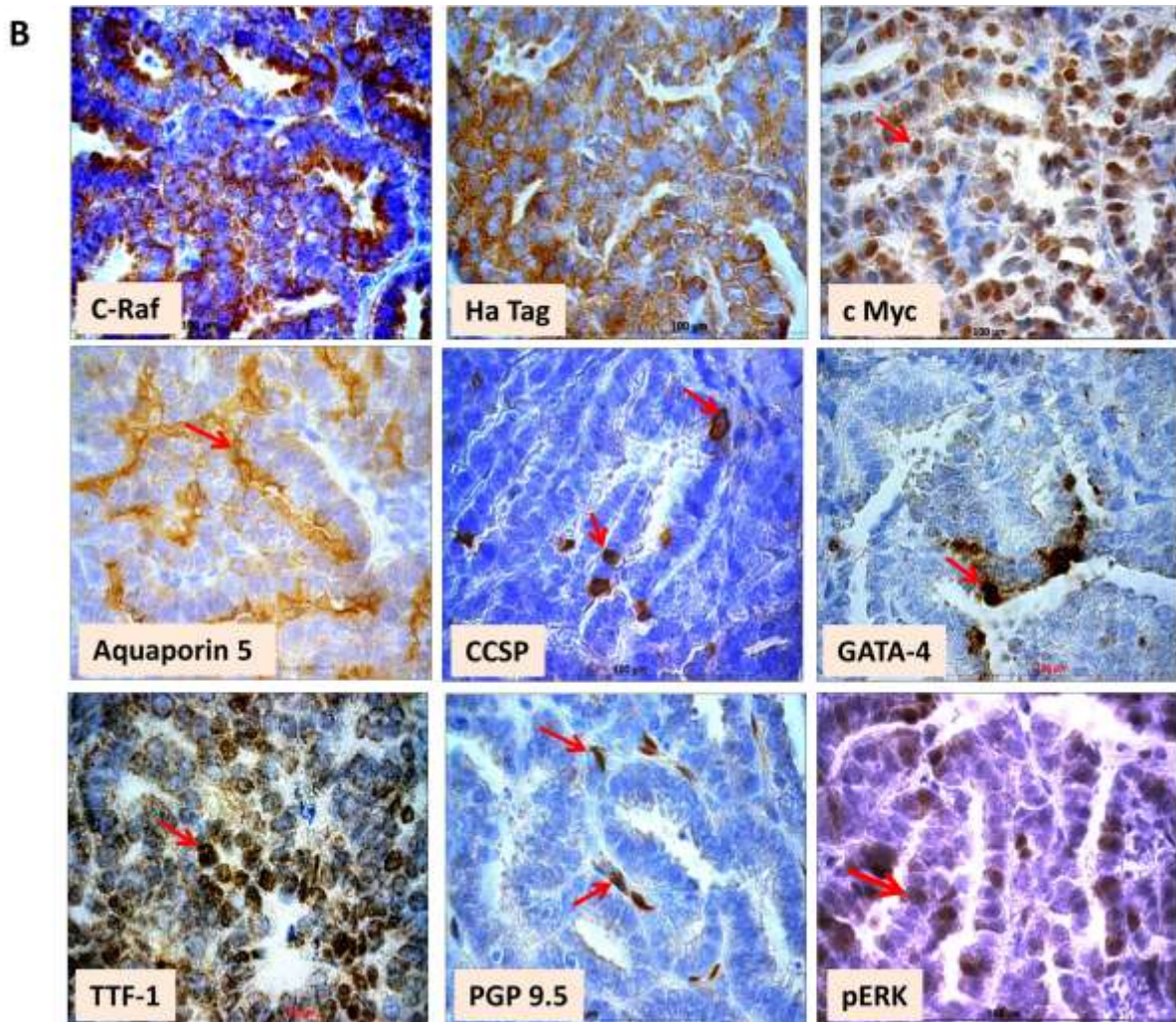


Fig 14.1B Immunohistochemical analysis of the tumors obtained from Myc-BXB-DsRed mice (>12 months) for lung differentiation markers. Paraffin embedded tumor-bearing lungs were immunostained for the indicated markers. Haematoxylin was used as a counter-stain. Scale bar =100 μ m

5.1.8 Tumor progression concomitant with angiogenesis in the absence of EMT

Angiogenesis is an important step in both tumor growth and metastasis (Onn et al, 2003). Immunostaining of paraffin embedded lung tumor sections from Myc-BXB-DsRed mice (> 12 months) displayed tumor vascularization with unusual vessels in a mosaic pattern expressing Pecam-1, a marker for blood vessels (Fig 14.2).

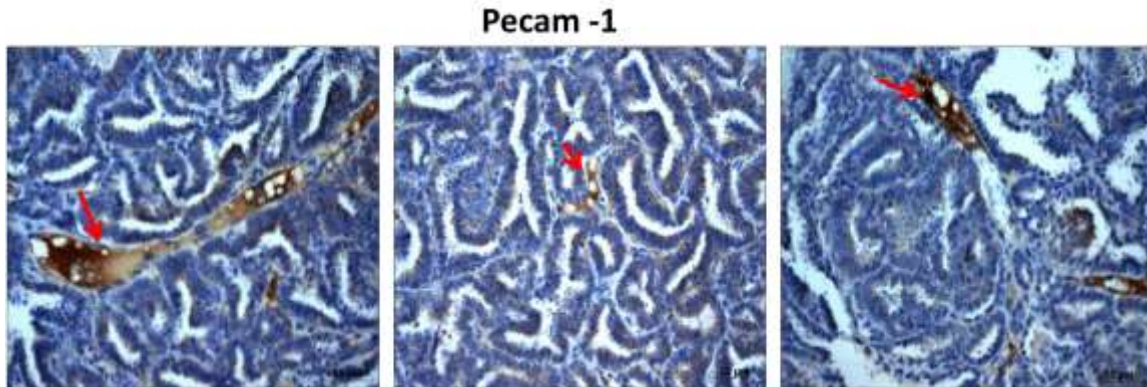


Fig 14.2 Angiogenic induction in tumor. Pecam-1 immunostaining of the paraffin embedded lung tumor sections from Myc-BXB-DsRed mice shows the presence of blood vessels within the tumor (in brown). Scale bar = 50 μ m

An important factor for maintaining normal tissue architecture is the E Cadherin-catenin complex (Bremnes et al, 2002). Loss of E Cadherin expression is observed in local lung cancer invasion as well as in regional metastasis and is associated with poor prognosis (Hirata et al, 2001; Kalogeraki et al, 2003). Paraffin embedded lung tumor section from Myc-BXB-DsRed mice (> 12 months) was stained with the epithelial marker, E-Cadherin. Small tumor lesions strongly express E- Cadherin which shows that the E-Cadherin junctions of columnar cells in tumor remained intact (Fig 14.3 A). Immuno blot of the tumor showed high E-Cadherin and feebly detected Vimentin (Fig 14.3 B). Taken together these results indicate that the tumor cells were not undergoing typical epithelial mesenchymal transition. Interestingly, in massive papillary tumors, there were certain regions observed that appeared to lose E-Cadherin (Fig 14.3 C). This may be the beginning of the transition phase from epithelial to acquiring mesenchymal phenotype. But while addressing issues of EMT, one has to be careful enough since catching the right time window when a cell undergoes EMT is very a critical criteria in detecting the markers up or down regulated during this transition.

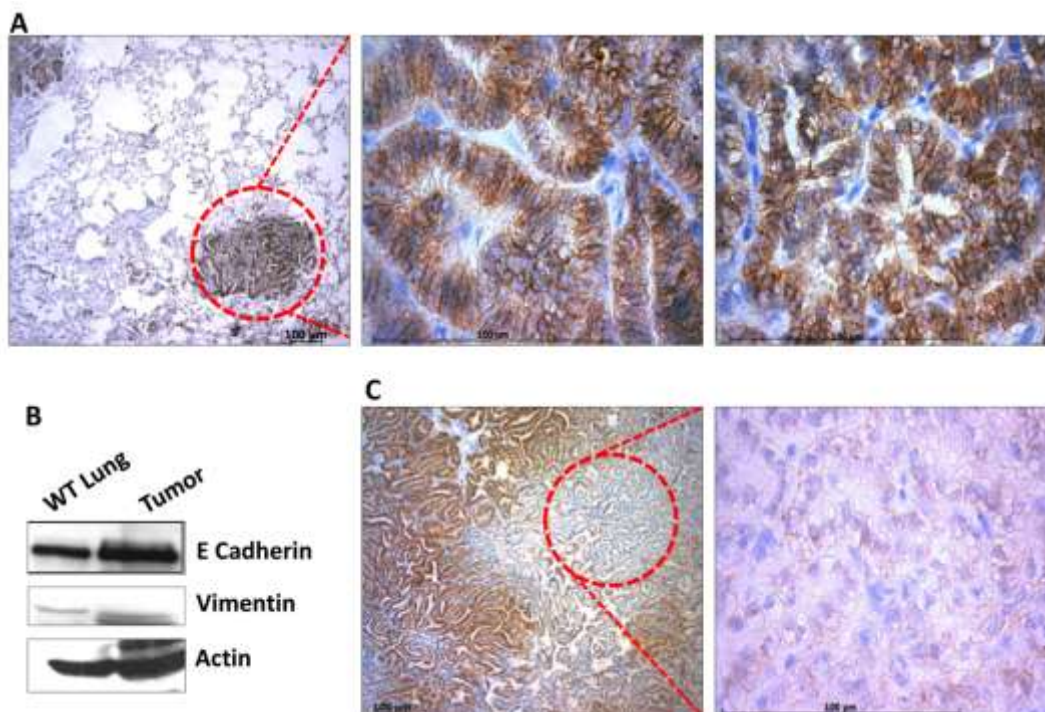


Fig 14.3 Analysis of Epithelial-Mesenchymal Transition (EMT) in lung tumor. Paraffin embedded tumor bearing lung sections were immunostained with the epithelial marker, E Cadherin. Tumor shows strong expression of E- Cadherin on the membranes of the tumor cells (A). Immunoblot of the lung tumor for E-Cadherin and Vimentin shows strong E-Cadherin and very feeble Vimentin (B). Some regions within the tumor are negative for the E-Cadherin expression (C). Scale bar = 100 μ m

5.1.9 Labeling efficiency in the transgenic compound reporter mice

The number of cells targeted by Cre would give an estimate of the percentage of lineage tagged cells in our transgenic system. Lungs from the two groups of transgenic mice viz C RAF BXB-DsRed and Myc-DsRed were paraffin embedded, sectioned and stained with SpC and DsRed antibodies. Ten random animals were chosen from each group and the number of DsRed positive cells in the entire lung per animal was counted. Gross morphological examination of the lungs displayed the expression of SpC and DsRed (Fig 15 A) in an entirely normal alveolar type II cell pattern. Calculation of labeling efficiency revealed that 40 % of the total lung was labeled in C RAF BXB-DsRed mice whereas Myc-DsRed mice showed a tendency of 35% labeling of the entire lung (Fig 15 B).

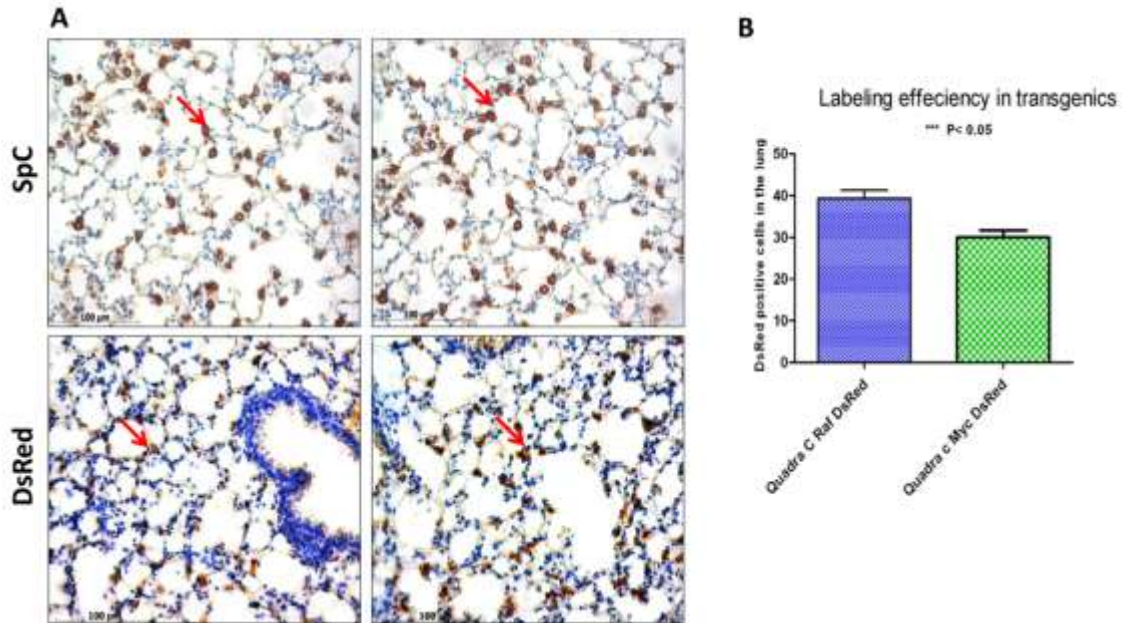


Fig 15 (A) Paraffin embedded lung sections from the C RAF BXB-DsRed and Myc-DsRed reporter mice immunostained for SpC and DsRed shows fair expression of the lineage markers throughout the lung without any abnormal expression pattern otherwise Scale bar = 100 μm. (B) Quantification of the DsRed positive cells in the total lung determines the efficiency of labeling in the compound transgenic reporter animals harbouring c Myc and Tet O C RAF BXB oncogenes.

5.1.10 Proliferation and apoptosis in the primary tumor

A tumor is more or less a collection of cells that grow more rapidly than the surrounding normal tissue. Hence we were interested to know how actively the cells in tumor are growing compared to the surrounding tissue. The measurement of Ki67 is one of the most common ways to measure the growth fraction of tumor cells. Ki-67 is a molecule that is found in growing, dividing cells but is absent in the resting phase of cell. In order to understand the rate at which the cells within a tumor are growing; lung tumor sections were immuno-stained with a Ki 67 antibody. Strong nuclear Ki67 was detected in abundance within the tumor (Fig 16 A). In conjunction with analyzing tumors for their growing status, it is important to study the cells undergoing apoptosis. Apoptosis can occur when a cell becomes too damaged to survive but is still able to die in a controlled way (to prevent inflammation and the release of proteins that could damage other cells). One of the things that triggerers

apoptosis is genetic mutations. Since cells become cancerous due to multiple genetic mutations, it becomes necessary for them to be eliminated via apoptosis. In view of this, lung tumor sections were stained with cleaved Caspase 3 antibody to detect the cells undergoing apoptosis. Quantifying the number of cells in total lung derived from C RAF BXB-DsRed and Myc-DsRed animals; positive for Ki 67 and Cleaved Caspase 3; a graph is plotted which shows that the mice transgenic for Myc-DsRed scores high for Ki 67, and thus contain cells that are rapidly dividing and growing (Fig 16 B).

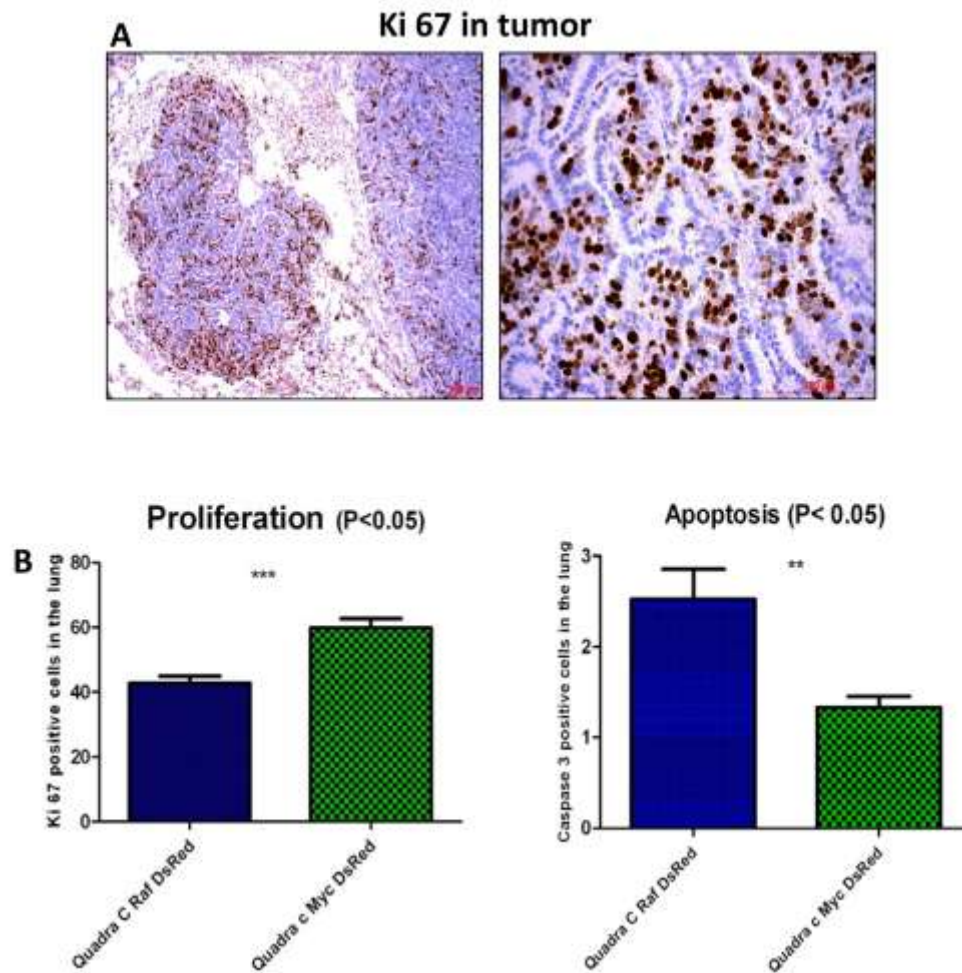


Fig 16 Proliferation and apoptosis in the compound transgenic reporter mice. (A) Ki-67 immunohistochemistry in paraffin embedded lung tumor sections. Right panel image is the magnified view of the randomly selected region of the tumor displayed in the left panel. Scale bar = 100 μ m (B) Quantification of proliferation and apoptosis, scored from the cells of the pulmonary epithelium in the compound transgenic reporter mice.

5.1.11 Status of p53 in the compound transgenic reporter animals

p53 is a tumor suppressor gene that is frequently mutated in lung cancer with mutations in approx. 50% of Non–small cell lung cancer and 70% of small cell lung cancer (Harris, 1996; Rom et al, 2000). The p53 protein is a transcription factor that induces the expression of several genes, including p21, an inhibitor of the cyclin/cyclin-dependent kinase complex mediating G1 cell cycle arrest; bax, which promotes apoptosis; and GADD45, which is involved in cell cycle arrest and DNA nucleotide excision repair (Levine, 1997). Most missense mutations occur in the DNA-binding domain, resulting in defective contacts with DNA and loss of the ability of p53 to act as a transcription factor, thereby hampering the function of this potent tumor suppressor. Functional p53 is short-lived in the cell as it triggers its own degradation. Mutant p53 however can accumulate. This forms the basis for the detection of mutant p53 via standard immunohistochemical staining. In accordance with this, the goal of the present study was to carry out p53 assessment in the lung tumors obtained from three different groups of transgenic animals viz C RAF BXB-DsRed, Myc-DsRed and Myc-BXB-DsRed respectively. Paraffin embedded lung tumor sections were immunostained with the p53 antibody. Pre-malignant lesions derived from the Myc-DsRed and Myc-BXB-DsRed exhibited p53 expression in the clusters of the pleomorphic cells, also a fraction of cells within the tumors showed strong p53 (Fig 17). In all cases, p53 was strongly confined to nucleus. Interestingly, we did not detect any p53 positive cells in the tumors generated from C RAF BXB-DsRed animals (Fig 17). Finally, the number of tumor cells positive for p53 signal were counted, quantified and represented in the graph (Fig 17) which shows that the Myc-BXB-DsRed labeled tumor exhibit strong p53 upregulation compared to the tumor form Quadra transgenic reporter mice driven by c Myc alone. This is our preliminary observation about the p53 status in the labeled transgenic mice. And the molecular mechanisms underling this observed phenomena has yet to be investigated in detail.

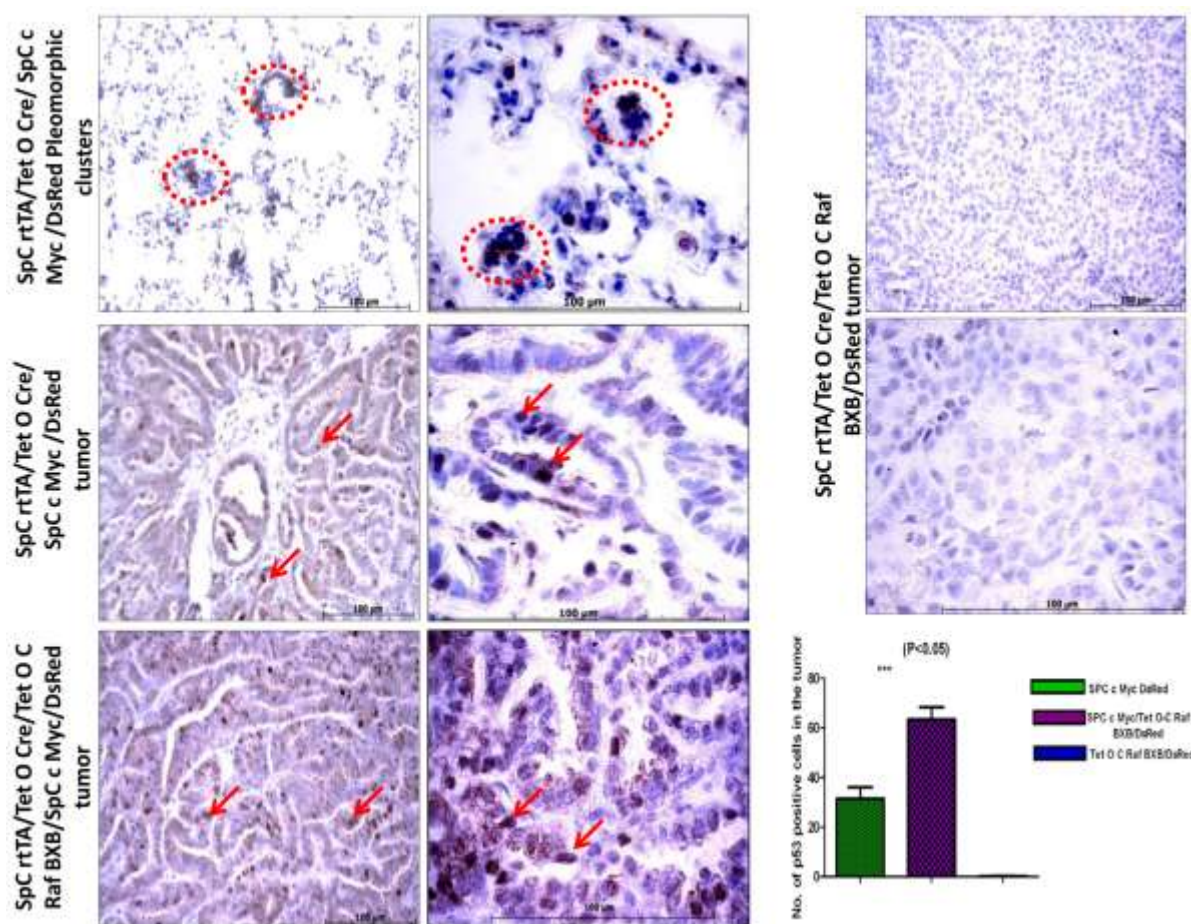


Fig 17 Analysis of the p53 in the lungs of the compound transgenic reporter mice (with the indicated genotypes). Pleomorphic clusters and tumors of the Myc-DsRed and Myc-BXB-DsRed mice displayed heterogenous, nuclear p53 expression whereas the tumors generated from C RAFBXB-DsRed mice showed the complete absence of p53 signal. Quantification of p53 positive cells were scored and a graph was plotted which shows that the tumors of the Myc-BXB-DsRed reporter mice have the maximum p53 expression when compared to others. Scale bar = 100 μ m

5.1.12 Screening for DsRed positive cells via Flow Cytometry

One of the advantages of fluorescent labeling is to detect the presence of the labeling molecule under suitable filters utilizing flow cytometry. For that purpose, single cell suspension from total organs which includes lung, liver and kidney from three animals (Myc-DsRed, ~10 to 14 months old) were subjected to FACS analysis for screening DsRed in the FLH-2 channel of the BD FACS caliber. Wild type organs

and tissue derived from non labeled mice (SpC c Myc/ BXB) served as control. Though no obvious visible metastasis and lung tumor were observed in these animals, but we detected fraction of cells from the total population; positive for the DsRed signal. This indicates that metastatic is an early event, yet it may require additional factors and time in-order to form a full fledged metastasis that can be readily detected via naked eyes.

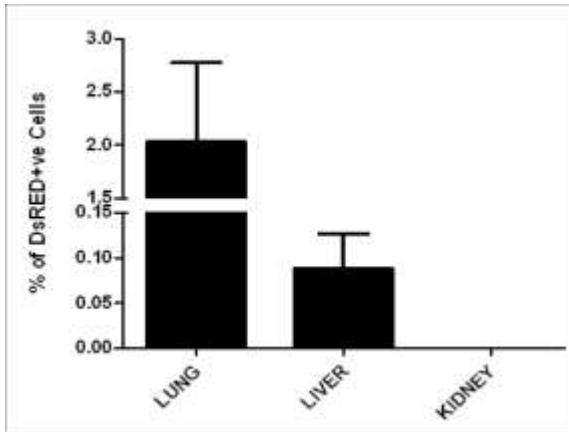


Fig 18 Quantification of DsRed positive cells in the parenchymal organs. Data represents the average of three animals.

5.1.13 Loss of SpC and TTF-1 in the primary tumors: Hallmarks for metastatic progression

NK2 homeobox 1 (NKX2-1), also known as thyroid transcription factor 1 (TTF-1), is a protein which in humans is encoded by the *NKX2-1* gene (Guazzi et al, 1990). Also known as Thyroid transcription factor 1 (TTF-1), it is the earliest known marker associated with commitment of endodermal cells to pulmonary and thyroid cell lineages; it appears before the definitive lung formation (Maeda et al, 2007). SpC is expressed in the distal epithelium during early lung development, and becomes restricted to alveolar type II cells late in gestation and postnatally. It is expressed in type II pneumocytes in the normal adult lung (Ikeda et al, 1995) and in approximately 75% of non-mucinous lung adenocarcinomas (Kaufmann & Dietel, 2000). Currently, testing for TTF-1 expression by immunohistochemistry is commonly used to confirm the pulmonary origin of a carcinoma (Kaufmann & Dietel, 2000; Stenhouse et al, 2004). Several studies have evaluated the prognostic significance of TTF-1

expression in NSCLC (Au et al, 2004; Berghmans et al, 2006) (Haque et al, 2002; Myong, 2003; Pelosi et al, 2001; Puglisi et al, 1999; Stenhouse et al, 2004). It has been shown that TTF-1 is a favorable prognostic factor for survival in patients with lung adenocarcinoma (Berghmans et al, 2006). Since the expression of TTF-1 is an early event during lung differentiation, the evaluation of TTF-1 expression in lung tumors would be of significant impact. For this purpose, paraffin embedded lung tumor sections from Myc-DsRed and Myc-BXB-DsRed (>12 months) were immunoreacted with the SpC and TTF-1 antibodies and were analysed for the presence or absence of their immunoreactivity. Lung tumor expressed strong nuclear TTF-1 and SpC proteins (Fig 19). But interestingly, certain regions within the massive tumor lesions were found negative for the expression of SpC and TTF-1, which states that these tumor cells are losing these markers in their course of malignant progression. A recent report from Tyler Jacks laboratory showed that the loss of TTF-1 is a pre-requisite for metastatic progression in lung cancer (Winslow et al, 2011). In view of this our observation are in consistent with the already published phenomena in the case of malignant progression.

Loss of SpC and TTF-1 in the primary tumors during tumor progression

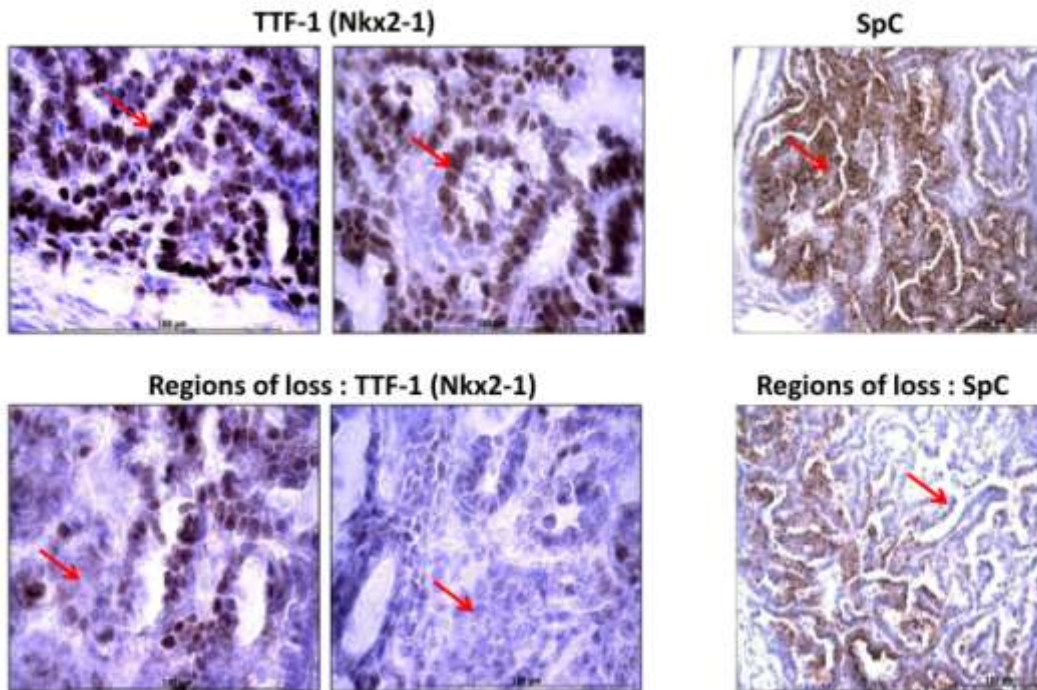


Fig 19 Lung tumors generated from the Myc-DsRed and Myc-BXB-DsRed reporter mice displayed abundant SpC and TTF-1 expression whereas certain tumor cells exhibited the loss of the indicated markers. Paraffin embedded lung tumor sections were immunostained with SpC and TTF-1 antibodies and shows membranous SpC and nuclear TTF-1 expression. Scale bar = 100 μ m

5.1.14 Evidence of circulating Bronchioalveolar stem cells (BASCs) in the tumors

Lung adenocarcinoma is the lethal form of lung cancer and has an overall poor prognosis with low 5-year survival due to late presentation, disease relapse and lack of curative systemic therapy. Recently, the cancer stem cells (CSC) theory proposes that cancers are maintained by subpopulations of tumor cells that possess stem or progenitor cell characteristics. These cells can initiate tumor formation, differentiate along multi-potent pathways and are relatively resistant to conventional chemotherapy (Lapidot et al, 1994). Bronchioalveolar stem cells (BASCs) were recently identified in adult mouse lung as a rare cell population located in the bronchoalveolar duct junction. (Kim et al, 2005; Mallick et al, 2009). BASCs were

characterized by its double positive staining characteristics for both the alveolar epithelial type II cell marker, Surfactant protein C (SpC), and the Clara cell marker, Clara cell secretory protein (CCSP). Viable BASCs were maintained through multiple passages in vitro under distinct culture conditions, and retained the ability to differentiate into either Clara cells or alveolar type II cells AT2 (Kim et al, 2005) and (Giangreco et al, 2002). In order to find the potential BASCs in the tumors generated from Myc-DsRed and Myc-BXB-DsRed mice, lung tumor sections were co-immunostained with SpC and CCSP antibodies. Double immunofluorescence staining revealed the presence of few double positive cells inside the tumor and near the BADC (Fig 20). These data suggest that the presence of rare circulating BASCs contribute as one of the potential candidate cell type that is capable of initiating and sustaining the tumor in these animals. Interestingly we have not detected a single BASC in the lung tumors derived from C RAF BXB-DsRed mice. A recent finding states that c-Myc regulates self renewal in Bronchoalveolar Stem Cells (Dong et al, 2011) may shed some light on our findings. Nevertheless, this phenomena need to be explored in detail.

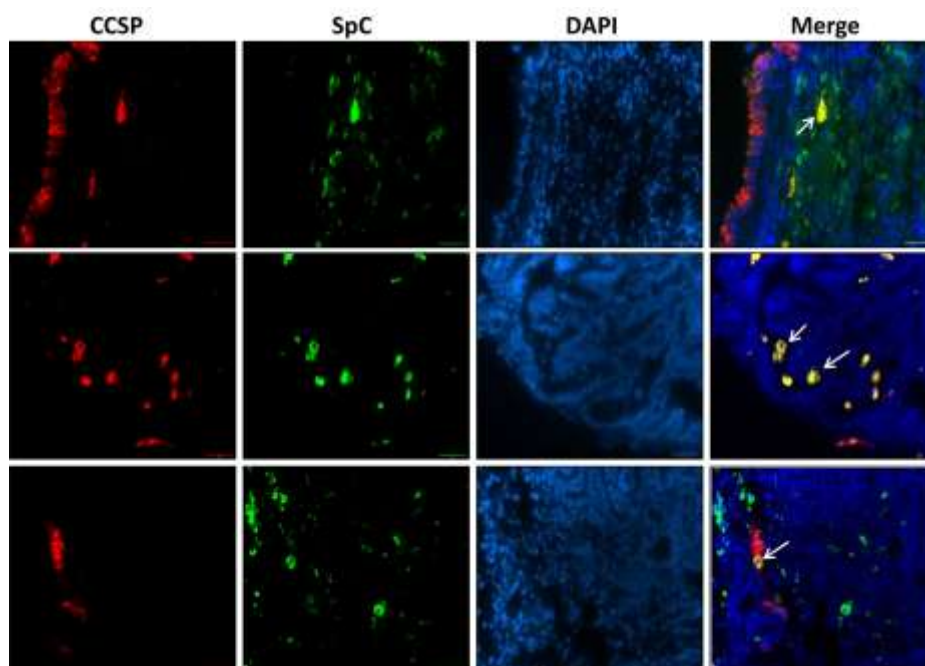


Fig 20 Representative images of lung tumor generated from Myc-BXB-DsRed mice (>12 months) showed the presence of BASCs. Paraffin embedded lung sections were co-immunostained with SpC and CCSP. DAPI depicts the nucleus. Double positive cells are indicated with white arrows. Scale bar = 100 μ m

5.1.15 Detection of the tumor specific transcripts in compound transgenic reporter mice via gene expression analysis.

Expression of lineage marker, DsRed was already determined in the primary lung tumors via Immuno histochemical stainings. In order to confirm our previous findings as well as to explore the presence of the lineage specific and type II cell marker in the primary tumors and their respective secondary organs, multigene real time PCR was carried out with the cDNA samples obtained from the lung, liver and kidney of the reporter transgenic animals viz. DsRed, Myc-DsRed and Myc-BXB-DsRed (metastatic animal). DsRed mice served as a control of this experiment. Probes were normalized with the HPRT (hypoxanthine-guanine phosphoribosyltransferase) as an internal control. Real time PCR detected the differential presence of the transcripts under study that comprises of DsRed, SpC, cMyc, C RAF-BXB, and TTF-1 respectively. As expected metastatic mice displayed DsRed, SpC, c Myc and TTF-1 in both the primary lung tumor and in the liver metastasis. Whereas the liver metastasis displayed minimal levels of CCSP.

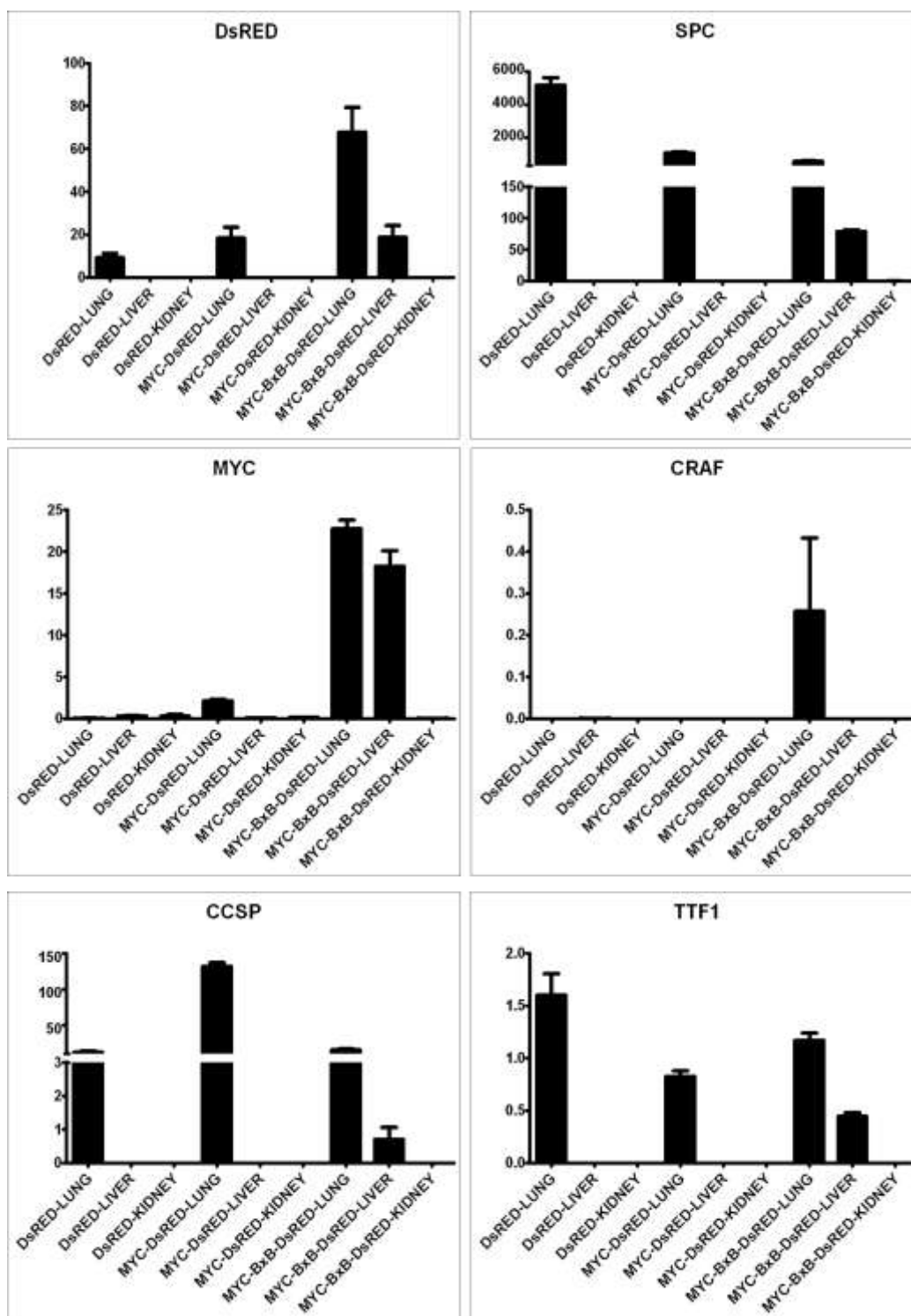


Fig 21 Relative mRNA levels expressed in the transgenic reporter mice screened for the presence/absence of the transcripts (DsRed, SpC, c Myc, C RAF-BXB, CCSP, and TTF-1) in the tissues (lung, liver and kidney) analysed. DsRed mice served as control. Genotypes of the derived tissue are indicated on the Y axis.

5.1.16 Gene expression profiling of the primary lung tumor

The discovery of rare cells with stem cell-like properties in solid tumors is emerging as an important area of cancer research and may help explain the resistance of these tumors to current therapeutics. In view of this, we investigated the presence of cancer stem cells in our NSCLC mouse model. For this, a panel of cancer stem cell markers was screened at the gene expression level exclusively in the pure tumor nodules dissected from the lung lobes of Myc-BXB-DsRed mice. Among them includes the cluster of differentiation group of molecules namely CD 44, CD 24, CD 34, and CD 133 along with Sca 1, c kit and TERT. Wild type lung served as a control. The expression of the CD 44, Sca 1 and TERT genes was significantly higher in tumor than compared to the normal lung tissue (Fig 22 A and B). LEF 1, CD 34, Axin 2, CD 24, LGR 5, CD 133, MMP 2, MMP 9 and SYK mRNA levels were not significantly different in the tumor relative to the normal healthy lung; whereas c kit, Vimentin and TCF 1 were found to be downregulated in the tumors (Fig 22 A).

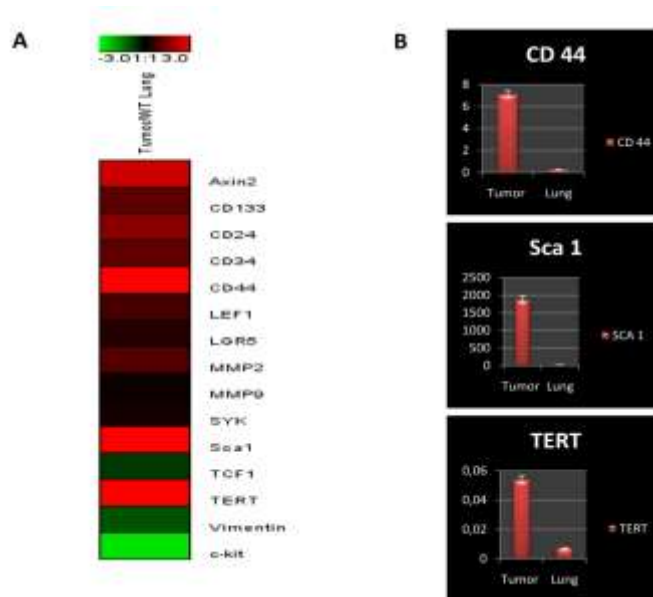


Fig 22 Gene expression profiling of the primary lung tumor obtained from Myc-BXB-DsRed transgenic reporter mice showed elevated expression of CD 44, Sca-1 and TERT. (A) Heat map generated from the fold expression values for the indicated genes. (B) Individual graphs depicting the genes up regulated in the tumor. Wildtype lungs were used as a control.

The establishment of metastasis requires that tumor cells acquire new adhesion and migration properties to emigrate from primary sites and colonize distant organs. The CD44 antigen is a cell-surface glycoprotein involved in cell-cell interactions, cell adhesion and migration. It participates in a wide variety of cellular functions including lymphocyte activation, recirculation and homing, hematopoiesis, and tumor metastasis. CD 44 may be involved in cloning selection of metastasis prone cells within early primary tumors. Since it is a cell membrane protein often over expressed on tumor cells and being both a cell–cell and cell–extracellular matrix adhesion protein, is well positioned to contribute to the early events of metastasis (Jothy, 2003). Hence the high levels of CD 44 expression in our tumors is in accordance with the earlier findings which has demonstrated that many NSCLC cell lines are enriched with stem cell like properties thereby having elevated levels of CD 44 expression (Leung et al, 2010). Stem cell antigen-1, Sca-1 is one of the important determinants of cell lineage which is expressed on hematopoietic stem cells which proliferate and differentiate into progenitors that then go on to become various cell lineages. Reports are available which states that aggressive breast cancer tumors express higher levels of this stem cell marker (Welm et al, 2002). Such elevated levels of Sca -1 in the tumors suggest its influential effect on the maintenance of rare cancer stem cells resulting in the prolonged diseased state. The *TERT* (telomerase reverse transcriptase) gene encodes the catalytic subunit of telomerase, which elongates the telomere ends using the RNA subunit TERC as a template (Gulmann et al, 2005). The stabilization of telomere size is a prerequisite for malignant cells to erase the senescence checkpoint and acquire the capacity to proliferate unlimitedly. Thus, telomerase reactivation is an obligatory event in carcinogenesis and, in fact, increased telomerase activity or *TERT* mRNA expression has been detected in up to 90% of human cancers (Shay & Wright, 2005). Presence of high levels of TERT in the tumors explains the plausible reason as to why the cells within a tumor sustain themselves for a longer period until a fully-fledged metastasis happens succumbing the animal to death (Catarino R 2010).

5.1.17 Survival curve and tumor burden of the reporter transgenic animals

To test whether the introduction of the reporter tag, DsRed interfered/affected the life span of the compound mice harbouring this allele; transgenic mice were observed for their mortality rate, general health and parameters regarding tumor incidence were studied. The animals under investigation consisted of C RAF-DsRed and Myc-DsRed mice. Observation for a period of ≥ 2 years demonstrated accelerated death in the DsRed labeled (Myc-DsRed and C RAF-BXB-DsRed) reporter transgenic mice compared to their unlabeled counterpart animals (Fig 23.1 A and B, respectively). Compound reporter mice exhibited the percent survival that significantly differed from the control single SpC c MYC and Double SpCrtTA/Tet O C RAF BXB transgenic mice by log-rank analysis.

This clearly demonstrates that labeling affects the overall life span of the labeled compound animals. The labeled animals start dying in a small interval of time after their birth compared to the non-labeled transgenic animals. These results indicate that DsRed influences the survival of labeled animals. For instance; though there is not much significant difference in the C RAF BXB- DsRed Quadro Vs SpC rtTA /Tet O C RAF BXB in terms of their median survival values but there is a tendency that prevails (Median survival C RAF BXB-DsRed = 54 and Tet O C RAF BXB = 56). In the case of Myc-DsRed Quadro Vs SpC c Myc animals analyzed there occurs a significant difference in their survival pattern due to labeling. The labeled mice die much earlier and have a vast difference in their median survival values (Median survival Myc-DsRed Quadro = 51 and SpC c Myc = 77.5).

Kaplan-Meier : Survival proportions

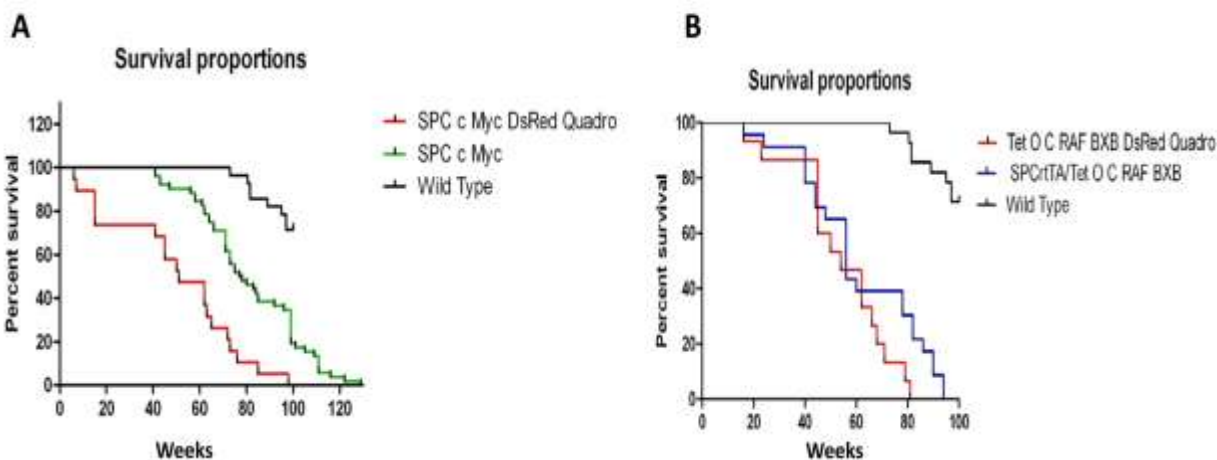


Fig 23.1 Kaplan-Meier plot for (A) Myc-DsRed (n = 19), SpC c MYC (n = 52), and (B) C RAF BXB-DsRed (n=15), SpCrtTA/Tet O C RAF BXB (n= 23).

Wild type (n = 28) littermate control mice. Log-rank analysis for percent survival for labeled compound mice Myc-DsRed vs SpC-c Myc = $p > 0.05$; labeled C RAF BXB-DsRed Vs SpCrtTA/Tet O C RAF BXB = $p < 0.0001$. n= number of animals.

Another important observation that came to our knowledge is that the majority of the DsRed labeled animals (analysed ~8-12 months) indicated reduced incidence of tumor burden (Fig 23.2 A and B). More-over the size of the tumors generated from the labeled animals showed a marked decrease in its overall area occupying the lung; when compared with the tumor foci obtained from the non-labeled transgenic mice (Fig 23.2 C). H&E section of the lungs from the transgenic animals was analyzed for the presence of tumor and the tumor sizes were compared with the indicated animals for their specific genotype. The figure displays the representative examples of lung sections analysed from the animals that were generated for the project.

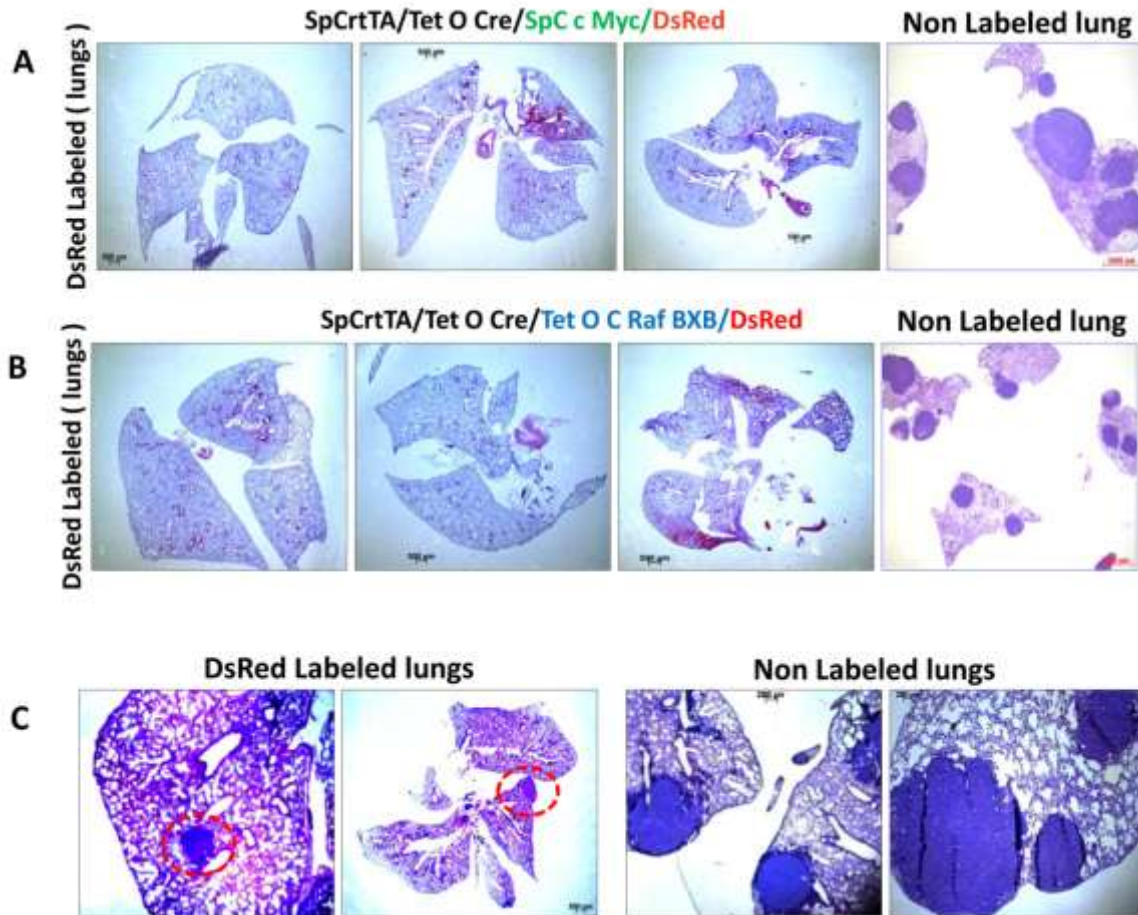


Fig 23.2 Labeling the lungs of the transgenic animals with DsRed decreases the tumor incidence and tumor size in the compound transgenic reporter mice. H&E stained lung sections (formalin fixed) were analysed for the presence of tumor foci (A and B). Most of the labeled lungs showed complete absence of tumor when compared to the age matched non-labeled lungs. (C) Tumor size also decreased in the labeled lungs when compared to the unlabeled tumors of the age matched transgenic animals. (Age group ranging from 8 to 12 months)

Put together the existing data obtained from a cohort of animals clearly indicate that DsRed (First Generation DsRed, Clontech™) expression interferes with CRafBxB and c Myc induced tumorigenesis in the lung and influences the survival of labeled animals.

5.2 Analysis of liver metastases

As we have previously determined the expression of DsRed in the primary tumor, our goal was to trace the fate of DsRed labeled cells and to identify their expression at the secondary sites elsewhere in the body as in the case of metastatic development in the compound reporter transgenic mice that were generated for this purpose. We examined mice for metastasis starting from the age of 12 to 15 months. None of the C RAF-BXB-DsRed mice developed metastasis. Consistent with the frequency of metastasis, in a cohort of 10 inducible Myc-BXB-DsRed compound reporter mice that were induced 12-18 months, one mouse developed multiple macroscopic liver metastases (Fig 24.1).

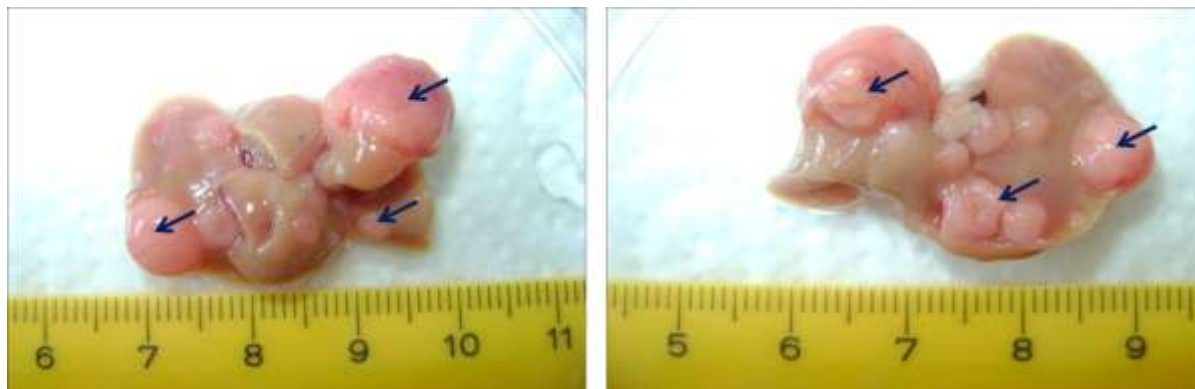


Fig 24.1 Macrometastases in the liver of a Myc-BXB-DsRed mouse (17 months). Whole liver photograph shows macroscopic tumor nodules on the liver (arrows with front and back view)

5.2.1 Anatomical and morphological characterization of the metastatic lesions

On histopathological examination of metastases via an H & E staining on paraffin embedded liver sections; we find three types of metastasis prevailing in the liver. Cystic, mixed-cystic papillary and papillary (Fig 24.2). On closer examination, we found that the central portion of the cysts contained empty vacuole like gaps and tumor cells were found predominantly outside the well-developed fibrous capsules in the liver. While the cystic metastases have an intact periphery, papillary projections were usually recognized within the cystic lesions of the mixed cystic papillary

metastases. Whereas papillary metastases have condensed cellular architecture with compact tumor cells composed of columnar cells resembling that of the primary tumor. Interestingly streaming single cells and clusters of cells were found scattered in the liver, indicative of initial seeds in metastatic colonization. Furthermore, to evaluate the presence of the lineage tag DsRed and the type II cell in the liver metastases, immunoblotting was performed using the protein lysates obtained from the primary lung tumor and the liver metastases. Actin served as the loading control. Interestingly both SpC and DsRed protein were detected in the primary tumor as well in its metastatic derivative (Fig 24.2). To facilitate tracking of both DsRed positive tumor cells and lineage tagged SpC derived cells in vivo, metastatic lesions were immunostained with the DsRed and SpC antibodies respectively. Subsequent results would focus on the expression pattern of SpC and DsRed in the different subtypes of liver metastases.

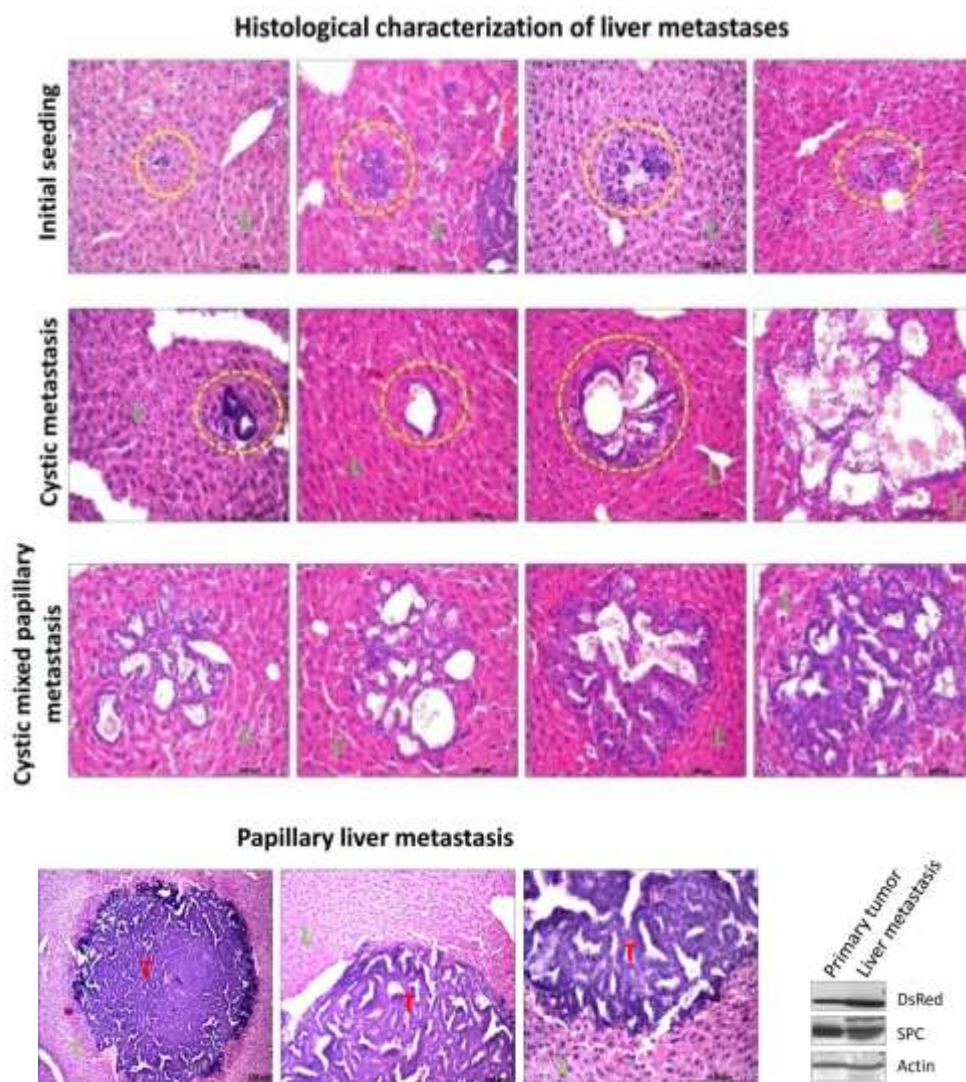


Fig 24.2 Histological analysis of the liver metastases from 17 months induced Myc-BXB-DsRed mouse shows the presence of three types of metastatic lesions viz. cystic, mixed cystic papillary and papillary metastases. Small clusters of foreign cells are also found streaming in the liver (yellow circles depicts the small clusters and cystic metastasis). Cystic lesions have a well defined periphery comprised of the tumor cells enclosing an empty space like structure. Cystic mixed papillary lesions have a less organized structure with small papillary like projections invading/protruding the adjacent/nearby liver. As the cysts advances to a papillary metastases; the space within the lesions becomes less empty and more condensed with the tumor cells making it appear like the primary tumor of the lung resembling the papillary structure composed of columnar cells. (T = tumor and L = liver). Scale bar = 100 μ m. Immunoblot for SpC and DsRed of the primary tumor and its liver metastases.

5.2.2 SpC expression is detected in cystic metastases

Since the primary tumor cells were positive for SpC, we next examined the expression of SpC in the liver metastases. Small clusters of tumor cells were negative for the SpC and the first expression of few SpC positive cells were observed only in the cystic metastasis. Notably, in the stroma-rich border area of the cystic lesions, isolated clusters of tumor cells that were positive for SpC were observed (Figure 24.3) consistent with invasion by collective migration. The number of SpC expressing cells increased in the mixed cystic papillary metastases and advanced in the papillary metastases as abundant SpC positive cells were present in them. This result is consistent with the earlier observation of liver metastases in which few SPC positive cells occur only at the cystic stage (Rapp et al, 2009).

First appearance of SpC expressing Type II cells in the Cystic metastases

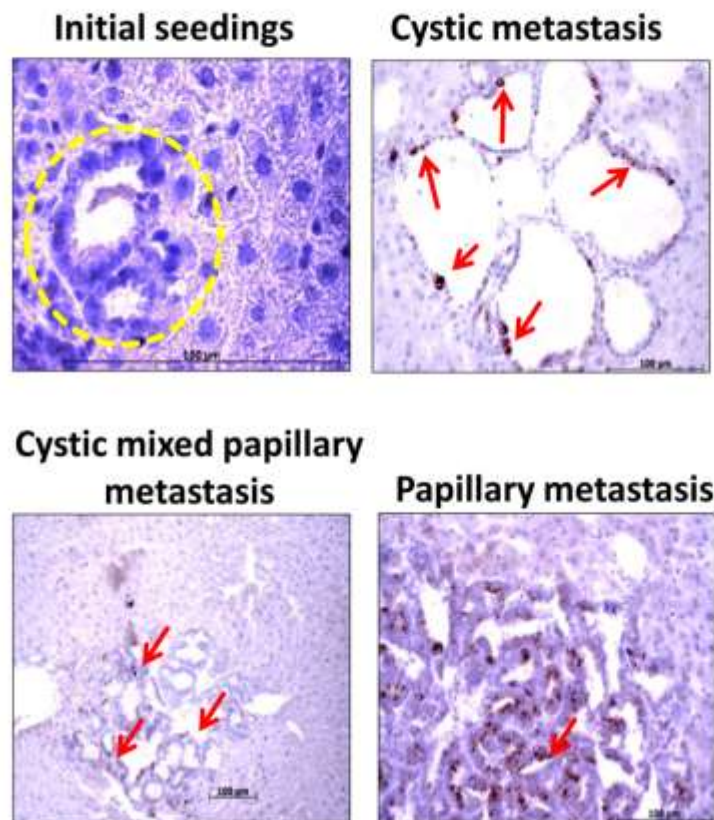


Fig 24.3 SpC expressing type II cells (arrow) are detected only at the cystic metastatic lesions (very few in numbers) and are abundantly found in the papillary metastasis. Paraffin embedded liver metastases was immunostained with the SpC antibody. Small clusters are negative for the SpC expression (yellow circles). Scale bar=100 µm

5.2.3 DsRed is detected in the single cluster of cell including the cystic and the papillary lesions of metastatic colonization

In-order to dissect the involvement of SpC expressing alveolar type II cells, tagged with a DsRed reporter; paraffin embedded liver metastases sections were immunostained with anti-DsRed antibody. Strikingly interesting observations were made by analyzing the distinct pattern of DsRed expressing cells in the metastases. Small clusters comprising of few cells strongly expressed the lineage marker DsRed. Cells contributing to cystic metastases were all positive for DsRed. Individual DsRed positive cells were also observed in the liver other than the metastatic lesions. While cystic metastases were completely DsRed positive, cells comprising the mixed cystic papillary and papillary metastases were heterogenous for DsRed expression (Fig 24.4). This specific pattern of DsRed expression clearly indicates that the cystic lesions are indeed metastases and are solely derived from type II cells. Earlier results for investigating the expression of SpC in metastases identified the cystic metastasis to be negative for SpC expression, yet retaining the DsRed lineage label, identifying them to be originated from type II cell precursors. To further confirm these findings, double immunofluorescence staining was performed on the consecutive metastatic sections with SpC and DsRed antibodies. Clusters of tumor cells and cystic metastases were found to be positive for the lineage label DsRed but haven't gained any SpC expression yet (Fig 24.5). This pattern of DsRed expression in small clusters of tumor cells and cysts in the liver symbolize the initial phase of metastatic colonization where the lineage tagged cells landed in the foreign tissue.

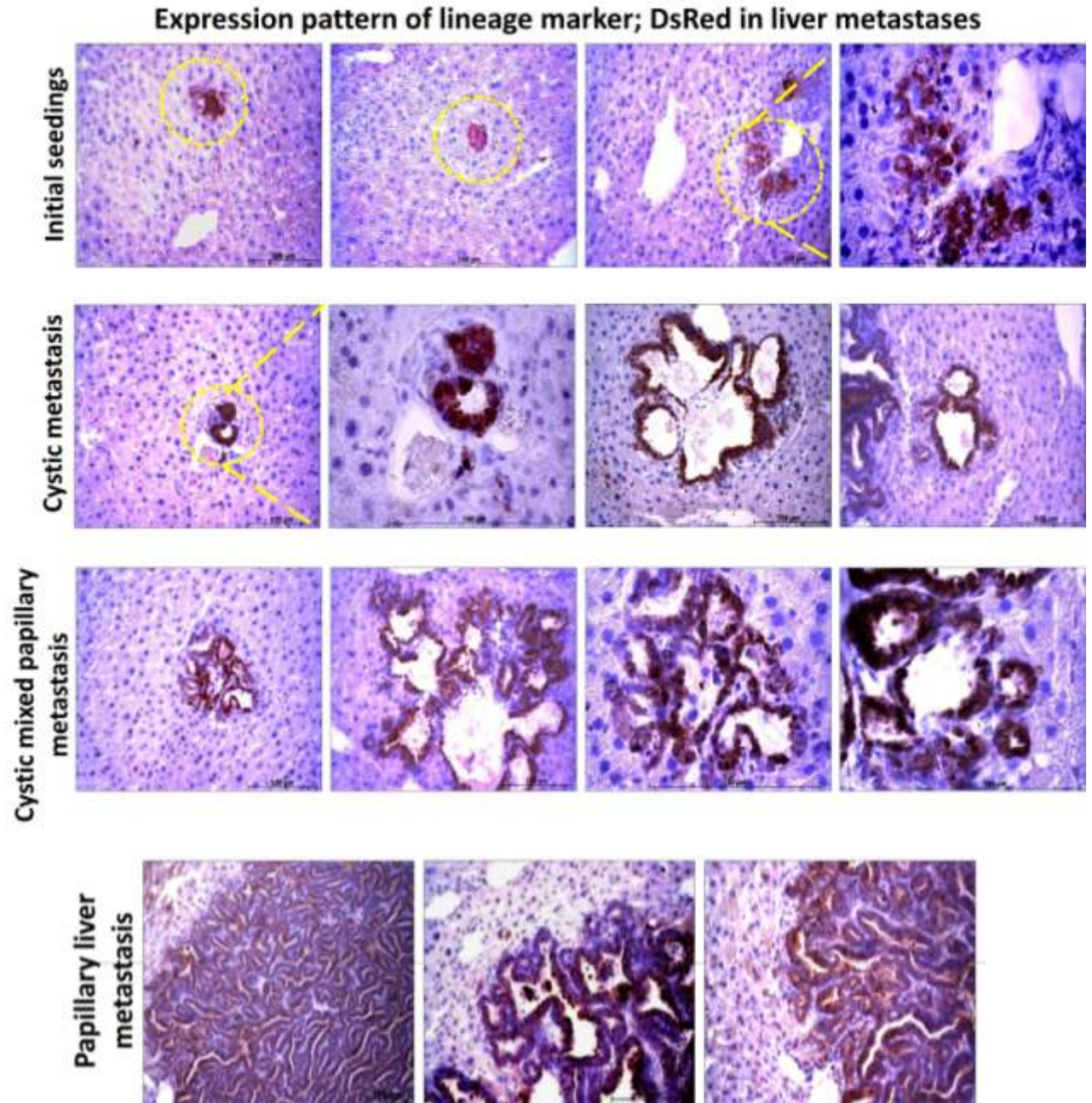
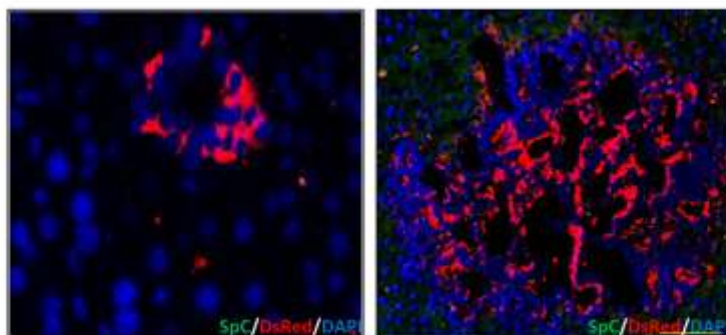


Fig 24.4 Lineage tracing of alveolar type II cells through histochemical analysis of the tagged marker (DsRed) expression in the liver metastases. DsRed is highly detectable in all the subtypes of metastases beginning from the single cluster of cells, including the cystic lesions and the mixed cystic papillary lesions. DsRed acquires a heterogenous expression pattern only in the papillary metastases. Scale bar = 100 μm

Early clusters and Cystic metastasis express DsRed



Emergence of SpC in Cystic metastasis

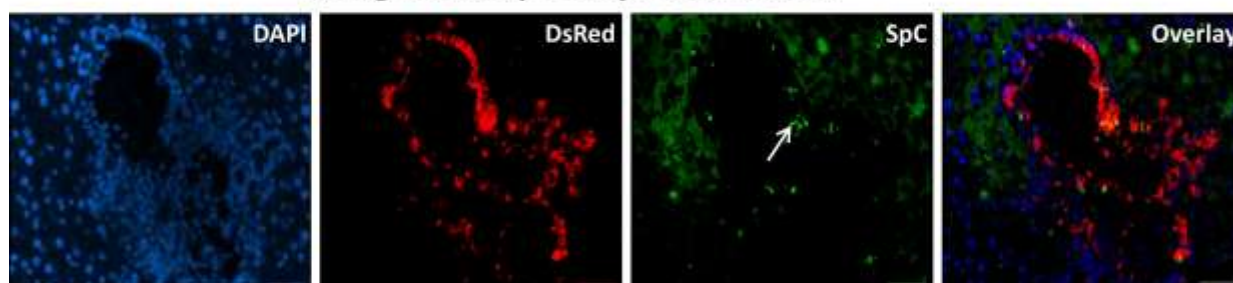


Fig 24.5 Lineage marker DsRed is present in the small clusters and cysts which were still negative for the SpC expression. Cryo embedded liver metastases sections were co-stained with SpC and DsRed antibodies. No double positive cells were observed in the clusters and cysts which retained only DsRed expression, whereas one to two SpC positive cells (white arrow) appear near the papillary projections of a cystic metastasis which is strongly positive for DsRed. Scale bar =100 μ m

5.2.4 Evaluation of metastases for the expression of progenitor markers/lineage selectors

We evaluated additional progenitor markers/lineage selectors for their expression in the metastases. Candidate markers were selected based on their role during lung development and expression in emerging lung foci from compound transgenic reporter mice. These included Transcription factor Gata4, Thyroid transcription factor-1 (TTF-1) ; a tissue-specific transcription factor expressed in the epithelial cells of thyroid and lung (type II pneumocytes and Clara cells) , alveolar type I cell marker; Aquaporin 5, and Protein gene product 9.5 (PGP 9.5); marker for neuroendocrine cells. Liver metastases retained heterogeneous expression of pan-

Cytokeratin, Aquaporin 5, GATA 4 and TTF-1. Pan-Cytokeratin and Aquaporin 5 were expressed in all the subtypes of metastases including small clusters to cystic, mixed cystic papillary and papillary metastasis. Mucin, a target gene of Gata4 is also detected in the metastatic lesions. Finally PGP 9.5 which was identified as a novel marker for tumor vasculature in mouse NSCLC (Rapp et al, 2009) was highly expressed in the vasculature of liver metastases (Fig 24.6). Hence, these markers may therefore be suitable for early detection of metastases of NSCLC.

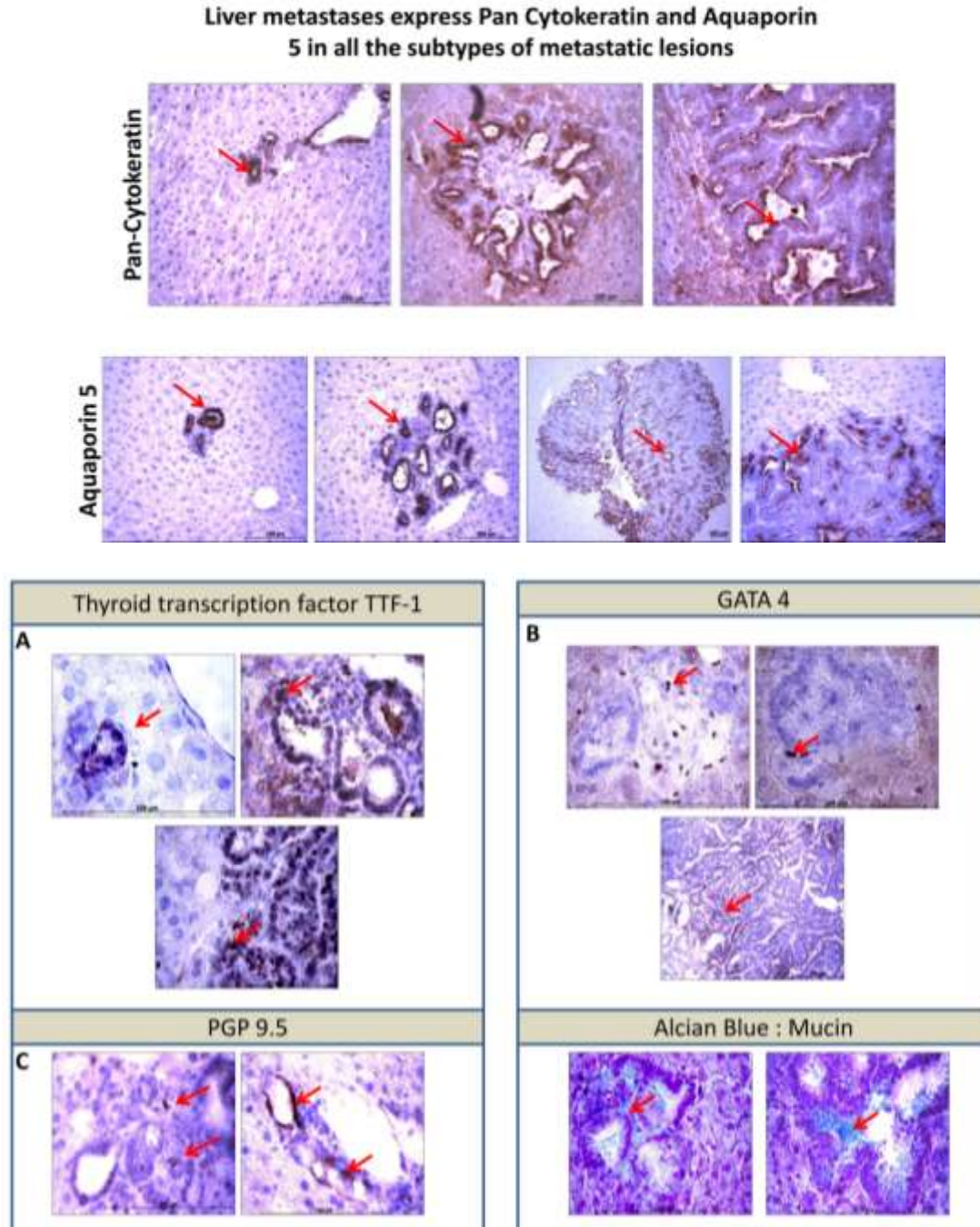


Fig 24.6 Liver metastases express the markers of pulmonary lineage. Lung differentiation markers are indicated. Pan-cytokeratin and Aquaporin 5 (marker for type I cells) are sustained in all the subtypes of metastases. TTF-1 and GATA 4 transcription factors are expressed in the small clusters as well as in the subsequent cystic and papillary metastasis. Mucin, a target gene for GATA 4 is also expressed as Alcian blue positive cells which mark the mucin positive cells (blue). Neuro-endocrine marker PGP 9.5 was present in few cells of the metastases (Brown). Scale bar =100 μ m

5.2.5 Clara cell emerges at the mixed cystic papillary stage of liver metastases

Since a fraction of primary tumors exhibit the columnar cell phenotype, displaying the participation of non-ciliated columnar Clara cells in tumor formation, it was obvious to screen the metastases for the appearance of Clara cell which is one among the cell type (s) responsible for initiating lung adenocarcinoma. Hence, the liver metastases sections were immunostained with a Clara cell marker, CCSP (Clara Cell secretory protein). Small clusters and cystic metastasis were devoid of CCSP expression. Whereas few CCSP expressing cells were detected in the mixed cystic papillary metastases and the CCSP positive cells showed a pronounced increase in their number in the papillary metastases. This clearly indicates that the Clara cells appears late during the metastatic progression, since we have not detected any Clara cell in the initial clusters and cystic metastasis (Fig 24.7). Given the fact that Clara cells are abundantly present in the papillary metastases, we were interested in delineating its origin. Here we exploited the DsRed expression in type II cells, which would facilitate us to know whether the cell originated from alveolar lineage if at all we observe any double positive cell stained for CCSP and DsRed. Subsequently double immuno-fluorescence staining was performed on liver metastases sections for the DsRed and CCSP proteins. No double positive cell was detected indicating that Clara cell evolved from bronchiolar lineage rather than an alveolar one (Fig 24.8).

Expression pattern of Clara cell specific marker; CCSP in liver metastases

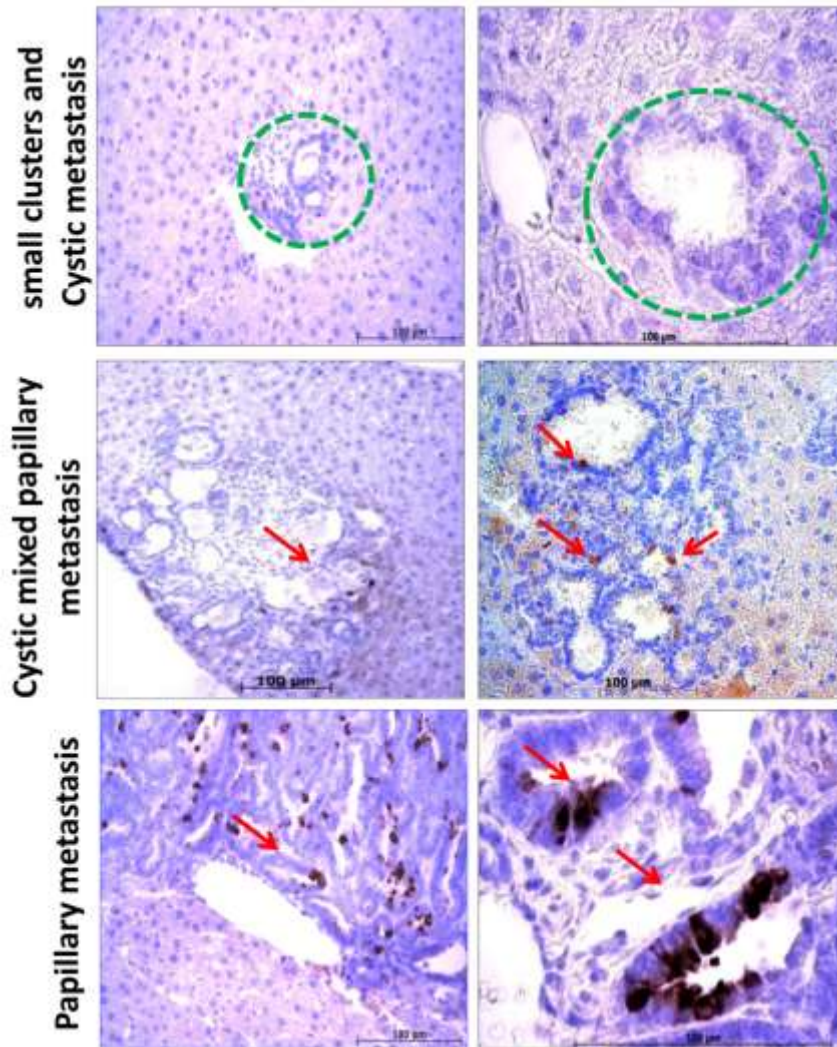


Fig 24.7 Clara cells appear only in the cystic mixed papillary metastases (yet few in number) and is abundantly present in the papillary metastases (red arrows). Small clusters and cystic metastasis are negative for the CCSP expression (green circle). Scale bar =100 µm

Clara cell is not derived from the alveolar (DsRed positive) lineage in the liver metastases

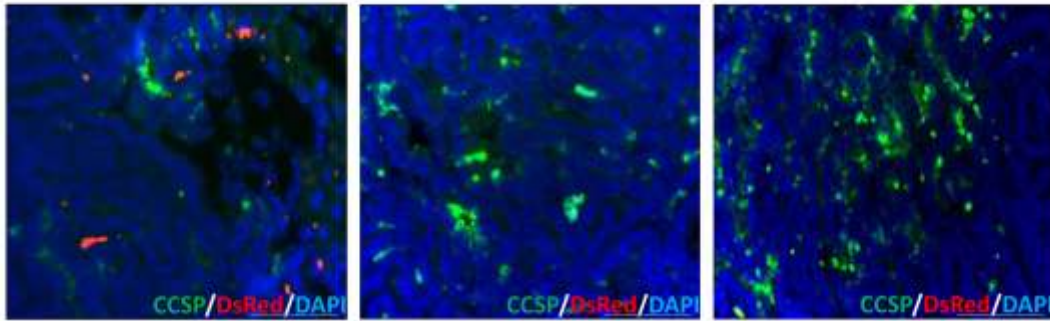
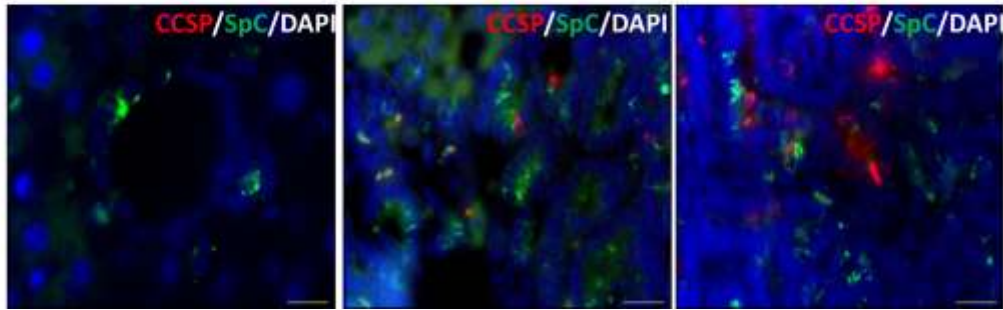


Fig 24.8 Identification of the origin of Clara cell lineage in the liver metastases. Co-immunofluorescence staining with the CCSP and DsRed revealed the absence of any double positive cells which indicates that Clara cells are derived from a bronchiolar lineage rather than from an alveolar one. Scale bar = 50 μ m

5.2.6 Presence of Bronchioalveolar stem cells (BASCs) in the metastases

Above mentioned findings which indicate the presence of CCSP and SpC in liver metastases, gave us an opportunity to screen for the presence of BASCs. While few double positive BASC cells were detected in papillary metastases (Fig 24.9B); cystic metastases were found negative for BASCs (Fig 24.9B). More-over CCSP and DsRed double positive cells were detected in the papillary metastases, again confirming the presence of BASCs, with DsRed as readout for SPC positive cells (Fig 24.9 B). These results suggest that CCSP positive cells in the liver metastases might have been generated by multipotent cells with BASCs as intermediates.

A Absence of BASCs in cystic, mixed cystic papillary and papillary metastases



B

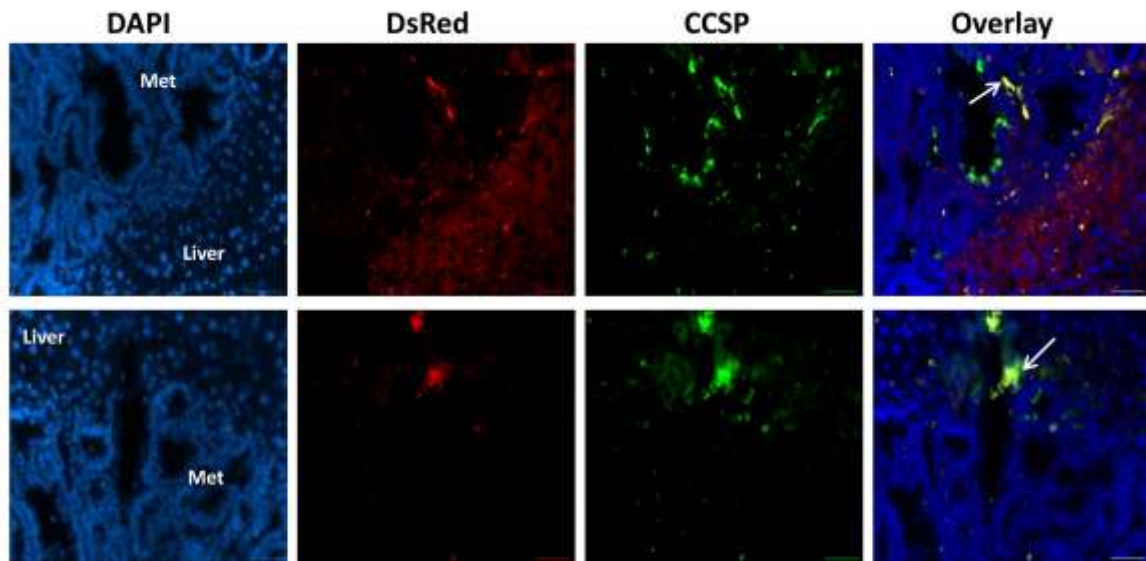


Fig 24.9 No evidence of BASCs within the liver metastases (A) but few BASCs were observed near the periphery of the metastatic lesions (B) indicating the existence of circulating BASCs in the foreign tissue (in this case, liver). Paraffin embedded liver metastases section, co-immunostained with CCSP and SpC (A) and CCSP and DsRed (B). Scale bar = 100 μ m

6 Discussion

6.1 Novel transgenic murine model for lineage tracing of alveolar type II cells in NSCLC metastasis

Lung cancer is the leading cause of cancer deaths worldwide (Jemal et al, 2004) and adenocarcinoma is currently the most common type of lung cancer. Unlike squamous cell carcinoma, the stages of progression have not been well described for adenocarcinoma, and little is known about the cell type of origin or the characteristics of precursor lesions of pulmonary adenocarcinoma. Mouse models are well suited to sample distinct cell populations for their propensity to give rise to specific tumors (Visvader, 2011). Such approach has been nicely demonstrated in pancreatic cancer models using cell type-specific Cre expression (Gidekel Friedlander et al, 2009; Wang et al, 2009). Here, we have addressed this question in lung focusing on the likely cell of origin of NSCLC via a genetic lineage tracing approach.

Cell turnover in the adult lung is normally very low (Kauffman, 1980). However, epithelial injury elicits rapid proliferation of surviving cells, and the tissue is soon repaired. Several lines of evidence suggest that alveolar epithelium is repaired by the type II cells, hence serving as the progenitor cells (Kauffman, 1974). Despite the evidence that type II cells are the progenitor cells of the alveolar epithelium compartment; relatively little is known about their biology and the mechanisms regulating their behavior and participation in the metastatic progression in malignant tumors. To address this issue, we have generated a transgenic mouse line to more efficiently lineage trace and genetically manipulate alveolar type II pneumocytes. To target alveolar type II cells, we chose to use the Cre-loxP system, which is an effective method for expressing or deleting a target gene in Cre-expressing cells. We generated a series of compound mice lines expressing Cre recombinase from specific lung alveolar epithelial type II cell promoter, SpC. The attempt to study the metastatic potential of type II cells was determined through introduction of a genetic tag into SpC expressing cells of the alveolar epithelium. This model used the SpC

rtTA/Tet O Cre transgene in combination with the Lac Z floxed DsRed allele to generate tagged SpC expressing cells. Regulation of the recombined allele by the ubiquitous Chicken beta actin promoter allowed expression of the lineage tag in all cells derived from a SpC expressing progenitor cell. We introduced a new line in which a 37 kb human Surfactant Protein C (SpC) promoter drives Cre. We used this allele, in combination with the *lacZ/DsRed reporter*, to lineage trace alveolar type II cells in adult mice. Soon after the induction, most of the labeled cells (65%) were scored as type II cells (data not shown). This is the first report of genetic lineage tracing studies by doxycycline inducible expression of Cre in SpC expressing type II cells.

We made bi-transgenic mice expressing *SpCrtTA and Tet O Cre* under the control of the same *SpC* promoter elements (Fig 8.1). Crossing the *SPCrtTA/Tet O Cre* mouse line to the *Actin Lac Z/DsRed* reporter strain and exposing the adult offspring to doxycycline gave widespread activation of the heritable reporter gene in alveolar epithelial type II cells throughout the airways (Fig 9.1 and 9.2) The DsRed tag was identified at the nucleo-cytoplasmic membrane of type II cells. Tagged type II cells displayed fair distribution throughout the lung. Sections were stained SpC which is expressed by type II cells and DsRed, which strongly labels type II cells; to confirm that recombination of the reporter gene was restricted to type II cells (Fig 10.3 C). The proportion of type II cells that were lineage-labeled varied from 65% to 70%. The lineage-labeled cells were visualized by using DsRed staining and colabeled with SpC (marker for type II cells). Within the non-neoplastic lungs, the tagging system is highly specific for type II cells. DsRed expression was not observed in the Clara cells of the bronchioles (Fig 9.3 A).

Cellular heterogeneity is a common histopathologic feature in lung cancer. Cancer cells undertake progressive morphologic and behavioral changes during disease progression and metastasis. Because these changes are often correlated with the malignant state of the disease, investigating the morphologic and behavioral alterations may reveal clues to the mechanism by which tumor cells acquire more aggressive phenotype and metastatic potential. Subsequently with our transgenic

strategy, we tagged the cancer cells with red fluorescent protein to sensitively detect tumor cell metastasis in the mouse and to identify cancer cells that adopted significant morphologic changes. Fluorescence protein tagging is also a sensitive technique to track xenograft tumor cells metastasis. To identify, purify and track the fate of type II cell progenitors, this lineage tracing approach with a Cre/loxP system has enabled us to mark irreversibly SpC expressing type II cells and their differentiated progeny in the context of tumor progression and metastasis. Cre expression from the tet-o- locus mediates the excision of the floxed stop sequence on the chicken beta actin flox lac Z DsRed reporter compound transgenic resulting in the irreversible expression of the DsRed MST (DsRed-MST is a variant DsRed protein) in type II progenitors and their differentiated progeny. Immunostaining displayed co-expression of SpC and DsRed in the cells obtained from the induced triple transgenic mice (DsRed). To obtain purified populations of type II progenitors, we isolated DsRed cells by fluorescence-activated cell sorting (FACS) and were able to culture them under special regimes.

Earlier results of lineage tracing in the developing lung, using a transgene driven by a regulatory region of the human *SpC* gene, are consistent with the presence of a multipotent epithelial population, but suggest that it does not include progenitors of NE (Neuro Endocrine) cells (Perl et al, 2002b).

Current study provides an in vivo description of an adult proliferative differentiated cell compartment (ie. The alveolar epithelium) where we have observed a specific population, identified by *DsRed* expression in the liver metastasis that enables us to explore the contribution of type II cells in the metastatic colonization in NSCLC model.

6.2 Alveolar type II cells in NSCLC tumor initiation; perspective and facts

The cell of origin of pulmonary adenocarcinomas remains unknown and candidates include multipotent stem cells, Clara cells, and alveolar type II cells (Dermer, 1982). Human pulmonary adenocarcinomas are classified into six cytologic subtypes including both Clara cell type and alveolar type II cell type (Kobayashi et al, 1990),

suggesting different cells of origin. Tumors might arise from Clara cells, alveolar type II cells, multipotent stem cells, or from derivative lineages from these cells (Beer & Malkinson, 1985; Jackson et al, 2001; Magdaleno et al, 1998; Mason et al, 2000; Rehm et al, 1991; Thaete & Malkinson, 1991). Most often, the cell of origin of a lung tumor is determined by immunohistochemical staining with anti-SpC antibodies marking the alveolar type II cell lineage and anti-CC10 antibodies that identify cells from the Clara cell lineage. There is, however, increasing evidence that tumor cells can transdifferentiate or down regulate CC10 expression (Linnoila et al, 2000; Wikenheiser & Whitsett, 1997). The staining with these lineage markers might therefore not necessarily identify the cell of origin of the tumor. Solid tumors appear to originate from alveolar type II cells, but the origin of papillary tumors remains unclear (Malkinson, 1991). Papillary adenocarcinomas can express either SpC or Clara cell-specific markers (Thaete & Malkinson, 1990). Interestingly, both solid and papillary adenocarcinomas developed in CCSP, as well as in SpC Tag transgenic mice. This supports an argument in favor of a common multipotent precursor cell and/or transdifferentiation (Wikenheiser et al, 1992) for NSCLC.

In an attempt to get closer to identifying candidate target genes in our mouse models generated, doxycycline administration to the transgenic mice (C RAF BXB-DsRed, Myc-DsRed and Myc-BXB-DsRed) marked SpC expressing type II cells in a mosaic fashion and led to the generation of labeled progeny. Compound transgenic reporter mice gave rise to lung tumors with cuboidal, papillary and mixed cuboidal-papillary tumor cells. Expression of DsRed in these tumors functioned as a readout for SpC expression. Immunohistochemical analysis of the tumor cells for the expression of cell type-specific and lineage marker revealed prominent results. Consistent with the DsRed expression in all the tumor types, SpC expression was also detected in cuboidal as well as in columnar cell tumors. Next, we examined expression of TTF-1, a homeodomain transcription factor known to be involved in lung development and in SpC expression. TTF-1 nuclear staining was also detectable in the columnar cells of papillary tumors. Although type II cells appear the predominant cancer-initiating population in NSCLC, our data also support the presence of a SpC positive progenitor cell population that can give rise to NSCLC following overexpression of c

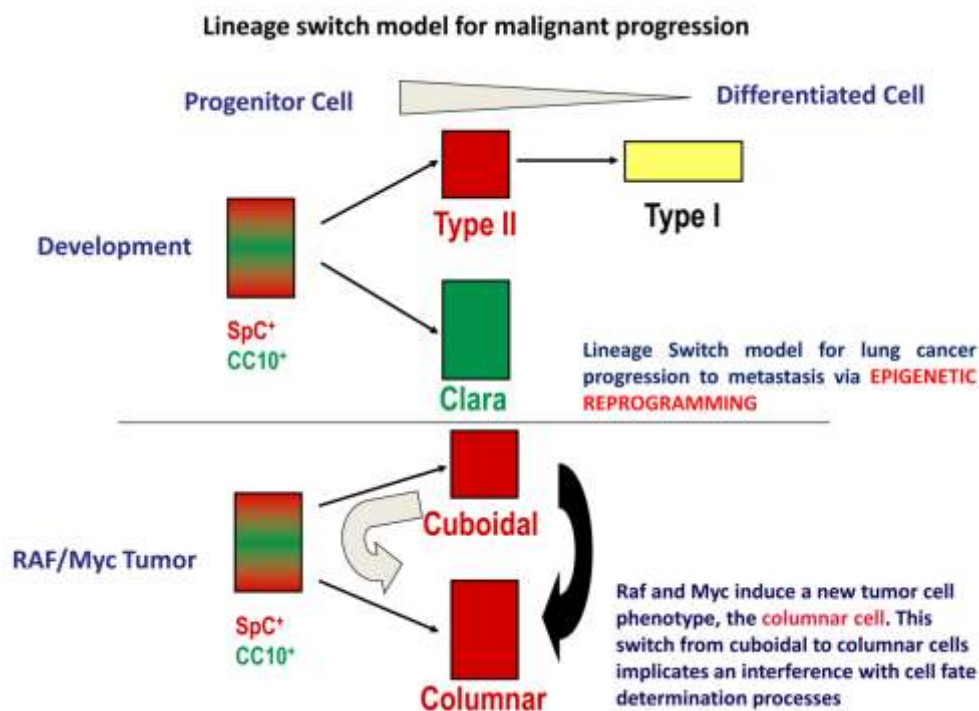
Myc and C RAF switch albeit with a lower penetrance; as evidenced by the fact that we detected a fraction of tumor cells always positive for DsRed. This observation implies that there might be a population of SpC positive cells that, upon gain of C RAF activation and c Myc amplification, acquire the capacity to give rise to NSCLC.

Another cell type that immediately comes to mind is the Bronchio-alveolar stem cell (BASC). BASCs have been proposed to be the cell of origin of K-ras-induced NSCLC (Kim et al, 2005). This rare cell type located at the Bronchio-alveolar duct junction (BADJ) expresses both CCSP and SpC, and thus would be targeted by our SpCrtTA/Tet O Cre system.

The double immunofluorescence experiments in the current study clearly demonstrate the existence of SpC/CCSP double-positive cells within the tumors. These findings shed new light lead us to propose the existence of a pathway in the development of adenomas in which tumors arise from a cell type with characteristics of both Clara cells and type II cells. There are two possible models to describe this pathway. In the first model, oncogene activation induces hyperproliferation of Clara cells, which then undergo transdifferentiation as they move into the alveolar compartment. An alternative model is that may be these intermediate cells are the consequence of *K-ras* activation in a stem cell that has the potential to develop into either Clara cells or alveolar type II cells. Hyperplasia of such a cell type could give rise to adenomas in later time points. It is more likely that other cell types that express CCSP have the capacity to give rise to NSCLC. In this respect, it is noteworthy that a fraction of the NSCLC tumors also expresses CCSP, suggesting that CCSP is expressed in the lineage of the cell of origin of NSCLC. This indicates to the existence of an early progenitor that expresses low levels of CCSP and has the capacity to differentiate along the alveolar lineage. This could be a common progenitor residing in the lung or a committed progenitor that trans-differentiates under pressure of the concomitant expression of c Myc. In support of this hypothesis, it is interesting to note that there is evidence for a multipotent progenitor cell in the immature and developing lung (Rawlins et al, 2009a; Wuenschell et al, 1996). One can also not underestimate the influence specific genetic mutations may

have on the target cell. *c Myc* is a critical controller of cell differentiation and is a reprogramming factor and induces a lineage switch in the cell fate determination process. Its overexpression loss could be a mechanism by which a progenitor-like AT2 cell could differentiate toward a more Neuro-epithelial and bronchiolar cell-like state. (Fig.20). A primary tumor's metastatic propensity may be dictated in large measure by transforming oncogenes that are active early in tumorigenesis (and regulate the expression of prognostic signatures) rather than solely by metastasis enabling mutations per se, which supposedly arise in rare metastatic precursors later in tumor progression (Ramaswamy et al, 2003). Most transforming oncogenes ultimately drive *Myc* expression either directly or indirectly thus assuring that deregulation of the *Myc* pathway is one of the most common features of human tumorigenesis. The *Myc* oncoprotein confers a selective advantage on cancer cells in differing contexts by promoting proliferation, cell survival, differentiation blockade, epithelial to mesenchymal transition and genetic instability, all of which can contribute to metastasis indirectly. (Grandori et al, 2000). *Myc* is also a powerful reprogramming factor that can determine normal and cancer cell differentiation (Takahashi & Yamanaka, 2006). Cancer cells in an undifferentiated, more stem-like state might more easily migrate to and seed distant sites therefore promoting metastasis.

A



B

Columnar cells in the c Myc mediated primary tumor express SpC but negative for the Clara cell marker, CCSP

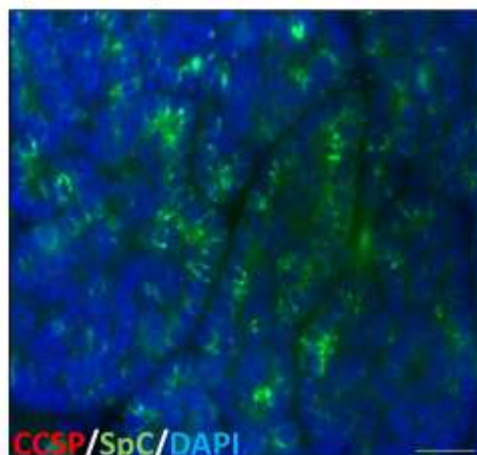


Fig 25 (A) The proposed model which demonstrate the existence of a common multipotent progenitor cell exhibiting the phenotype that expresses both SpC and CCSP and finally differentiates into Clara cells and type II cells during the development of the pulmonary epithelium. In the case of tumorigenesis with the introduction of c Myc in particular, interferes with the normal cell fate determination process and reprograms the progenitor cell contained in the neoplasias to acquire a columnar phenotype, yet producing SPC (Fig 25 B)

It should be noted that it is unlikely that every SpC positive cell has the capacity to develop a tumor with alveolar features following the overexpression of c Myc and C RAF. Instead, the susceptibility of a subset of SpC positive cells to tumor development might be a consequence of intrinsic capabilities inherent to progenitor cells.

6.3 Contribution of alveolar type II cells in the metastases; an insight

Although SpC positive type II cells were abundantly found in the lung tumors generated from the inducible expression of oncogenic C RAF and constitutive expression of c Myc; it was unknown whether these cells represent a specialized population in the metastasis and at what stages of metastatic progression, one can detect type II cells in them. We asked whether DsRed positive progeny of the type II cells, persisted in the metastases. After 17 months of induction, macrometastasis in the liver was observed comprising of multiple tumor nodules visualized by the naked eyes (Fig 24.1). Although DsRed protein was readily detected in the liver metastases (Fig 24.2) we wanted to explore its localization and distribution pattern in the metastases via further experimental approach.

On histopathological examination of the liver metastases, three predominant subtypes were observed; cystic, mixed cystic papillary and papillary forms (Fig 24.2). Commonly all the three forms coexist in the same target organ. Whether these forms can interconvert or whether cysts are early precursor forms of mixed cystic-papillary metastasis was so far unknown. Micrometastatic clusters of DsRed positive cells attached to each other were also observed (Fig 24.4, initial seedings) demonstrating that single emboli could have invaded from the primary tumor site and reached the liver as a cluster. The presence of DsRed positive cluster of cells in the cystic metastasis suggests that these have been originated from the SpC producing type II cells. This shows that the resulting metastases were clonal at this

stage of cystic appearance which suggests that these cystic metastases might have resulted from the proliferation of a single viable DsRed positive cell (type II) within a circulating tumor embolus which is likely to be homogenous for DsRed expression, because it might have been originated from a clonal zone of a DsRed positive primary neoplasm. However the fact that we found many purely cystic liver metastases which shows DsRed positive cells in the lining epithelium (Fig 24.4) argues that cysts may be a transitional state to development of frank malignancy. Hence with our lineage tracing results in metastases, we propose that cysts are the precursors of advanced liver metastases.

Of the metastatic lesions observed, only cystic lesions uniformly expressed DsRed in all the cells comprising the lesions and small clusters indicative of type II cells origin. Papillary lesions displayed heterogenous distribution of DsRed among the cells, which states the fact that cell types of other lineage have participated in the tumor formation that might include endothelial cells, macrophages, stromal cells and other cells types of the lung. These lesions express SpC and TTF-1, characteristics of early progenitor markers. GATA4 transcription factor is also expressed and its direct target gene mucin as evident by the Alcian blue positive cells in the metastatic lesions. The expression of these early progenitor markers within the metastases strongly supports the existence of cells; characteristics of early cancer precursors.

The presence of up to 5 to 10 cells in clusters of DsRed positive cells in some regions within the liver indicates that the originally labeled cells are going through multiple rounds of duplication and self-renewal. Moreover we noticed that few SpC cells emerge late at a stage in a cystic lesion and advanced in the mixed cystic papillary metastases; whereas DsRed positive cells were fully prevalent right from the single cell seedings to the small clusters and cystic metastases (Fig 24.4). However, in the papillary metastasis, heterogeneity in the DsRed expression has been observed (Fig 24.4). Analysis of metastases for the expression the Clara cell marker CCSP revealed that the small clusters and cystic metastases which were all found to

be positive for the lineage label DsRed; were negative for the CCSP expression. Few Clara cells appeared only in the mixed cystic papillary metastases and subsequently their number increased in the papillary metastases. This shows that the occurrence of bronchiolar lineage in the liver metastases is not an early event and Clara cells populate the metastases, once a full-fledged metastatic colonization has been established.

Type II pneumocytes : contribution towards malignancy

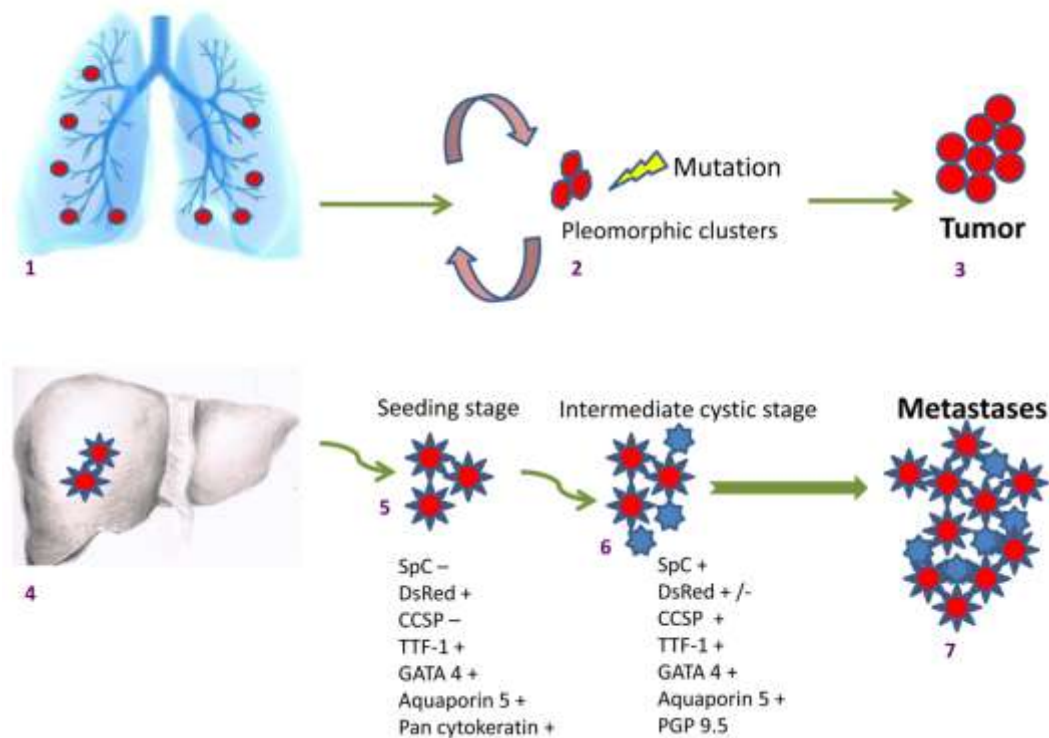


Fig 26 Lineage tracing of metastasis reveals the contribution of lineage tagged DsRed positive alveolar type II cells. type II cells of the lung were labeled with DsRed which are expressed in the pleomorphic clusters of the premalignant lesions (2) which are in a constant state of proliferation and dying, unless hit by a mutation (K Ras or loss of LKB 1B) which with c Myc as a driver forms a primary tumor in the lung expressing DsRed (3). Upon long term sustainance of the oncogene, finally results in metastasis in the liver (4) and displays differential expression of the early progenitor and lineage markers (5 and 6) and finally culminating to a papillary metastases with the lesions exactly resembling the primary tumor (7). Red stars = DsRed positive type II cells.

The fact that liver metastasis and primary tumours share markers of alveolar lineage, DsRed, and others which include, TTF-1 and Aquaporin 5, suggests that aggressive malignant cell progenies are derived from a parental primary tumour. This is in accordance with the fact that metastatic and primary tumours share somatic mutations. In view of this the assumption that primary and metastatic tumours have common ancestry is inherent in the design of systemic treatment strategies for advanced cancers. Important examples include *HER2* amplification in breast cancers and their subsequent lymph node or distant organ metastasis (Strien et al, 2010). Hence our findings that has been focused on characterizing the cell type(s) contributing to metastasis demonstrate that alveolar type II cells are one among the other unknown cell types, which harbours the potential in context to metastatic colonization, since we have identified single DsRed positive cells streaming in the liver, and abundant and strong DsRed expression in several small clusters including the cystic metastases.

6.4 Putative metastatic initiating cells; contribution of the alveolar lineage

With our lineage tracing approach we were able to show that the oral administration of doxycycline induces the expression of Cre that rapidly mediates excision of the transcriptional roadblock by catalyzing recombination across the flanking LoxP sites. The DsRed reporter gene is thereby activated in the SPC producing type II cells and subsequently transmitted to their progeny as they repopulate the tissue during normal homeostasis (in non neoplastic, DsRed animals) and in tumor formation. Because the DsRed labeled, SPC positive type II cells are progenitors of the alveolar epithelium, they would continuously generate DsRed progeny, which contributes to tissue renewal over the entire lifetime of the mouse and would also exhibit its expression in the very late stages of abnormalities as in the case of metastasis formation. However it is not possible to rule out the existence of undifferentiated progenitor compartment existing and such a pool does

contribute to the metastasis at late stages once the tumor cell has been recruited at a foreign site.

In view of this our data support the existence of three progenitor cell pool in pulmonary epithelium of the lung which acts as a putative metastatic initiating cell. First is an actively proliferating stem cell compartment responsible for the daily maintenance of the alveolar and the bronchiolar epithelium that is characterized by the expression of SpC and CCSP; preferably termed as BASCs. (Fig 27 A)

In accordance with this, it would be highly justifiable to rely on the notion that the cancer stem cells may be the source of metastasis based on the assumption that these cells are rare, resistant to therapy and therefore responsible for cancer recurrences (Reya et al, 2001). It is also presumed that the capacity to self-renew is required not only during primary tumorigenesis but also for the re-initiation of growth by disseminated cancer cells. In line of these assumptions, we were able detect few BASCs in the primary tumor as well as in the papillary metastasis. Second is the SPC expressing cuboidal type II cells that later acquire a columnar phenotype (Fig 27 B). Once the cells attain a bronchiolar like columnar structure, it starts producing CCSP, to sustain it throughout. The negative expression of CCSP in the columnar tumor cells that are still positive for SpC (Fig 25 B) proves this hypothesis that tumor cell acquires a more aggressive phenotype, (the columnar cells which forms a major cell mass of the papillary tumors in advanced cancers) during later stages of malignancy. Third is the SpC expressing columnar type II cells that later acquire a cuboidal phenotype and gain some neuroendocrine feature (Fig 27C).

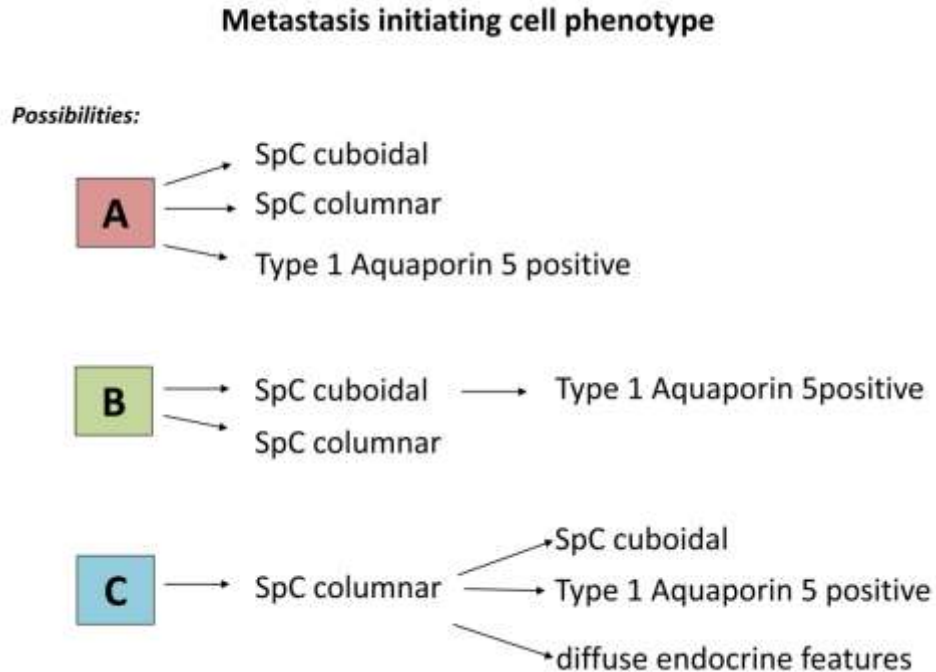


Fig 27 Proposed identity of the cell types responsible for metastasis in the NSCLC model.

Nevertheless, metastases formed from a primary tumor most probably as the result of a complex interplay of several factors: the initial transforming mutation and additional mutations in subpopulations of the primary tumor, the genetic background of the organism and the cell type from which the tumor develops and the response of the host to the tumor in terms of innate tumor immunity and inflammation as well as the constitution of the stroma. The crucial point is that in most cases none of these factors alone is sufficient to determine whether a metastasis actually forms or not.

7 Critical parameters, troubleshooting and time considerations

In the compound transgenic reporter lungs, (Myc-BXB-DsRed, C RAF BXB-DsRed and Myc-DsRed) there are certain region in the primary tumors where the expression of Cre is silenced (i.e. there occurred a silence of the knock-in allele in a region-dependent fashion). Hence there prevails a population of cells that are Cre escapers. Even the transgenes are not 100 % activated in all the type II cells. Such variegated expression of transgenes is commonly observed in the lungs derived from the compound reporter mice.

The Myc-BXB-DsRed, C RAF BXB-DsRed and Myc-DsRed mice are only viable as heterozygotes. Apart from that, DsRed bred to homozygosity leads to the death of the littermates (prenatal as well as post natal). In vivo lineage tracing is therefore always performed with DsRed-*het* mice. Nevertheless, in principle, in vivo lineage tracing can be performed using SpCrtTA/Tet O Cre/Tet O C RAF BXB/SpCc Myc/DsRed mice in combination with any inducible reporter mouse strain that is activated using standard Cre/*loxP* technology.

The dose of doxycycline used to induce adult transgenic reporter mice (500 mg/kg body weight via DOX food) is shown to achieve stochastic activation of the *DsRed/Lac Z* reporter gene within the SPC positive population of the lung. Higher doses of doxycycline may be used to increase the frequency of lineage tracing if desired (But not tested in the current study).

Advantage of labeling

Given that the SPC positive cells belong to a progenitor cell compartment, the frequency of DsRed positive alveolar epithelial type II units present will remain constant even after the alveolar epithelium has undergone multiple rounds of complete renewal. Thus, we expect to see multiple tracing units even 24 months after induction. (As in the case of metastases development which takes approx. more than 12 months)

Time considerations and Animal numbers

Generation of Triple, Quadra and Penta Transgenic mice via multiple rounds of inter breeding takes more than a year to get statistically justifiable number of animals for the experiments. Induction of the transgenic reporter mice for tumor development takes 9 to 13 months and metastasis being a late event is usually observed between 15 to 24 months. Hence the current project with animal generation and their analysis takes more than 3 years to conclude something reproducible about the outcome of the present study.

Due to shifting of the complete animal facility twice in two different years (from MSZ, Würzburg) to Charles River laboratories and from Charles River labs to *Max-Planck-Institut für Herz- und Lungenforschung, Bad Nauheim*; it was very difficult to control the number of animals available to me for carrying out the experiments, in a statistically justifiable number at regular time points. Hence the data presented are the representative analysis and findings that I observed in a small group of animals analyzed during this time period. Additionally, a severe contamination/infection in the Animal Facility (year 2011) prohibited us to get access to more number of animals (cessation of breeding and harvesting) to reproduce the results including large number of animals that was initially generated for the project.

Here I describe the number of animals that were incorporated for studies that represent the results section.

Total compound transgenic reporter animals generated for the project includes 49 Quadra Myc-DsRed mice (20 dead), 62 Quadra C RAF-DsRed (15 dead) and 11 Penta Myc-BXB-DsRed (1 dead).

Induction of the transgenic animals lead us to the following number of animals that were ready to be analysed after they reached the required age for being harvested. 29 Myc-DsRed, 47 C RAF-DsRed and 10 Myc-BXB-DsRed animals. 15 animals were analysed from the two groups i.e. Myc-DsRed and C RAF-DsRed that reached the age of ≥ 12 months and between 9 to 12 months, respectively. 2 animals developed tumors in Myc-DsRed mice (13%), 5 animals developed tumors in C

RAF-DsRed (33%) and 2 animals developed tumors and 1 of them developed macro liver metastasis in Myc-BXB-DsRed mice from 10 animals.

The results described are the representative data from the tumor bearing animals as well as the lungs of the transgenic compound reporter mice; that were processed for experimental procedures.

1. Section 5.1.3: representative data from a group of 5 animals.
2. Section 5.1.4: representative data from a group of 3 tumor bearing animals. analyzed, whereas, fig 12.4 and fig 12.5 are the results from 10 animals.
3. Section 5.1.5 which includes, fig 13.1 and fig 13.2 are the representative for 2 animals.
4. Section 5.1.6: representative data from 5 animals (fig 13.3).
5. Section 5.1.7: representative data from 2 animals.
6. Section 5.1.8: representative data from 2 animals.
7. Section 5.1.9: representative data from 10 animals.
8. Section 5.1.10: representative data from 5 animals.
9. Section 5.1.11: representative data from 2 animals per genotype.
10. Section 5.1.12: representative data from 3 animals.
11. Section 5.1.13 representative data from 2 animals.
12. Section 5.1.14: representative data from 2 animals.
13. Section 5.1.15: representative data from 3 animals.
14. Section 5.1.16: representative data from 1 tumor bearing animal (repeated thrice to confirm the results).
15. Section 5.2: Data shown from one animal that was detected for metastases development.

Nevertheless, the purpose for lineage tracing has been depicted well. Although it would have been much easier and more informative if we could have analyzed all the animals, which was somehow not feasible due to animal deaths occurring during the time period and unexpected delays in experiments caused from certain factors which includes, animals transport from different animal facilities, and inability to

monitor the animals regularly and frequently for analysis. It is plausible that if the transgenic animals were analysed at a later time point including more mice, we would have been readily detected more metastases and tumors. Still the observation that we made would have not been changed in terms of the data reflecting the lineage tracing strategy that worked well. We were able to mark the primary tumors (cells) with DsRed and were successful in monitoring the different stages of metastasis in context to DsRed and SpC expression which has broadened our knowledge regarding the cystic liver lesions. This is the first report which tends to declare that hepatic cysts occurring in the NSCLC metastatic animals (readily detected at earlier time points by the previous investigators of Rapp's lab) are not simply any pathological liver condition, but are indeed a metastasis. However future work needs to be done in this area which will help us in finding the identity of the cell type solely responsible for metastasis/metastatic potential.

8 Appendix

Abbreviations

Abbreviation	Full name
APS	Ammoniumpersulfate
ATP	Adenosine-5'-triphosphate
BCP	1-Bromo-3-Chloropropane (C ₃ H ₆ BrCl)
BASCs	Bronchioalveolar stem cells
BADJ	Bronchioalveolar duct junction
BSA	Bovine Serum Albumin
°C	Degree Celsius
CCSP	Clara cell secretory protein
cDNA	Complementary DNA
CMV	Cytomegalovirus
CO ₂	Carbon dioxide
DPCs	Double positive cells
DAPI	4',6-Diamidino-2-phenylindol
DMEM	Dulbecco's Modified Eagle Medium
DMSO	Dimethylsulphoxide
DNA	Deoxyribonucleic acid
DOX	Doxycycline
dNTP	(Di)Desoxynucleotide triphosphate
DOX	Doxycycline
ECL	Enhanced Chemiluminescence
EDTA	Ethylenediaminetetraacetic acid
et al.	Et alii
FCS	Fetal calf serum
FITC	Fluorescein isothiocyanate
Fig	Figure
Floxed	Flanked by loxP site
g	Gram
GAPDH	Glyceraldehyde-3-phosphate dehydrogenase
GFP	Green Fluorescent Protein

HCl	Hydrochloric acid
H&E	Hematoxylin/eosin staining
hm	Hyper methylation
HPRT	Hypoxanthine guanine phosphoribosyl transferase
Kb	Kilo basepair
het	heterozygotes
kDa	Kilo dalton
ko	Knock-out
L	Liter
LOH	Loss of heterozygosity
M	Month
mA	Milliampere
mg	Milligram
min	Minutes
mM	Millimolar
ml	Millilitre
NaOH	Sodium hydroxide
NEBs	Neuro-epithelial bodies
NP40	Nonidet P-40 (octyl phenoxy polyethoxy ethanol)
NSCLC	Non-Small-Cell Lung Cancer
N	Normal
OCT	Optimal cutting temperature
OD	Optical density
PAGE	Polyacrylamide Gel Electrophoresis
PCR	Polymerase Chain Reaction
PBS	Phosphate Buffered Saline
PFA	Paraformaldehyde
rpm	Rounds per minute
RT	Room temperature
RTK	Receptor tyrosine kinase
RT-PCR	Reverse transcriptase polymerase chain reaction
RFP	Red Fluorescent Protein

rtTA	Reverse tetracycline transactivator
SCLC	Small-Cell Lung Cancer
sq.m	Square meter
SDS	Sodium dodecylsulfate
SP-C	Surfactant Protein C
sq.m	Square meter
TAE	Tris-Acetate-EDTA
TEMED	N,N,N',N'-Tetramethylethylenediamine
tet	tetracycline-regulated
Tet-O	tetracycline operator
Tris	Tris(hydroxymethyl)aminomethane
TRE	Tetracycline responsive elements
TRITC	Tetramethylrhodamine isothiocyanate
TTF-1/Nkx2.1	Thyroid transcription factor 1
V	Volt
wt	Wild type
µg	Microgram
µl	Microlitre
%	Percentage
+ve	positive
-ve	negative

9 References

Au NH, Cheang M, Huntsman DG, Yorida E, Coldman A, Elliott WM, Bebb G, Flint J, English J, Gilks CB, Grimes HL (2004) Evaluation of immunohistochemical markers in non-small cell lung cancer by unsupervised hierarchical clustering analysis: a tissue microarray study of 284 cases and 18 markers. *J Pathol* **204**: 101-109

Avruch J, Zhang XF, Kyriakis JM (1994) Raf meets Ras: completing the framework of a signal transduction pathway. *Trends Biochem Sci* **19**: 279-283

Beer DG, Malkinson AM (1985) Genetic influence on type 2 or Clara cell origin of pulmonary adenomas in urethan-treated mice. *J Natl Cancer Inst* **75**: 963-969

Belteki G, Haigh J, Kabacs N, Haigh K, Sison K, Costantini F, Whitsett J, Quaggin SE, Nagy A (2005) Conditional and inducible transgene expression in mice through the combinatorial use of Cre-mediated recombination and tetracycline induction. *Nucleic Acids Res* **33**

Berghmans T, Paesmans M, Mascaux C, Martin B, Meert AP, Haller A, Lafitte JJ, Sculier JP (2006) Thyroid transcription factor 1--a new prognostic factor in lung cancer: a meta-analysis. *Ann Oncol* **17**: 1673-1676

Boguski MS, McCormick F (1993) Proteins regulating Ras and its relatives. *Nature* **366**: 643-654

Borges M, Linnoila RI, van de Velde HJ, Chen H, Nelkin BD, Mabry M, Baylin SB, Ball DW (1997) An achaete-scute homologue essential for neuroendocrine differentiation in the lung. *Nature* **386**: 852-855

Borthwick DW, Shahbazian M, Krantz QT, Dorin JR, Randell SH (2001) Evidence for stem-cell niches in the tracheal epithelium. *Am J Respir Cell Mol Biol* **24**: 662-670

Brabletz T, Jung A, Spaderna S, Hlubek F, Kirchner T (2005) Opinion: migrating cancer stem cells - an integrated concept of malignant tumour progression. *Nat Rev Cancer* **5**: 744-749

Bremnes RM, Veve R, Gabrielson E, Hirsch FR, Baron A, Bemis L, Gemmill RM, Drabkin HA, Franklin WA (2002) High-throughput tissue microarray analysis used to evaluate biology and prognostic significance of the E-cadherin pathway in non-small-cell lung cancer. *J Clin Oncol* **20**: 2417-2428

Brinster RL, Chen HY, Messing A, van Dyke T, Levine AJ, Palmiter RD (1984) Transgenic mice harboring SV40 T-antigen genes develop characteristic brain tumors. *Cell* **37**: 367-379

Brooks AI, Cory-Slechta DA, Federoff HJ (2000) Gene-experience interaction alters the cholinergic septohippocampal pathway of mice. *Proc Natl Acad Sci U S A* **97**: 13378-13383

Cardoso WV, Lu J (2006) Regulation of early lung morphogenesis: questions, facts and controversies. *Development* **133**: 1611-1624

- Chalfie M, Tu Y, Euskirchen G, Ward WW, Prasher DC (1994) Green fluorescent protein as a marker for gene expression. *Science* **263**: 802-805
- Creuwels LA, van Golde LM, Haagsman HP (1997) The pulmonary surfactant system: biochemical and clinical aspects. *Lung* **175**: 1-39
- Decaestecker C, Debeir O, Van Ham P, Kiss R (2007) Can anti-migratory drugs be screened in vitro? A review of 2D and 3D assays for the quantitative analysis of cell migration. *Med Res Rev* **27**: 149-176
- Deisboeck TS, Couzin ID (2009) Collective behavior in cancer cell populations. *Bioessays* **31**: 190-197
- Dermer GB (1982) Origin of bronchioloalveolar carcinoma and peripheral bronchial adenocarcinoma. *Cancer* **49**: 881-887
- Dong J, Sutor S, Jiang G, Cao Y, Asmann YW, Wigle DA (2011) c-Myc regulates self-renewal in bronchoalveolar stem cells. *PLoS One* **6**: 17
- Dorsam RT, Gutkind JS (2007) G-protein-coupled receptors and cancer. *Nat Rev Cancer* **7**: 79-94
- Downward J (1998) Ras signalling and apoptosis. *Curr Opin Genet Dev* **8**: 49-54
- Ehrhardt A, Bartels T, Geick A, Klocke R, Paul D, Halter R (2001) Development of pulmonary bronchiolo-alveolar adenocarcinomas in transgenic mice overexpressing murine c-myc and epidermal growth factor in alveolar type II pneumocytes. *Br J Cancer* **84**: 813-818
- Emura M (2002) Stem cells of the respiratory tract. *Paediatr Respir Rev* **3**: 36-40
- Engelhardt JF (2001) Stem cell niches in the mouse airway. *Am J Respir Cell Mol Biol* **24**: 649-652
- Engelhardt JF, Schlossberg H, Yankaskas JR, Dudus L (1995) Progenitor cells of the adult human airway involved in submucosal gland development. *Development* **121**: 2031-2046
- Engelhardt JF, Yankaskas JR, Wilson JM (1992) In vivo retroviral gene transfer into human bronchial epithelia of xenografts. *J Clin Invest* **90**: 2598-2607
- Flory E, Hoffmeyer A, Smola U, Rapp UR, Bruder JT (1996) Raf-1 kinase targets GA-binding protein in transcriptional regulation of the human immunodeficiency virus type 1 promoter. *J Virol* **70**: 2260-2268
- Forbes S, Clements J, Dawson E, Bamford S, Webb T, Dogan A, Flanagan A, Teague J, Wooster R, Futreal PA, Stratton MR (2006) Cosmic 2005. *Br J Cancer* **94**: 318-322
- Forgacs E, Zochbauer-Muller S, Olah E, Minna JD (2001) Molecular genetic abnormalities in the pathogenesis of human lung cancer. *Pathol Oncol Res* **7**: 6-13
- Friedl P, Hegerfeldt Y, Tusch M (2004) Collective cell migration in morphogenesis and cancer. *Int J Dev Biol* **48**: 441-449

Furth PA, St Onge L, Boger H, Gruss P, Gossen M, Kistner A, Bujard H, Hennighausen L (1994) Temporal control of gene expression in transgenic mice by a tetracycline-responsive promoter. *Proc Natl Acad Sci U S A* **91**: 9302-9306

Giangreco A, Reynolds SD, Stripp BR (2002) Terminal bronchioles harbor a unique airway stem cell population that localizes to the bronchoalveolar duct junction. *Am J Pathol* **161**: 173-182

Gidekel Friedlander SY, Chu GC, Snyder EL, Girnius N, Dibelius G, Crowley D, Vasile E, DePinho RA, Jacks T (2009) Context-dependent transformation of adult pancreatic cells by oncogenic K-Ras. *Cancer Cell* **16**: 379-389

Gossen M, Bujard H (1992) Tight control of gene expression in mammalian cells by tetracycline-responsive promoters. *Proc Natl Acad Sci U S A* **89**: 5547-5551

Grandori C, Cowley SM, James LP, Eisenman RN (2000) The Myc/Max/Mad network and the transcriptional control of cell behavior. *Annu Rev Cell Dev Biol* **16**: 653-699

Gschwind A, Fischer OM, Ullrich A (2004) The discovery of receptor tyrosine kinases: targets for cancer therapy. *Nat Rev Cancer* **4**: 361-370

Guazzi S, Price M, De Felice M, Damante G, Mattei MG, Di Lauro R (1990) Thyroid nuclear factor 1 (TTF-1) contains a homeodomain and displays a novel DNA binding specificity. *Embo J* **9**: 3631-3639

Gulmann C, Lantuejoul S, Grace A, Leader M, Patchett S, Kay E (2005) Telomerase activity in proximal and distal gastric neoplastic and preneoplastic lesions using immunohistochemical detection of hTERT. *Dig Liver Dis* **37**: 439-445

Hadjantonakis AK, Dickinson ME, Fraser SE, Papaioannou VE (2003) Technicolour transgenics: imaging tools for functional genomics in the mouse. *Nat Rev Genet* **4**: 613-625

Hadjantonakis AK, Nagy A (2000) FACS for the isolation of individual cells from transgenic mice harboring a fluorescent protein reporter. *Genesis* **27**: 95-98

Hanahan D, Weinberg RA (2000) The hallmarks of cancer. *Cell* **100**: 57-70

Hanawalt PC, Ford JM, Lloyd DR (2003) Functional characterization of global genomic DNA repair and its implications for cancer. *Mutat Res* **544**: 107-114

Haque AK, Syed S, Lele SM, Freeman DH, Adegboyega PA (2002) Immunohistochemical study of thyroid transcription factor-1 and HER2/neu in non-small cell lung cancer: strong thyroid transcription factor-1 expression predicts better survival. *Appl Immunohistochem Mol Morphol* **10**: 103-109

Harris CC (1996) The 1995 Walter Hubert Lecture--molecular epidemiology of human cancer: insights from the mutational analysis of the p53 tumour-suppressor gene. *Br J Cancer* **73**: 261-269

- Hibi K, Westra WH, Borges M, Goodman S, Sidransky D, Jen J (1999) PGP9.5 as a candidate tumor marker for non-small-cell lung cancer. *Am J Pathol* **155**: 711-715
- Higashiyama M, Doi O, Kodama K, Yokouchi H, Kasugai T, Ishiguro S, Takami K, Nakayama T, Nishisho I (1997) MDM2 gene amplification and expression in non-small-cell lung cancer: immunohistochemical expression of its protein is a favourable prognostic marker in patients without p53 protein accumulation. *Br J Cancer* **75**: 1302-1308
- Hirata T, Fukuse T, Naiki H, Wada H (2001) Expression of E-cadherin and lymph node metastasis in resected non-small-cell lung cancer. *Clin Lung Cancer* **3**: 134-140
- Hoess RH, Abremski K (1984) Interaction of the bacteriophage P1 recombinase Cre with the recombining site loxP. *Proc Natl Acad Sci U S A* **81**: 1026-1029
- Hoffman RM (2005) The multiple uses of fluorescent proteins to visualize cancer in vivo. *Nat Rev Cancer* **5**: 796-806
- Hoffman RM (2008) A better fluorescent protein for whole-body imaging. *Trends Biotechnol* **26**: 1-4
- Hong KU, Reynolds SD, Giangreco A, Hurley CM, Stripp BR (2001) Clara cell secretory protein-expressing cells of the airway neuroepithelial body microenvironment include a label-retaining subset and are critical for epithelial renewal after progenitor cell depletion. *Am J Respir Cell Mol Biol* **24**: 671-681
- Hong KU, Reynolds SD, Watkins S, Fuchs E, Stripp BR (2004a) Basal cells are a multipotent progenitor capable of renewing the bronchial epithelium. *Am J Pathol* **164**: 577-588
- Hong KU, Reynolds SD, Watkins S, Fuchs E, Stripp BR (2004b) In vivo differentiation potential of tracheal basal cells: evidence for multipotent and unipotent subpopulations. *Am J Physiol Lung Cell Mol Physiol* **286**: 18
- Hotte SJ, Hirte HW (2002) BAY 43-9006: early clinical data in patients with advanced solid malignancies. *Curr Pharm Des* **8**: 2249-2253
- Ihrie RA, Reczek E, Horner JS, Khachatryan L, Sage J, Jacks T, Attardi LD (2003) Perp is a mediator of p53-dependent apoptosis in diverse cell types. *Curr Biol* **13**: 1985-1990
- Ikeda K, Clark JC, Shaw-White JR, Stahlman MT, Boutell CJ, Whitsett JA (1995) Gene structure and expression of human thyroid transcription factor-1 in respiratory epithelial cells. *J Biol Chem* **270**: 8108-8114
- Jackson EL, Willis N, Mercer K, Bronson RT, Crowley D, Montoya R, Jacks T, Tuveson DA (2001) Analysis of lung tumor initiation and progression using conditional expression of oncogenic K-ras. *Genes Dev* **15**: 3243-3248
- Jemal A, Tiwari RC, Murray T, Ghafoor A, Samuels A, Ward E, Feuer EJ, Thun MJ (2004) Cancer statistics, 2004. *CA Cancer J Clin* **54**: 8-29

- Johnson BE, Russell E, Simmons AM, Phelps R, Steinberg SM, Ihde DC, Gazdar AF (1996) MYC family DNA amplification in 126 tumor cell lines from patients with small cell lung cancer. *J Cell Biochem Suppl* **24**: 210-217
- Johnson L, Mercer K, Greenbaum D, Bronson RT, Crowley D, Tuveson DA, Jacks T (2001) Somatic activation of the K-ras oncogene causes early onset lung cancer in mice. *Nature* **410**: 1111-1116
- Jothy S (2003) CD44 and its partners in metastasis. *Clin Exp Metastasis* **20**: 195-201
- Kalogeraki A, Bouros D, Zoras O, Karabekios S, Chalkiadakis G, Stathopoulos E, Sifakas N, Delides GS (2003) E-cadherin expression on fine-needle aspiration biopsies in primary lung adenocarcinomas is related to tumor differentiation and invasion. *Anticancer Res* **23**: 3367-3371
- Karremans C (2002) AiO, combining DNA/protein programs and oligo-management. *Bioinformatics* **18**: 884-885
- Karreth FA, Tuveson DA (2009) Modelling oncogenic Ras/Raf signalling in the mouse. *Curr Opin Genet Dev* **19**: 4-11
- Kaspar BK, Vissel B, Bengoechea T, Crone S, Randolph-Moore L, Muller R, Brandon EP, Schaffer D, Verma IM, Lee KF, Heinemann SF, Gage FH (2002) Adeno-associated virus effectively mediates conditional gene modification in the brain. *Proc Natl Acad Sci U S A* **99**: 2320-2325
- Katz MH, Takimoto S, Spivack D, Moossa AR, Hoffman RM, Bouvet M (2003) A novel red fluorescent protein orthotopic pancreatic cancer model for the preclinical evaluation of chemotherapeutics. *J Surg Res* **113**: 151-160
- Kauffman SL (1974) Kinetics of alveolar epithelial hyperplasia in lungs of mice exposed to urethane. I. Quantitative analysis of cell populations. *Lab Invest* **30**: 170-175
- Kauffman SL (1980) Cell proliferation in the mammalian lung. *Int Rev Exp Pathol* **22**: 131-191
- Kaufmann O, Dietel M (2000) Expression of thyroid transcription factor-1 in pulmonary and extrapulmonary small cell carcinomas and other neuroendocrine carcinomas of various primary sites. *Histopathology* **36**: 415-420
- Kerkhoff E, Fedorov LM, Siefken R, Walter AO, Papadopoulos T, Rapp UR (2000) Lung-targeted expression of the c-Raf-1 kinase in transgenic mice exposes a novel oncogenic character of the wild-type protein. *Cell Growth Differ* **11**: 185-190
- Khanna KK, Jackson SP (2001) DNA double-strand breaks: signaling, repair and the cancer connection. *Nat Genet* **27**: 247-254
- Kilby NJ, Snaith MR, Murray JA (1993) Site-specific recombinases: tools for genome engineering. *Trends Genet* **9**: 413-421

References

- Kim CF, Jackson EL, Woolfenden AE, Lawrence S, Babar I, Vogel S, Crowley D, Bronson RT, Jacks T (2005) Identification of bronchioalveolar stem cells in normal lung and lung cancer. *Cell* **121**: 823-835
- Kim KK, Kugler MC, Wolters PJ, Robillard L, Galvez MG, Brumwell AN, Sheppard D, Chapman HA (2006) Alveolar epithelial cell mesenchymal transition develops in vivo during pulmonary fibrosis and is regulated by the extracellular matrix. *Proc Natl Acad Sci U S A* **103**: 13180-13185
- Kobayashi T, Tsuda H, Noguchi M, Hirohashi S, Shimosato Y, Goya T, Hayata Y (1990) Association of point mutation in c-Ki-ras oncogene in lung adenocarcinoma with particular reference to cytologic subtypes. *Cancer* **66**: 289-294
- Kolch W, Kotwaliwale A, Vass K, Janosch P (2002) The role of Raf kinases in malignant transformation. *Expert Rev Mol Med* **4**: 1-18
- Landis SH, Murray T, Bolden S, Wingo PA (1999) Cancer statistics, 1999. *CA Cancer J Clin* **49**: 8-31
- Langley RR, Fidler IJ (2007) Tumor cell-organ microenvironment interactions in the pathogenesis of cancer metastasis. *Endocr Rev* **28**: 297-321
- Lapidot T, Sirard C, Vormoor J, Murdoch B, Hoang T, Caceres-Cortes J, Minden M, Paterson B, Caligiuri MA, Dick JE (1994) A cell initiating human acute myeloid leukaemia after transplantation into SCID mice. *Nature* **367**: 645-648
- Leung EL, Fiskus RR, Tung JW, Tin VP, Cheng LC, Sihoe AD, Fink LM, Ma Y, Wong MP (2010) Non-small cell lung cancer cells expressing CD44 are enriched for stem cell-like properties. *PLoS One* **5**
- Levine AJ (1997) p53, the cellular gatekeeper for growth and division. *Cell* **88**: 323-331
- Lewis PD, Parry JM (2004) In silico p53 mutation hotspots in lung cancer. *Carcinogenesis* **25**: 1099-1107
- Linnoila RI, Szabo E, DeMayo F, Witschi H, Sabourin C, Malkinson A (2000) The role of CC10 in pulmonary carcinogenesis: from a marker to tumor suppression. *Ann N Y Acad Sci* **923**: 249-267
- Lippincott-Schwartz J, Patterson GH (2003) Development and use of fluorescent protein markers in living cells. *Science* **300**: 87-91
- Liu X, Driskell RR, Engelhardt JF (2006) Stem cells in the lung. *Methods Enzymol* **419**: 285-321
- Lutz W, Leon J, Eilers M (2002) Contributions of Myc to tumorigenesis. *Biochim Biophys Acta* **14**: 61-71
- Maeda Y, Dave V, Whitsett JA (2007) Transcriptional control of lung morphogenesis. *Physiol Rev* **87**: 219-244

- Magdaleno SM, Barrish J, Finegold MJ, DeMayo FJ (1998) Investigating stem cells in the lung. *Adv Pediatr* **45**: 363-396
- Malkinson AM (1991) Genetic studies on lung tumor susceptibility and histogenesis in mice. *Environ Health Perspect* **93**: 149-159
- Mallick B, Ghosh Z, Chakrabarti J (2009) MicroRNome analysis unravels the molecular basis of SARS infection in bronchoalveolar stem cells. *PLoS One* **4**
- Marchant JS, Stutzmann GE, Leissring MA, LaFerla FM, Parker I (2001) Multiphoton-evoked color change of DsRed as an optical highlighter for cellular and subcellular labeling. *Nat Biotechnol* **19**: 645-649
- Marshall C (1999) How do small GTPase signal transduction pathways regulate cell cycle entry? *Curr Opin Cell Biol* **11**: 732-736
- Mason RJ, Kalina M, Nielsen LD, Malkinson AM, Shannon JM (2000) Surfactant protein C expression in urethane-induced murine pulmonary tumors. *Am J Pathol* **156**: 175-182
- Matz MV, Fradkov AF, Labas YA, Savitsky AP, Zraisky AG, Markelov ML, Lukyanov SA (1999) Fluorescent proteins from nonbioluminescent Anthozoa species. *Nat Biotechnol* **17**: 969-973
- McDowell EM, Newkirk C, Coleman B (1985) Development of hamster tracheal epithelium: II. Cell proliferation in the fetus. *Anat Rec* **213**: 448-456
- Metzger RJ, Klein OD, Martin GR, Krasnow MA (2008) The branching programme of mouse lung development. *Nature* **453**: 745-750
- Meuwissen R, Berns A (2005) Mouse models for human lung cancer. *Genes Dev* **19**: 643-664
- Miyawaki A, Sawano A, Kogure T (2003) Lighting up cells: labelling proteins with fluorophores. *Nat Cell Biol* **7**: S1-7
- Mizuno H, Sawano A, Eli P, Hama H, Miyawaki A (2001) Red fluorescent protein from *Discosoma* as a fusion tag and a partner for fluorescence resonance energy transfer. *Biochemistry* **40**: 2502-2510
- Mori S, Ito G, Usami N, Yoshioka H, Ueda Y, Kodama Y, Takahashi M, Fong KM, Shimokata K, Sekido Y (2004) p53 apoptotic pathway molecules are frequently and simultaneously altered in nonsmall cell lung carcinoma. *Cancer* **100**: 1673-1682
- Myong NH (2003) Thyroid transcription factor-1 (TTF-1) expression in human lung carcinomas: its prognostic implication and relationship with expressions of p53 and Ki-67 proteins. *J Korean Med Sci* **18**: 494-500
- Nagy A (2000) Cre recombinase: the universal reagent for genome tailoring. *Genesis* **26**: 99-109

- Okabe M, Ikawa M, Kominami K, Nakanishi T, Nishimune Y (1997) 'Green mice' as a source of ubiquitous green cells. *FEBS Lett* **407**: 313-319
- Okubo T, Knoepfler PS, Eisenman RN, Hogan BL (2005) Nmyc plays an essential role during lung development as a dosage-sensitive regulator of progenitor cell proliferation and differentiation. *Development* **132**: 1363-1374
- Onn A, Isobe T, Itasaka S, Wu W, O'Reilly MS, Ki Hong W, Fidler IJ, Herbst RS (2003) Development of an orthotopic model to study the biology and therapy of primary human lung cancer in nude mice. *Clin Cancer Res* **9**: 5532-5539
- Oster SK, Ho CS, Soucie EL, Penn LZ (2002) The myc oncogene: Marvelously Complex. *Adv Cancer Res* **84**: 81-154
- Otani EM, Newkirk C, McDowell EM (1986) Development of hamster tracheal epithelium: IV. Cell proliferation and cytodifferentiation in the neonate. *Anat Rec* **214**: 183-192
- Otto WR (2002) Lung epithelial stem cells. *J Pathol* **197**: 527-535
- Peake JL, Reynolds SD, Stripp BR, Stephens KE, Pinkerton KE (2000) Alteration of pulmonary neuroendocrine cells during epithelial repair of naphthalene-induced airway injury. *Am J Pathol* **156**: 279-286
- Pelosi G, Frassetto F, Pasini F, Maisonneuve P, Sonzogni A, Iannucci A, Terzi A, Bresaola E, Valduga F, Lupo C, Viale G (2001) Immunoreactivity for thyroid transcription factor-1 in stage I non-small cell carcinomas of the lung. *Am J Surg Pathol* **25**: 363-372
- Perl AK, Tichelaar JW, Whitsett JA (2002a) Conditional gene expression in the respiratory epithelium of the mouse. *Transgenic Res* **11**: 21-29
- Perl AK, Wert SE, Nagy A, Lobe CG, Whitsett JA (2002b) Early restriction of peripheral and proximal cell lineages during formation of the lung. *Proc Natl Acad Sci U S A* **99**: 10482-10487
- Puglisi F, Barbone F, Damante G, Bruckbauer M, Di Lauro V, Beltrami CA, Di Loreto C (1999) Prognostic value of thyroid transcription factor-1 in primary, resected, non-small cell lung carcinoma. *Mod Pathol* **12**: 318-324
- Ramaswamy S, Ross KN, Lander ES, Golub TR (2003) A molecular signature of metastasis in primary solid tumors. *Nat Genet* **33**: 49-54
- Rapp UR, Ceteci F, Schreck R (2008) Oncogene-induced plasticity and cancer stem cells. *Cell Cycle* **7**: 45-51
- Rapp UR, Heidecker G, Huleihel M, Cleveland JL, Choi WC, Pawson T, Ihle JN, Anderson WB (1988) raf family serine/threonine protein kinases in mitogen signal transduction. *Cold Spring Harb Symp Quant Biol* **1**: 173-184

- Rapp UR, Korn C, Ceteci F, Karreman C, Luetkenhaus K, Serafin V, Zanucco E, Castro I, Potapenko T (2009) MYC is a metastasis gene for non-small-cell lung cancer. *PLoS One* **4**
- Rawlins EL (2008) Lung epithelial progenitor cells: lessons from development. *Proc Am Thorac Soc* **5**: 675-681
- Rawlins EL, Clark CP, Xue Y, Hogan BL (2009a) The Id2+ distal tip lung epithelium contains individual multipotent embryonic progenitor cells. *Development* **136**: 3741-3745
- Rawlins EL, Hogan BL (2006) Epithelial stem cells of the lung: privileged few or opportunities for many? *Development* **133**: 2455-2465
- Rawlins EL, Okubo T, Xue Y, Brass DM, Auten RL, Hasegawa H, Wang F, Hogan BL (2009b) The role of Scgb1a1+ Clara cells in the long-term maintenance and repair of lung airway, but not alveolar, epithelium. *Cell Stem Cell* **4**: 525-534
- Reddy R, Buckley S, Doerken M, Barsky L, Weinberg K, Anderson KD, Warburton D, Driscoll B (2004) Isolation of a putative progenitor subpopulation of alveolar epithelial type 2 cells. *Am J Physiol Lung Cell Mol Physiol* **286**: 15
- Rehm S, Lijinsky W, Singh G, Katyal SL (1991) Mouse bronchiolar cell carcinogenesis. Histologic characterization and expression of Clara cell antigen in lesions induced by N-nitrosobis-(2-chloroethyl) ureas. *Am J Pathol* **139**: 413-422
- Reya T, Morrison SJ, Clarke MF, Weissman IL (2001) Stem cells, cancer, and cancer stem cells. *Nature* **414**: 105-111
- Reynolds SD, Giangreco A, Power JH, Stripp BR (2000) Neuroepithelial bodies of pulmonary airways serve as a reservoir of progenitor cells capable of epithelial regeneration. *Am J Pathol* **156**: 269-278
- Richardson GE, Johnson BE (1993) The biology of lung cancer. *Semin Oncol* **20**: 105-127
- Robbins DJ, Zhen E, Cheng M, Xu S, Ebert D, Cobb MH (1994) MAP kinases ERK1 and ERK2: pleiotropic enzymes in a ubiquitous signaling network. *Adv Cancer Res* **63**: 93-116
- Rock JR, Onaitis MW, Rawlins EL, Lu Y, Clark CP, Xue Y, Randell SH, Hogan BL (2009) Basal cells as stem cells of the mouse trachea and human airway epithelium. *Proc Natl Acad Sci U S A* **106**: 12771-12775
- Rom WN, Hay JG, Lee TC, Jiang Y, Tchou-Wong KM (2000) Molecular and genetic aspects of lung cancer. *Am J Respir Crit Care Med* **161**: 1355-1367
- Salgia R, Skarin AT (1998) Molecular abnormalities in lung cancer. *J Clin Oncol* **16**: 1207-1217
- Sauer B, Henderson N (1988) Site-specific DNA recombination in mammalian cells by the Cre recombinase of bacteriophage P1. *Proc Natl Acad Sci U S A* **85**: 5166-5170

- Schiller JH (2001) Current standards of care in small-cell and non-small-cell lung cancer. *Oncology* **1**: 3-13
- Schmitt CA, Fridman JS, Yang M, Lee S, Baranov E, Hoffman RM, Lowe SW (2002) A senescence program controlled by p53 and p16INK4a contributes to the outcome of cancer therapy. *Cell* **109**: 335-346
- Schonig K, Schwenk F, Rajewsky K, Bujard H (2002) Stringent doxycycline dependent control of CRE recombinase in vivo. *Nucleic Acids Res* **30**
- Schreck R, Rapp UR (2006) Raf kinases: oncogenesis and drug discovery. *Int J Cancer* **119**: 2261-2271
- Shay JW, Wright WE (2005) Senescence and immortalization: role of telomeres and telomerase. *Carcinogenesis* **26**: 867-874
- Slebos RJ, Kibbelaar RE, Dalesio O, Kooistra A, Stam J, Meijer CJ, Wagenaar SS, Vanderschueren RG, van Zandwijk N, Mooi WJ, et al. (1990) K-ras oncogene activation as a prognostic marker in adenocarcinoma of the lung. *N Engl J Med* **323**: 561-565
- Srinivas S, Watanabe T, Lin CS, Williams CM, Tanabe Y, Jessell TM, Costantini F (2001) Cre reporter strains produced by targeted insertion of EYFP and ECFP into the ROSA26 locus. *BMC Dev Biol* **1**: 27
- Stec DE, Davisson RL, Haskell RE, Davidson BL, Sigmund CD (1999) Efficient liver-specific deletion of a floxed human angiotensinogen transgene by adenoviral delivery of Cre recombinase in vivo. *J Biol Chem* **274**: 21285-21290
- Stenhouse G, Fyfe N, King G, Chapman A, Kerr KM (2004) Thyroid transcription factor 1 in pulmonary adenocarcinoma. *J Clin Pathol* **57**: 383-387
- Stewart TA, Pattengale PK, Leder P (1984) Spontaneous mammary adenocarcinomas in transgenic mice that carry and express MTV/myc fusion genes. *Cell* **38**: 627-637
- Strien L, Leidenius M, von Smitten K, Heikkila P (2010) Concordance between HER-2 and steroid hormone receptor expression between primary breast cancer, sentinel node metastases, and isolated tumor cells. *Pathol Res Pract* **206**: 253-258
- Sutherland KD, Berns A (2010) Cell of origin of lung cancer. *Mol Oncol* **4**: 397-403
- Takahashi K, Yamanaka S (2006) Induction of pluripotent stem cells from mouse embryonic and adult fibroblast cultures by defined factors. *Cell* **126**: 663-676
- Talmadge JE, Fidler IJ (2010) AACR centennial series: the biology of cancer metastasis: historical perspective. *Cancer Res* **70**: 5649-5669
- Terskikh AV, Fradkov AF, Zaraisky AG, Kajava AV, Angres B (2002) Analysis of DsRed Mutants. Space around the fluorophore accelerates fluorescence development. *J Biol Chem* **277**: 7633-7636

Thaete LG, Malkinson AM (1990) Differential staining of normal and neoplastic mouse lung epithelia by succinate dehydrogenase histochemistry. *Cancer Lett* **52**: 219-227

Thaete LG, Malkinson AM (1991) Cells of origin of primary pulmonary neoplasms in mice: morphologic and histochemical studies. *Exp Lung Res* **17**: 219-228

Toyooka S, Tsuda T, Gazdar AF (2003) The TP53 gene, tobacco exposure, and lung cancer. *Hum Mutat* **21**: 229-239

Travis WD (2011) Pathology of lung cancer. *Clin Chest Med* **32**: 669-692

Troppmair J, Rapp UR (2003) Raf and the road to cell survival: a tale of bad spells, ring bearers and detours. *Biochem Pharmacol* **66**: 1341-1345

Tsien RY *Rosy dawn for fluorescent proteins*: Nat Biotechnol. 1999 Oct;17(10):956-7.

van Zandwijk N, Mooi WJ, Rodenhuis S (1995) Prognostic factors in NSCLC. Recent experiences. *Lung Cancer* **12**: S27-33

Verkhusha VV, Lukyanov KA (2004) The molecular properties and applications of Anthozoa fluorescent proteins and chromoproteins. *Nat Biotechnol* **22**: 289-296

Verkhusha VV, Otsuna H, Awasaki T, Oda H, Tsukita S, Ito K (2001) An enhanced mutant of red fluorescent protein DsRed for double labeling and developmental timer of neural fiber bundle formation. *J Biol Chem* **276**: 29621-29624

Visvader JE (2011) Cells of origin in cancer. *Nature* **469**: 314-322

Wall MA, Socolich M, Ranganathan R (2000) The structural basis for red fluorescence in the tetrameric GFP homolog DsRed. *Nat Struct Biol* **7**: 1133-1138

Wang L, Heidt DG, Lee CJ, Yang H, Logsdon CD, Zhang L, Fearon ER, Ljungman M, Simeone DM (2009) Oncogenic function of ATDC in pancreatic cancer through Wnt pathway activation and beta-catenin stabilization. *Cancer Cell* **15**: 207-219

Welm BE, Tepera SB, Venezia T, Graubert TA, Rosen JM, Goodell MA (2002) Sca-1(pos) cells in the mouse mammary gland represent an enriched progenitor cell population. *Dev Biol* **245**: 42-56

Wikenheiser KA, Clark JC, Linnoila RI, Stahlman MT, Whitsett JA (1992) Simian virus 40 large T antigen directed by transcriptional elements of the human surfactant protein C gene produces pulmonary adenocarcinomas in transgenic mice. *Cancer Res* **52**: 5342-5352

Wikenheiser KA, Whitsett JA (1997) Tumor progression and cellular differentiation of pulmonary adenocarcinomas in SV40 large T antigen transgenic mice. *Am J Respir Cell Mol Biol* **16**: 713-723

References

- Winslow MM, Dayton TL, Verhaak RG, Kim-Kiselak C, Snyder EL, Feldser DM, Hubbard DD, DuPage MJ, Whittaker CA, Hoersch S, Yoon S, Crowley D, Bronson RT, Chiang DY, Meyerson M, Jacks T (2011) Suppression of lung adenocarcinoma progression by Nkx2-1. *Nature* **473**: 101-104
- Wuenshell CW, Sunday ME, Singh G, Minoo P, Slavkin HC, Warburton D (1996) Embryonic mouse lung epithelial progenitor cells co-express immunohistochemical markers of diverse mature cell lineages. *J Histochem Cytochem* **44**: 113-123
- Yamamoto N, Yang M, Jiang P, Xu M, Tsuchiya H, Tomita K, Moossa AR, Hoffman RM (2003) Real-time imaging of individual fluorescent-protein color-coded metastatic colonies in vivo. *Clin Exp Metastasis* **20**: 633-638
- Yang M, Li L, Jiang P, Moossa AR, Penman S, Hoffman RM (2003) Dual-color fluorescence imaging distinguishes tumor cells from induced host angiogenic vessels and stromal cells. *Proc Natl Acad Sci U S A* **100**: 14259-14262
- Yilmaz M, Christofori G (2010) Mechanisms of motility in metastasizing cells. *Mol Cancer Res* **8**: 629-642
- Yu TS, Dandekar M, Monteggia LM, Parada LF, Kernie SG (2005) Temporally regulated expression of Cre recombinase in neural stem cells. *Genesis* **41**: 147-153
- Yuan B, Li C, Kimura S, Engelhardt RT, Smith BR, Minoo P (2000) Inhibition of distal lung morphogenesis in Nkx2.1(-/-) embryos. *Dev Dyn* **217**: 180-190
- Zhao M, Yang M, Baranov E, Wang X, Penman S, Moossa AR, Hoffman RM (2001) Spatial-temporal imaging of bacterial infection and antibiotic response in intact animals. *Proc Natl Acad Sci U S A* **98**: 9814-9818

10 Curriculum Vitae

Personal Information

Name: Chitra Thakur
Gender: Female
Date of Birth: 4th November 1982
Place of Birth: Bhopal, India
Nationality: Indian
Marital Status: Single

Education

2010-2012: Max Planck Institute of Biochemistry, Martinsreid Germany
Graduate Fellow

2007- 2010: University of Würzburg, Germany
Graduate School of Life Sciences Fellow

2006-2007: Centre for Cellular and Molecular Biology, Hyderabad, A.P.
India
Project, Junior Research Fellow

2004- 2006: University Teaching Department Barkatullah University Bhopal
(M.P.) India
Master of Science in Microbiology (University Topper)

2001-2004: Govt. Motilal Vigyan Mahavidyalaya, Barkatullah University
Bhopal (M.P.) India
Bachelor of Science in Microbiology (College Topper)

Awards and Acheivements

2007-2010: University of Würzburg, Germany
Graduate School of Life Sciences Fellowship (DFG Excellence Initiative)

2006-2007: Molecular Markers Laboratory; Centre for Cellular and Molecular Biology, Hyderabad, A.P., India

JRF Fellowship from a DBT (Department of Biotechnology, India) sponsored project

2006: University Teaching Department, Dept. of Microbiology, Barkatullah University Bhopal

University topper : Rank 1st

Class Representative of the Department of Microbiology, 2005-2006

2004: Govt. Motilal Science College, Barkatullah University Bhopal (M.P.) India

College topper: Rank 1st

Associated Member

2007-2010: University of Würzburg, Germany

Graduate College Würzburg-Nice: “Signal Transduction: Where Cancer and Infection Converge”

Associate member of the AACR, American Association for Cancer Research. Card Id: 242823

Associate member of the Association of the Microbiologist of India, South Campus, Delhi University, New Delhi, India

Presentations and Talks:

Poster:

1. Title of the paper: Lineage tracing of metastasis in a Non-small cell lung cancer (NSCLC) mouse model”

Authors: Chitra Thakur, Ulf R Rapp

Presenter: Chitra Thakur

Conference: MRS-AACR Joint Conference on Metastasis and the Tumor Microenvironment, September 12th -15th, 2010 at the Sheraton Center City, Philadelphia, PA, USA.

2. *Title of the paper:* "Lineage tracing of metastasis in a Non-small cell lung cancer (NSCLC) mouse model"

Authors: Chitra Thakur, Ulf R Rapp

Presenter: Chitra Thakur

Conference: Max Planck Institute's Day on 18th May 2011 at the MPI Biochemistry, Martinsreid, Germany.

3. *Title of the paper:* Is Cancer initiation restricted to replicative cells?

Authors: Chitra Thakur, Fatih Ceteci, Ulf R Rapp

Presenter: Chitra Thakur

Conference: 4th International Symposium organized by the students of Graduate School Of Life Sciences , on " Research Revolution "University of Wurzburg, 26 -27 March, 2009.

Talk

"Lineage tracing of metastasis in a murine lung adenocarcinoma model" in the 11th Graduate Program of the Max Planck Institute of Biochemistry , Martinsreid Germany at Ringberg Castle, 21st -23rd March 2011.

Trainings

Compact-course on laboratory animals, animal experiments and alternatives (FELASA)

Conducted by: Charite-Universitätsmedizin Berlin and ZEBE

Certified by: GV- SOLAS (Gesellschaft für Versuchstierkunde-Society of Laboratory Animal Science)

Light Microscopy for Biologists

Conducted by: Max Planck Institute of Biochemistry, Core Facility

Proteomics and Mass Spectrometry

Conducted by: Max Planck Institute of Biochemistry, Core Facility

Applied Statistics for Life Scientists

Conducted by: Graduate School of Life Sciences University of Würzburg
Ethics, Science and Bioethics, Genetic testing

Conducted by: Graduate School of Life Sciences University of Würzburg

Publication

Conditional Expression of Oncogenic C-RAF in Mouse Pulmonary Epithelial Cells Reveals Differential Tumorigenesis and Induction of Autophagy Leading to Tumor Regression. *Ceteci F, Xu J, Ceteci S, Zanucco E, Thakur C, Rapp UR. Neoplasia. 2011 Nov; 13(11):1005-18.*

Combinatorial treatment of mammospheres with trastuzumab and salinomycin efficiently eradicates HER2-positive cancer cells and cancer stem cells. *Prajakta S. Oak, Florian Kopp, Chitra Thakur, Joachim W. Ellwart, Ulf R. Rapp, Axel Ullrich, Ernst Wagner, Pjotr Knyazev and Andreas Roidl (In review)*

Treatment of salinomycin targets metastatic breast cancer cells and reduces their migration. *Prajakta S. Oak, Florian Kopp, Chitra Thakur, Axel Ullrich, Pjotr Knyazev, Ulf R. Rapp, Ernst Wagner, Rajkumar Savai, and Andreas Roidl (In preparation)*

Hepatic Cysts mark the early stage of metastatic tumor development in a mouse model for metastasis of NSCLC. *Chitra Thakur, Vijay Kumar Ulaganathan, Prajakta Oak, Nefertiti Elenkhelly, Andreas Roidl, Raj Kumar Savai, Ulf R.Rapp. (In preparation)*

Acknowledgements

The writing of a dissertation can be an exciting or an isolating experience; yet it is obviously not possible without the personal & practical support of numerous people. Any attempt to list the people and opportunities with which my life has been richly blessed would be like trying to count stars in the heaven. Yet among these stand some individuals whose profound impact deserves special acknowledgement.

Prime most I thank Almighty God for his immeasurable love and mercy. His soul grace was my strength in all my knowledge and wisdom.

With a deep sense of humbleness & gratitude, I express my heartfelt thanks to Prof. Dr. Ulf R. Rapp, who gave me the opportunity to pursue my PhD under his excellent supervision. I thank him for providing me the interactive environment that has enhanced my ability of analysis and shaping up the projects independently.

As Newton wrote, "if I see further; it is because I stand upon the shoulders of giants." This is what I feel when I think of my mentor Prof. Dr. Axel Ullrich (Director, Department of Molecular Biology, Max Planck Institute, Martinsried). I extend my sincerest thanks to him for his guidance, support, inspiration and constant encouragement. I thank him for giving me an opportunity to practical training in one of the well equipped & prestigious molecular biology labs of Europe and helping me in the successful completion of my PhD project in his department.

I extend my profound gratitude to Prof. Thomas Rudel, my immediate supervisor, for his enriching guidance and support. My heartfelt thanks to Dr. Rudolf Götz and Dr. Jörg Wischhusen for their critical feedback and suggestions on my PhD work.

I thank Dr. Nikolaos Deliolanis, (Institute for Biological and Medical Imaging (IBMI) Helmholtz Zentrum München, German Research Center for Environmental Health (GmbH), Neuherberg) for collaborating with us and their assistance in animal imaging experiments. Sincere thanks to Miss Prajakta Oak and Dr. Andreas Roidl (Pharmaceutical Biology, Department of Pharmacy, Ludwig Maximilians University Munich) for being a wonderful collaborator. I thank them for the endless discussions which have helped me to gain new insights in carrying out my PhD work.

Acknowledgements

I am also grateful to Dr. Eva Hesse and Dr. Heinz Brandstetter (Animal Authority Officers at the MPI, Martinsreid). I thank them for timely providing me with their suggestions required to carry out animal experiments at MPI and helping me in the administrative work for establishing collaboration for imaging project.

I would like to thank Dr. Michael Sixt (Department of Molecular Medicine, MPI, Martinsreid) for his support in cell sorting experiments. I also thank Mr. Ralf Zenke for his guidance in using Laser Scanning microscope (MPI Core facility). I am indebtedly grateful to Miss Nefertiti El-Nikhely and Dr. Raj Kumar Savai (Laboratory for Molecular Mechanisms in Lung Cancer, Max-Planck-Institut für Herz- und Lungenforschung Bad Nauheim) for their support and cooperation in carrying several experiments and for the frequent scientific discussions.

I wish to extend my special acknowledgements to Dr. Vijay Kumar Ulaganathan (Dept. of Molecular biology, Max Planck institute of Biochemistry, Martinsreid) for being a great senior and guiding me in every possible way which has helped me in bringing my PhD project to fruition. I have benefitted enormously with the discussions I had with him. I also thank him sincerely for being there and encouraging me during odd circumstances.

I extend my thanks to Ms. Verena Theobald for supporting me in the entire official paper work. I thank Dr. Thomas Mayr and Dr. Pjotr Knyaze for scientific discussions.

A special thanks to Mrs. ML Rapp for helping and guiding me to proceed further. I thank her for the valuable time, she has offered me.

I thank the Graduate School of Life Sciences (GSLs), Würzburg for funding my PhD project. Sincere thanks to the 'Friday Worship group'; Luciana, Dr. Michael, Jenny, and Dr. Ruth. The little time spent with them in the church has strengthened me incredibly to progress positively in all the areas of my life in spite of facing challenges and setbacks.

Some people are always grumbling because roses have thorns. I am thankful that thorns have roses! This is what I feel when I remember Prajakta, Dity, Sayan, Megha Sneha, Padma, Ankita, Ruhel, Krishna, Bharti, Vaibhao, Pawan, Neha and Yamini. Their compassionate company made my stay in Germany homely and memorable. Special thanks to my lab colleagues Ema, Andreas (former lab mate), Fatih and Semra. I enjoyed their wonderful presence.

Friends are angels who lift us to our feet, when our wings have trouble remembering how to fly. This is really true of Shuchi, Tanmoy, Minarbha and K. Words are not sufficient to thank them.

My special appreciation goes to my enlightened teachers, because of whom our own genuine compassion can be born, flourish & gave rise to the power to benefit others.

When I start counting blessings my whole life turns around. This is still not enough when I think of my parents, brother Alok and sister Priya. I express my heartiest gratitude to all of them for being a source of inexhaustible encouragement, unconditional love and inspiration to build up my educational career. Their influence is all over these pages and all over my life.

Last but not the least; I thank Anand for his immense trust and faith in me which is helping me in realizing my dreams with each passing day.

Finally I owe great obligations for all those innocent mice that donated their lives for my project.

Nothing stokes the performance like feedback. The positive stuff of course is preferred, but even negative feedback does the concourse good. If it doesn't serve to improve the performance, it at least gets my Irish up and running nicely. Please keep it coming!

Affidavit

I hereby confirm that my thesis entitled:

Lineage tracing of metastasis in a mouse model for Non-small cell lung cancer (NSCLC)

is the result of my own work. I did not receive any help or support from commercial consultants. All sources and / or materials applied are listed and specified in the thesis.

Furthermore, I confirm that this thesis has not yet been submitted as part of another examination process neither in identical nor in similar form.

Place, Date

Signature

Eidesstattliche Erklärung

Hiermit erkläre ich an Eides statt, die Dissertation

Untersuchung metastatischer Prozesse durch genetische Zellmarkierung in einem Mausmodell des nichtkleinzelligen Lungenkarzinoms (NSCLC)

eigenständig, d.h. insbesondere selbständig und ohne Hilfe eines kommerziellen Promotionsberaters, angefertigt und keine anderen als die von mir angegebenen Quellen und Hilfsmittel verwendet zu haben.

Ich erkläre außerdem, dass die Dissertation weder in gleicher noch in ähnlicher Form bereits in einem anderen Prüfungsverfahren vorgelegen hat.

Ort, Datum

Unterschrift